SANTA FE INSTITUTE

Complexity in One-D Cellular Automata:

Gliders, Basins of Attraction and the Z Parameter

Andrew Wuensche

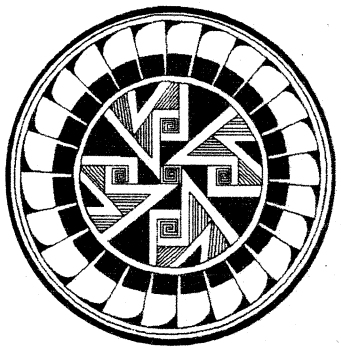

94-04-025

This research was supported in part by grants to the Santa Fe Institute, including core funding from the John D. and Catherine T. MacArthur Foundation; the National Science Foundation (PHY 9021437); and the U.S. Department of Energy (DE-FG05-88ER25054).

About the Santa Fe Institute

The Santa Fe Institute (SFI) is a multidisciplinary graduate research and teaching institution formed to nurture research on complex systems and their simpler elements. A private, independent institution, SFI was founded in 1984. Its primary concern is to focus the tools of traditional scientific disciplines and emerging new computer resources on the problems and opportunities that are involved in the multidisciplinary study of complex systems—those fundamental processes that shape almost every aspect of human life. Understanding complex systems is critical to realizing the full potential of science, and may be expected to yield enormous intellectual and practical benefits.

All Santa Fe Institute publications carry the SFI logo on the front cover, which is based on a Mimbres pottery design (circa A.D. 950-1150), drawn by Betsy Jones.

Complexity
in One-D Cellular Automata
Gliders, Basins of Attraction and the Z parameter

Andrew Wuensche

Santa Fe Institute
and University of Sussex
School of Cognitive and Computer Science
wuensch@santafe.edu
andywu@cogs.susx.ac.uk

contact address:
48 Esmond Road, London W4 1JQ
tel 081 995 8893 fax 081 742 2178
100020.2727@compuserve.com

February 1994

Abstract

What do we mean by complexity in the changing patterns of a discrete dynamical system? Complex one-D CA rules support the emergence of interacting periodic configurations - gliders, glider-guns and *compound* gliders made up of interacting sub-gliders - evolving within quiescent or periodic backgrounds. This paper examines gliders and their interactions in one-D CA on the basis of many examples. The basin of attraction fields of complex rules are typically composed of a small number of basins with long transients (interacting gliders) rooted on short attractor cycles (non-interacting gliders, or backgrounds free of gliders).

For CA rules in general, a relationship is proposed between the quality of dynamical behaviour, the topology of the basin of attraction field, the density of garden-of-Eden states counted in attractor basins or sub-trees, and the rule-table's Z parameter. High density signifies simple dynamics, and low - chaotic, with complex dynamics at the transition. Plotting garden-of-Eden density against the Z parameter for a large sample of rules shows a marked correlation that increases with neighbourhood size. The relationship between Z and the λ parameter is described. A method of recognising the emergence of gliders by monitoring the evolution of the lookup frequency spectrum, and its entropy, is suggested.

Contents

1. Introduction

So called *complex* cellular automata (CA) rules, such as Conway's 2-D *game of life*[2], support coherent, periodic, space-time configurations that propagate and interact on a quiescent background. The menagerie of configurations found have been grouped under various names such as blinkers, gliders, glider-guns, eaters, space ships, puffer-trains, etc. Langton suggests that such *virtual state machines*[7] may provide the 'molecular logic' for artificial life embedded in CA.

In one-D complex CA, analogous phenomena exist within a background that may be quiescent but is often periodic. These coherent structures are described variously as, solitary waves, gliders, virtual automata, information structures, particle-like structures and domain boundaries. Large scale complex dynamical behaviour emerges from disordered initial conditions as a result of many local small scale parallel processes; an instance of self-organisation at the *edge-of-chaos*[8]. Gliders are analogous to autocatalytic sets of polymers[6], in that a configuration C_1 sets off a sequence of transformations, $\rightarrow C_2 \rightarrow C_3 \rightarrow \cdots \rightarrow C_1$, with *catalytic closure*. Members of such sets have a survival advantage in occupying space, and the set acquires its own identity as an observed object at a higher level.

The possibility of a new level of description of dynamical behaviour, on the basis of observed glider collision rules without reference to the underlying low level CA rules, illustrates the concept of emergence, and may underlie the elusive notion of complexity. Gliders may eject or absorb a regular glider stream, or spontaneously combine to form *compound* gliders, which then interact at yet higher levels of description. The process could unfold without limit in large enough systems.

A CA may be regarded as a parallel processing computer[15]. Collisions between gliders, creating new gliders that collide in their turn, may encode logical operations supporting universal computation[2,8,15]. A CA may alternatively be viewed as a logical universe with its own local physics, with gliders as artificial molecules, from which more complex gliders with the capacity for self-reproduction and other essential functions of biomolecules might emerge, leading to the possibility of life-like behaviour[7].

How simple can a CA be and still exhibit complex behaviour? How and why is complexity able to emerge? What do we mean by complexity and emergence in the changing patterns of a discrete dynamical system? To begin to answer these questions it may be helpful to examine a relatively large sample of CA rules with glider-like properties that appear complex to us, but whose architecture is as simple as possible. In one-D CA, a few complex rules have been identified which feature emergent gliders. Among the 256 binary 3-neighbour rules (the elementary rules[15]) where an exhaustive search is practical, there are 2 sets of rules identified as complex[9,17], rule 54 and 110 (and their equivalents). Some examples of complex rules in 5-neighbour rule-space, have been documented[16,10,1,21]. Other examples are derived from one-D CA with more complicated architectures[8,16], such as a value range greater than binary.

In appendices 2 and 3, this paper presents a sample of about 60 subjectively complex one-D binary rules; the neighbourhood size is generally 5, with a few examples of 6 and 7. Figures 1 and 15 show typical examples. Complex rules are supposed to be rare[19]; most rules are *simple* or *chaotic*. However, complex rules can be found relatively easily by a method of artificially selecting random mutations similar to the proposal by Li[10]. As the neighbourhood increases the search becomes harder because the search space grows exponentially. A rule is selected at random from a likely region of rule space according to the Z parameter. As the space-time pattern iterates, the rule is mutated by random bitflips, bitflips-back, or bitflips that raise or lower Z, to select borderline rules until a complex space-time pattern is recognised. Alternatively, starting from a complex rule, other complex rules may be easily found, suggesting that related complex rules separated by small Hamming distances occur in clusters in rule space. Possible methods of automating the search by monitoring the frequency spectrum of neighbourhood lookup, and the variation of the spectrum's entropy, is suggested.

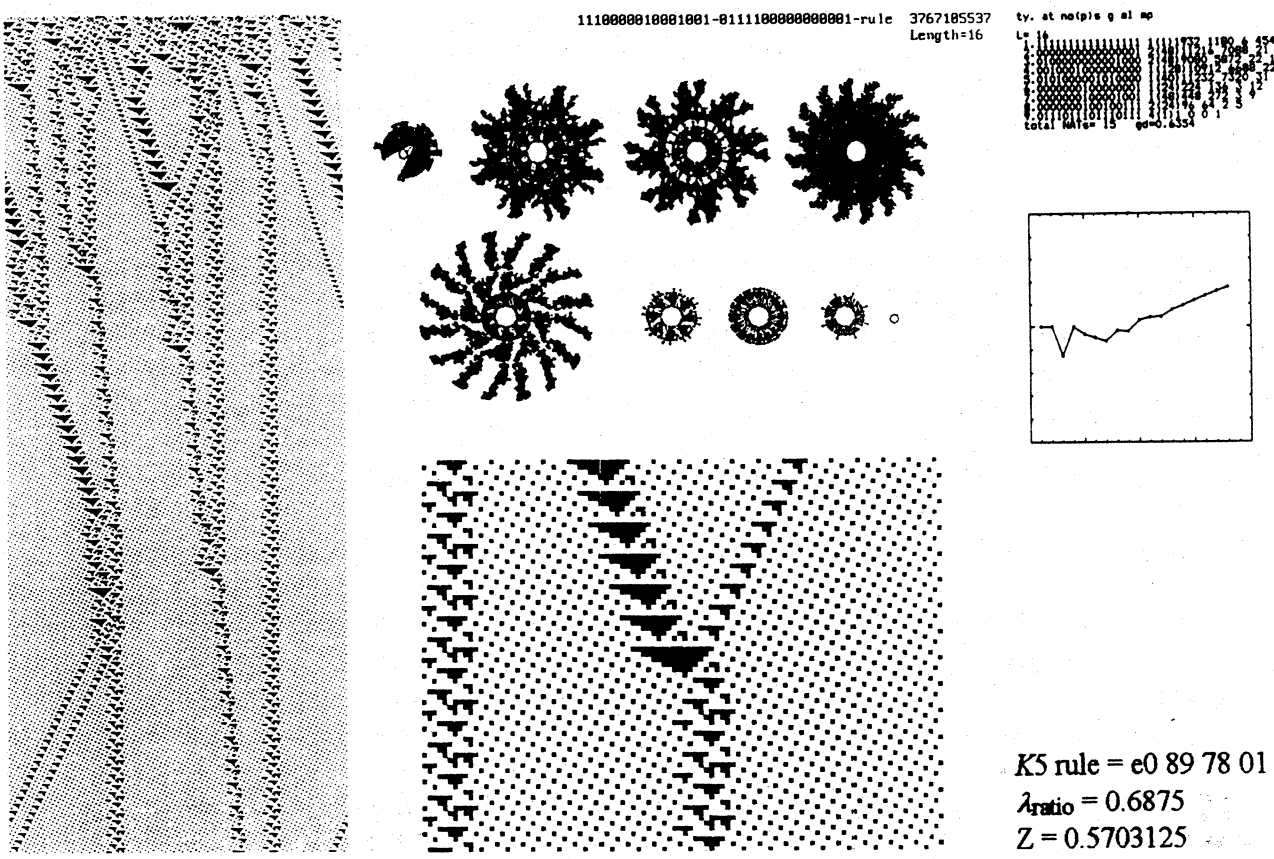

Figure 1.
A typical space-time pattern and basin of attraction field of a *K*5 rule that supports emerging gliders, taken from the sample in appendix 2 (2.17). *Left*: a typical space-time pattern, system size 200, periodic boundary conditions, 480 time-steps from the top down. *Top centre*: the basin of attraction field, system size 16, showing the 9 non-equivalent basins from a total of 15 in state space. *Top right*: basin field data (for key see appendix 2.1) and *below* a graph of garden-of Eden density (vertical axis) against system size, for $N = 1$ to 18. *Bottom centre*: a detail of glider interactions. *Bottom right*: the rule number in hex, its λ_{ratio} and Z parameter.

The basin of attraction field provides another, global, perspective for assessing complex rules, and may be contrasted with the basin fields of rules in general presented in[21]. The idea that complex rules occur at a phase transition in rule space based on Langton's λ parameter[8,20], is extended on the basis of the more focused Z parameter[21], which is shown to provide a good indication of the density of *garden-of-Eden* states in state space (*G-density*). G-density is a good measure of the degree of convergence, independent of system size, of the dynamical flow seen in the topology of the basin of attraction field. High density signifies simple dynamics, and low - chaotic, with complex dynamics at the transition. Graphs of G-density against the rule table's Z parameter for a large sample of rules shows a marked correlation, becoming more focused for larger neighbourhoods.

The availability of a relatively large sample of rules yielding space-time patterns that feature interacting gliders allows an attempt at a comparative description of what constitutes complex dynamics, in contrast to the simple or chaotic dynamics more generally apparent in CA behaviour space.

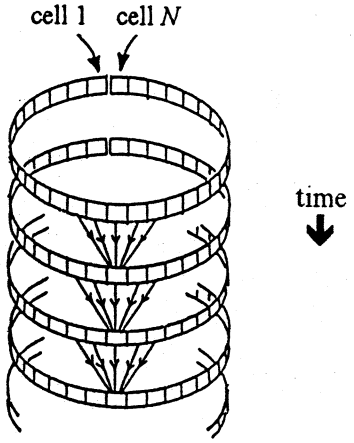

Figure 2.
One-D CA architecture, periodic boundary conditions. Neighbourhood size, K = 5, system size N. Updating is synchronous in discrete time-steps.

2. One-Dimensional CA architecture

A CA is a self-contained discrete dynamical system, where space is a lattice of cells with a regular geometry. Cells update their values, chosen from a finite alphabet, as an invariant function of a standard neighbourhood template (the *neighbourhood*). Updating is synchronous in discrete time-steps.

This paper considers the simplest CA architecture. The alphabet's size is just 2 (0,1). Space is a one-dimensional ring of N cells (periodic boundary conditions). A cell's neighbourhood (size K) is a continuous zone of up to 9 cells at the same time-step; odd sizes are centred, even sizes have an extra cell on the left. Most examples in this paper are for K=5 (radius 2) neighbourhoods; a diagram of the system is shows in figure 2. The direction of time is from the top down.

Consider a periodic one-D lattice with N cells and a size K neighbourhood. r_{left} and r_{right} are the neighbourhood radii to the left and right, where $K = r_{\text{left}} + 1 + r_{\text{right}}$. The time evolution of the i-th cell is given by,

$$C_i^{(t+1)} = f\left(C_{i-r_{\text{left}}}^{(t)}, \cdots C_{i-1}^{(t)}, C_i^{(t)}, C_{i+1}^{(t)}, \cdots C_{i+r_{\text{right}}}^{(t)}\right)$$

to satisfy periodic boundary conditions, for $x<1$, $C_x = C_{N+x}$; for $x>N$, $C_x = C_{x-N}$

A neighbourhood of size K has 2^K permutations of values. The most general expression of the function f is a lookup table (the *rule table*) with 2^K entries, giving 2^{2^K} possible rules. Sub-categories of rules can also be expressed as simple algorithms, Boolean derivatives[12], totalistic rules or threshold functions. The number of effectively different rules is reduced by symmetries in the rule table[14,21]. By convention[15,21] the rule table is arranged in descending order of the values of neighbourhoods, and the resulting bit string converts to the decimal or hexadecimal rule number. For example, the rule table for the K=3 rule 30 (hex 1e) is,

	7	6	5	4	3	2	1	0	←neighbourhoods (decimal)
	111	110	101	100	011	010	001	000	←neighbourhoods (binary)
rule-table→	0	0	0	1	1	1	1	0	←outputs

The rule table for the K=5 rule 906663673, hex 36 0a 96 f9, is ,

	neighbourhoods 31— 0 (shown vertically)																																
left cell→	1	1	1	1	1	1	1	1	1	1	1	1	1	1	1	1	0	0	0	0	0	0	0	0	0	0	0	0	0	0	0	0	0	0
	1	1	1	1	1	1	1	1	0	0	0	0	0	0	0	0	1	1	1	1	1	1	1	1	0	0	0	0	0	0	0	0	0	0
centre cell→	1	1	1	1	0	0	0	0	1	1	1	1	0	0	0	0	1	1	1	1	0	0	0	0	1	1	1	1	0	0	0	0		
	1	1	0	0	1	1	0	0	1	1	0	0	1	1	0	0	1	1	0	0	1	1	0	0	1	1	0	0	1	1	0	0		
right cell→	1	0	1	0	1	0	1	0	1	0	1	0	0	1	0	1	1	0	1	0	1	0	1	0	1	0	1	0	1	0	1	0		
rule-table→	0	0	1	1	0	1	1	0	0	0	0	0	1	0	1	0	1	0	0	1	0	1	1	0	1	1	1	1	1	0	0	1	←outputs	

$K \geq 5$ rules are referred to by their hexadecimal rule numbers for simplicity, but K=3 rules are also referred to by their more familiar decimal rule numbers.

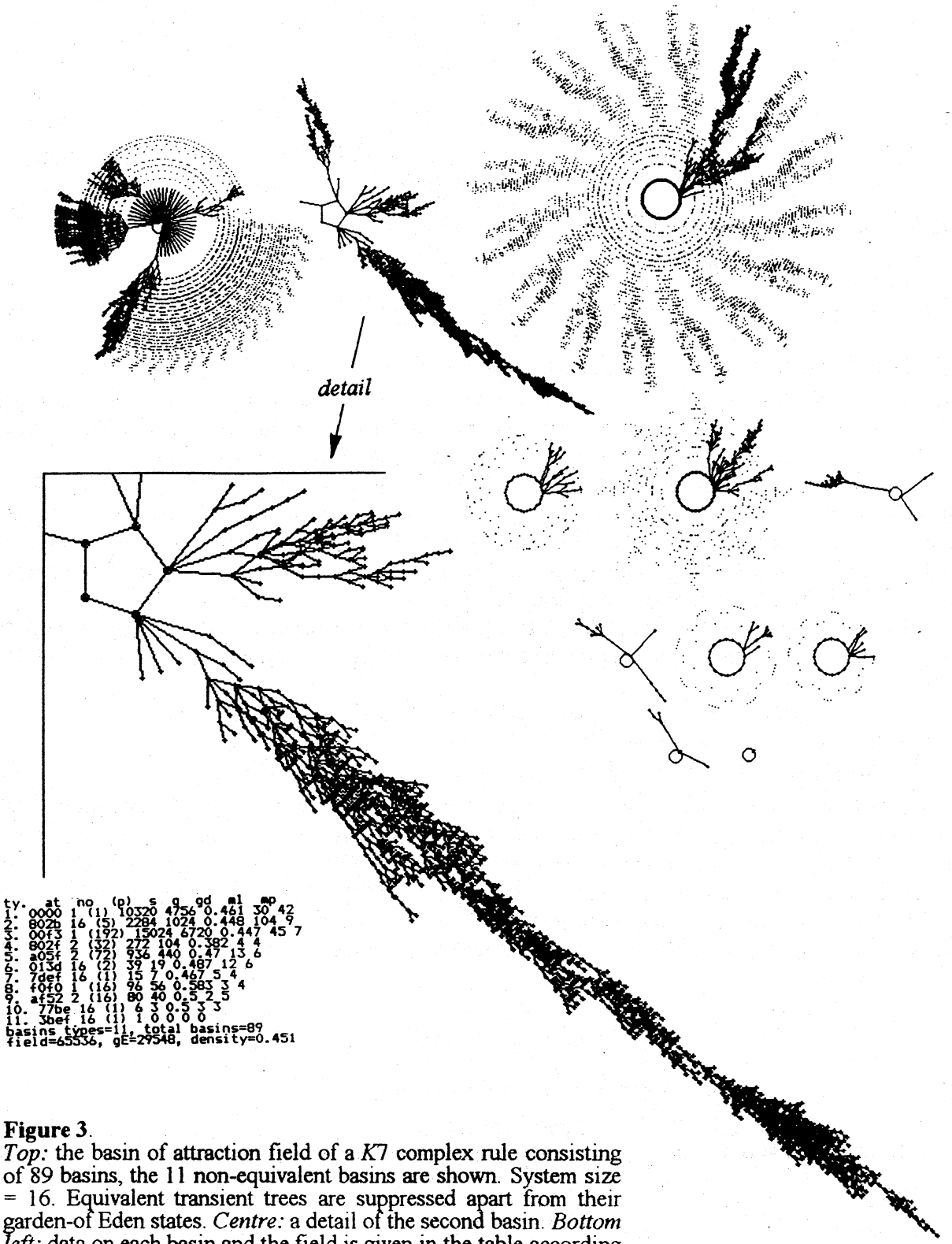

Figure 3.
Top: the basin of attraction field of a *K*7 complex rule consisting of 89 basins, the 11 non-equivalent basins are shown. System size = 16. Equivalent transient trees are suppressed apart from their garden-of Eden states. *Centre:* a detail of the second basin. *Bottom left:* data on each basin and the field is given in the table according to the key in appendix 2.1. The *K*7 rule number in hex is 3b 46 9c 0e e4 f7 fa 96 f9 3b 4d 32 b0 9e d0 e0, (see appendix 3.6).

3. Space-time patterns and basins of attraction

In this paper, two aspect of CA behaviour will be related, space-time patterns and the basin of attraction field.

A space-time pattern represents a single determined trajectory through state-space. An initial pattern or *seed* assigned to the lattice at time t_0 sets off a succession of patterns at times t_1, t_2, t_3,... by the iteration of the CA rule. The future dynamics is determined yet unpredictable; there seems in general to be no short cut for knowing the future more efficiently than the actual iteration itself[18]. The sequence of iterated states is a *trajectory*, and may be represented by a space-time pattern diagram. This is shown as successive rows of cells (the circular lattice is opened out), coloured according to value; 0-white, 1-black. The direction of time is down. A CA state has just one successor, but may have an arbitrary number of predecessors (its *pre-images*). States with no pre-images are so called *garden-of-Eden* states because they cannot be reached by normal CA evolution, they can only be imposed from outside. Although a seed determines a single future, each iteration may have many past histories.

The state-space of a CA with N cells is 2^N. Any path inevitably encounters a repeat of a previous state, and must lead to a state cycle (the *attractor cycle*). The attractor may have just one state, a stable point cycling to itself, or may have an arbitrarily long period*. The set of all possible paths leading to the same attractor, including the attractor itself, make up a *basin of attraction*, a concept familiar from continuous dynamical systems. State-space is typically divided into many basins, the *basin of attraction field*.

Any trajectory is just one particular path within a basin of attraction. A *transient* is the portion of the trajectory outside the attractor cycle and usually merges with other transients to form a branching tree with garden-of-Eden states as the leaves. A *sub-tree* is a branch of the *transient tree*. Basins of attraction typically have a topology of trees rooted on cycles. They are mathematical objects in space-time that link the system's global states according to their dynamical transitions.

Access to these objects opens up a new area of phenomenology. They provide a global perspective on CA dynamics, in addition to the study of space-time patterns alone. The relative length and *bushiness* of trees, and other features of basin field topology, reflect space-time phenomena.

4. Computing pre-images

Constructing a basin of attraction or subtree poses the problem of finding the pre-images of each state. A possible method is to exhaustively test the entire state space, but this becomes computationally intractable as the network's size increases beyond modest limits.

Algorithms have recently been invented[21,22], however, for computing pre-images directly, without exhaustive testing. The network's dynamics can be run *backwards* in time; backward trajectories will, as a rule, diverge. A *reverse algorithm* that directly computes pre-images for one-D cellular automata was presented in *The Global Dynamics of Cellular Automata*[21], and a *general* direct reverse algorithm for random Boolean networks (which includes higher dimensional cellular automata) in *The Ghost in the Machine*[22]. The computational performance depends on the extent to which the neighbourhood size K, is smaller than the system size N. Provide that $K < N$, on average the performance is many orders of magnitude faster than exhaustive testing, making basin portraits for these systems accessible.

*The attractor period cannot , however, exeed 2^N-M, where M is the number of states in state space made up of repeating segments on the circular lattice[21].

5. Drawing basins of attraction and subtrees

Basins of attraction are portrayed as computer diagrams in the same graphic format as presented in[21]. Global states may be represented by nodes, or by the state's binary, decimal or hexadecimal expression at the node position. Nodes are linked by directed arcs. Each node has one outgoing arc (one *out degree*) and zero or more incoming arcs from nodes at the previous time-step. Nodes with no pre-images have no incoming arcs, and represent garden-of-Eden states. The number of incoming arcs is referred to as the *degree of pre-imaging* (or *in degree*).

Figure 3 shows the basin of attraction field of a $K7$ CA with 16 cells from the examples of complex rules in appendix 3. The CA has organized the 65536 states in state-space into a field with 89 basins of attraction. Because of rotation symmetry in the circle of cells, many of these basins, and also transient trees within basins, are equivalent to each other. Only the 11 non-equivalent basins in the basin of attraction field are shown. If a basin has equivalent transient trees, only one example of each equivalent set of trees is shown in full, the others are indicated only by their garden-of-Eden states. Data on the field is shown according to the key in appendix 2.

6. The Z-parameter and basin topology

Various parameters, calculated directly from a CA's rule table, have been proposed to predict CA behaviour and mark the phase transition between order and chaos, notably Langton's λ parameter[7,8] and the equivalent idea of *internal homogeneity* introduced earlier by Walker[13]. I have proposed a new parameter[21], Z, which avoids many of the exceptions inherent in λ and tracks behaviour more closely. Whereas λ simply counts the fraction of 1s in a binary rule table, Z takes into account the allocation of rule-table values to sub-categories of related neighbourhoods.

Suppose that we know part of a pre-image (a partial pre-image) of an arbitrary CA state, and attempt to deduce the value of successive cells from *left* to right. The Z_{left} parameter is the probability that the next cell to the right in the partial pre-image has a unique value, and is calculated directly from the CA rule table by counting *deterministic* neighbourhoods, defined below. Z_{right} is the converse from *right* to left. The Z parameter itself is the greater of Z_{left} and Z_{right}.

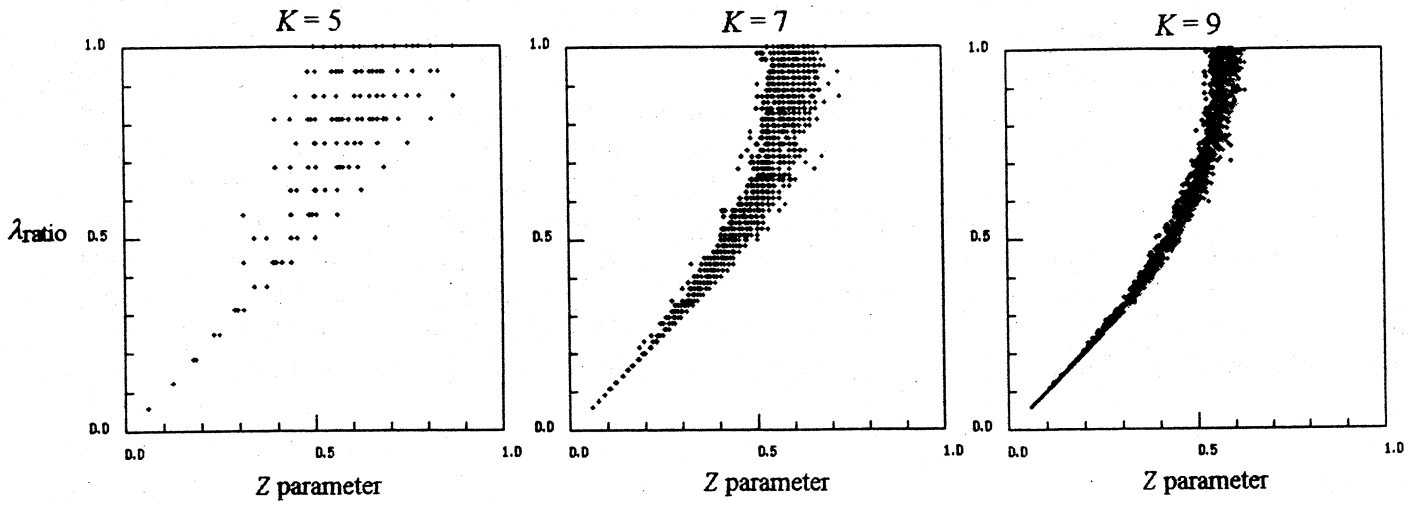

Figure 4.
The relationship between λ_{ratio} and the Z parameter for $K5$, $K7$ and $K9$ rules. Each graph shows 2200 rules chosen at random but biased to include a representative spread of λ_{ratio}.

If a partial pre-image ends with a pattern corresponding to a deterministic neighbourhood, then the next cell *must* have a unique value, thus preventing the partial pre-image from bifurcating into two valid partial pre-images, and restricting the potential for growth in the number of pre-images. This is the basis of the reverse algorithm for determining pre-images presented in[21], where the leading edge of each partial pre-image is continuously checked for a match with a deterministic neighbourhood.

Z is a probability, so varies between 0 and 1. If Z is high, the number of pre-images of an arbitrary CA state is likely to be small relative to system size. If Z=1 it was shown in[21] that maximum in-degree cannot exceed 2^{K-1}, and if only one of Z_{left} or Z_{right} =1, maximum in-degree must be smaller than 2^{K-1}. Conversely, if Z is low, the in-degree is likely to be relatively high (if Z=0, all state space becomes a single pre-image fan).

For CA rules in general, the quality of dynamical behaviour; simple–complex–chaotic is reflected by the degree of convergence of dynamical flow seen in the topology of the basin of attraction field. Consider a transient sub-tree with n nodes linked by n-1 edges. In the space of all possible topologies there are two extreme cases. Maximum convergence occurs where n-1 nodes converge in one step onto a single node; here the garden-of-Eden density is close to 1. Minimum convergence occurs where the nodes are strung out in a chain with pre-imaging never exceeding one; here the garden-of-Eden density is close to 0. Between these two extremes, it is possible to imagine a spectrum of degrees of convergence that describe the topology in terms of the "bushiness" of typical transient trees, high convergence for short and dense trees with many branching points of high in-degree, and low for long sparse trees, with few branching points of low in-degree.

A simple measure that seems to capture the degree of convergence (independently of system size) is the density of garden-of-Eden states (*G-density*) counted in attractor basins or sub-trees. High density signifies high convergence and simple dynamics, low density signifies low convergence and chaotic dynamics, with complex dynamics balanced at the transition.

By predicting the probable in-degree of an arbitrary CA state, the Z parameter predicts G-density and convergence. This in turn relates to attractor cycle and transient length, and the number and size of separate basins. The table below shows varying aspects of behaviour of increasingly large CA arrays as the Z parameter varies from 0 to 1 (Wolfram's behaviour classes[15,16] are shown in brackets).

		phase transition	
	simple (class 1&2) →	complex (class 4) →	chaotic(class 3)
Z parameter (0 - 1)	low	≈ 0.5 - 0.8	high
convergence	high	balanced	low
garden of Eden density	converges to 1	balanced	converges to 0
transient, attractor length	very short	moderately long	very long

7. Calculating the Z-parameter

The procedure to derive Z from the rule table is described below (refer to *The Global dynamics of Cellular Automata*[21] for a fuller discussion relating specifically to K3 and K5 rules).

Let n_K = the count of rule-table entries belonging to deterministic *pairs* of neighbourhoods such that,

the neighbourhood, $a_1,a_3,..a_{K-1},1 \rightarrow T$...(its output)

and $a_1,a_2,..a_{K-1},0 \rightarrow \overline{T}$ (not T)

The probability that the *next cell* is determined on the basis of deterministic *pairs* is given by $R_K = n_K/2^K$, a first approximation of Z_{left}, as deterministic *pairs* occur with the highest probability in a random rule-table.

Let n_{K-1} = the count of rule-table entries belonging to deterministic *4-tuples* of neighbourhoods (where "$*$" is a wildcard value, 0 or 1 with equal validity) of such that,

the neighbourhood, $a_1,a_3,..a_{K-2},1,\ * \rightarrow T$ (its output)

and $a_1,a_2,..a_{K-2},0,\ * \rightarrow \overline{T}$

The probability that the *next cell* is determined on the basis of deterministic *4-tuples* is given by $R_{K-1} = n_{K-1}/2^K$

Let n_{K-2} = the count of rule-table entries belonging to deterministic *8-tuples* of neighbourhoods such that,

the neighbourhood, $a_1,a_3,..a_{K-3},1,\ *,\ * \rightarrow T$ (its output)

and $a_1,a_2,..a_{K-3},0,\ *,\ * \rightarrow \overline{T}$

The probability that the *next cell* is determined on the basis of deterministic *4-tuples*, is given by $R_{K-2} = n_{K-2}/2^K$

This procedure is repeated if necessary to count rule-table entries belonging to deterministic *16-tuples* of neighbourhoods, *32-tuples* of neighbourhoods etc,... up to the special case of just one 2^K*-tuple* of neighbourhoods which occupies the whole rule-table.

The probability that the *next cell* is determined on the basis of at least one of these procedures is given by the following expression (order of the probabilities makes no difference to the result),

$$Z_{left} = R_K + R_{K-1}(1-R_K) + R_{K-2}(1-(R_K + R_{K-1}(1-R_K))) + R_{K-3}(1-(R_{K-2}(1-(R_K + R_{K-1}(1-R_K))))) + \ldots$$

Which simplifies to . . .

$$Z_{left} = R_K + R_{K-1}(1-R_K) + R_{K-2}(1-R_{K-1})(1-R_K) + R_{K-3}(1-R_{K-2})(1-R_{K-1})(1-R_K) + \ldots$$

And may be expressed as* $$Z_{left} = R_K + \sum_{i=1}^{K-1} R_{K-i}\left(\prod_{j=K-i+1}^{K}(1-R_j)\right)$$

where $R_i = n_i/2^K$, and n_i = the count of rule-table entries belonging of deterministic 2^{K-i}*-tuples*.

A converse procedure gives Z_{right}, and the Z parameter = the greater of Z_{left} and Z_{right}.

For example, take the $K5$ rule b9 89 3a f0 3 with a rule table set out in the conventional order (higher value neighbourhoods on the left). Left-to-right *n*-tuples are conveniently positioned in adjacent clusters. To calculate Z_{left}, count rule-table entries belonging to deterministic *n-tuples* of neighbourhoods. Deterministic *n-tuples* are indicated thus "_/", "___/___", "______/______" etc.

```
                neighbourhoods 31— 0 (shown vertically)
   left cell→   1 1 1 1 1 1 1 1 1 1 1 1 1 1 1 1   0 0 0 0 0 0 0 0 0 0 0 0 0 0 0 0
                1 1 1 1 1 1 1 1 0 0 0 0 0 0 0 0   1 1 1 1 1 1 1 1 0 0 0 0 0 0 0 0
 centre cell→   1 1 1 1 0 0 0 0 1 1 1 1 0 0 0 0   1 1 1 1 0 0 0 0 1 1 1 1 0 0 0 0
                1 1 0 0 1 1 0 0 1 1 0 0 1 1 0 0   1 1 0 0 1 1 0 0 1 1 0 0 1 1 0 0
  right cell→   1 0 1 0 1 0 1 0 1 0 1 0 1 0 1 0   1 0 1 0 1 0 1 0 1 0 1 0 1 0 1 0
                -------------------------------------------------------------------
  rule-table→   1 0 1 1 1 0 0 1 1 0 0 0 0 1 1 0   0 0 1 1 1 0 1 0 1 1 1 1 0 0 0 0  ←outputs
                \_/     \_/ \_/ \_/     \_/ \_/   \_____/ \_/ \_/ \_____________/
```

n_5=16, R_5 =16/32 = 0.5, n_4=4, R_4 =4/32 = 0.125, n_3=1, R_3 =8/32 = 0.25

Z_{left} = 0.5 + 0.125(1-0.5) +0.25(1-(0.5+ 0.125(1-0.5))) = 0.5 + 0.0625 + 0.109375 = 0.671875

To calculate Z_{right}, the diagram of neighbourhoods is reflected about its centre-cell axis, and the rule-table entries are rearranged according to the revised order (only asymmetric neighbourhoods change position). This groups right-to-left *n*-tuples in the same adjacent clusters as in the conventional order

*Acknowledgements to Guillaume Barreau and Phil Husbands for deriving this expression.

above. Count rule-table entries belonging to deterministic *n-tuples* of neighbourhoods. Deterministic *n-tuples* are indicated as above.

re-ordered neighbourhoods (shown vertically)

left cell→	1	0	1	0	1	0	1	0	1	0	1	0	1	0	1	0	1	0	1	0	1	0	1	0	1	0	1	0	1	0	1	0	
	1	1	0	0	1	1	0	0	1	1	0	0	1	1	0	0	1	1	0	0	1	1	0	0	1	1	0	0	1	1	0	0	
centre cell→	1	1	1	1	0	0	0	0	1	1	1	1	0	0	0	0	1	1	1	1	0	0	0	0	1	1	1	1	0	0	0	0	
	1	1	1	1	1	1	1	1	0	0	0	0	0	0	0	0	1	1	1	1	1	1	1	1	0	0	0	0	0	0	0	0	
right cell→	1	1	1	1	1	1	1	1	1	1	1	1	1	1	1	1	0	0	0	1	0	0	0	0	0	0	0	0	0	0	0	0	
rule-table→	1	0	1	1	1	0	0	0	1	1	0	1	0	1	1	0	0	0	0	1	0	0	1	0	1	1	1	1	1	0	0	0	←outputs

n_5=16, R_5 =16/32 = 0.5, n_4=4, R_4 =4/32 = 0.125

Z_{right} = 0.5 + 0.125(1-0.5) = 0.5 + 0.0625 = 0.5625, $Z_{left} > Z_{right}$, so Z = 0.671875

8. Relating the λ parameter and Z

The λ parameter and Z are related because λ indicates of the probability of the value of Z. Exceptions to λ's predictions of CA behaviour are due to the fact that λ only measures the proportions of the different values in the rule table, irrespective of the distribution. The three graphs in figure 4 show λ_{ratio} plotted against Z for a sample of K=5, 7 and 9 rules. λ_{ratio} = 2 × the ratio of 0s or 1s in the rule table, whichever is the less. This normalises the λ parameter, making 0s and 1s equivalent, for direct comparison with Z.

λ_{ratio} is plotted against Z for 2200 random rules for each K. The rule sample was biased to include a representative spread of λ_{ratio} values by varying the probability of setting a 1 in the rule table from 0.05 to 0.5, in 0.05 steps. An equal mix of 0s and 1s gives the highest probability of high Z values, at λ_{ratio} = 1 (λ = 0.5). However even at this setting of λ, high Z values are unlikely to be thrown up at random as they depend on unlikely distributions in the rule table. High Z values may be evolved (see below), but this is not done in the λ_{ratio} - Z graphs.

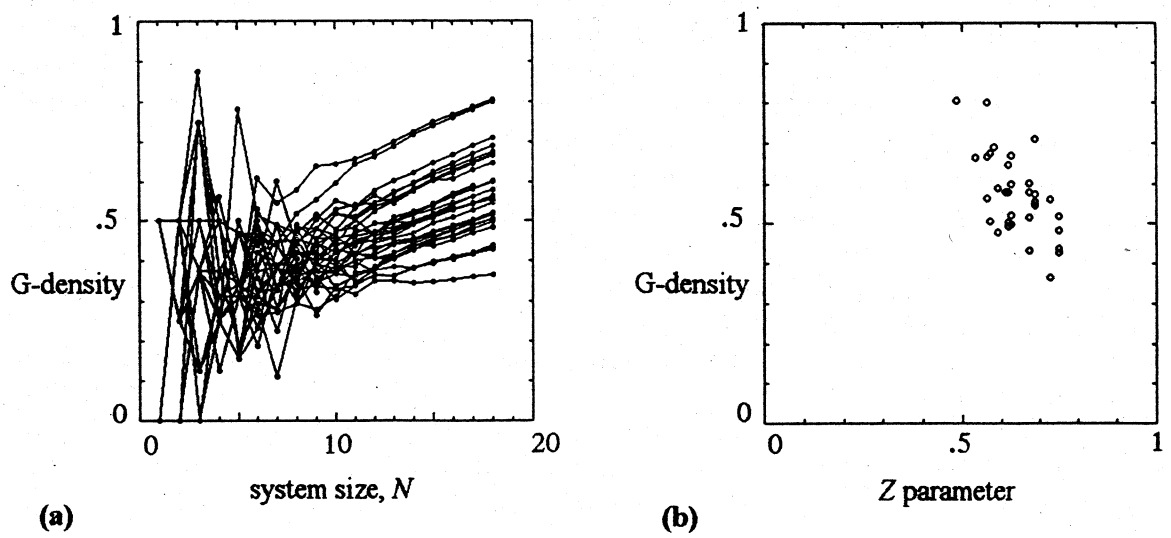

Figure 5.
G-density plotted against **(a)** system size, N, for N=1 to 18 and **(b)** the Z parameter (for N=18), for the sample of 38 complex rules in appendix 2. Graph **(a)** shows superimposed plots for all the rules. Separate graphs for each rule are shown in appendix 2. The G-density is based on the complete basin of attraction field.

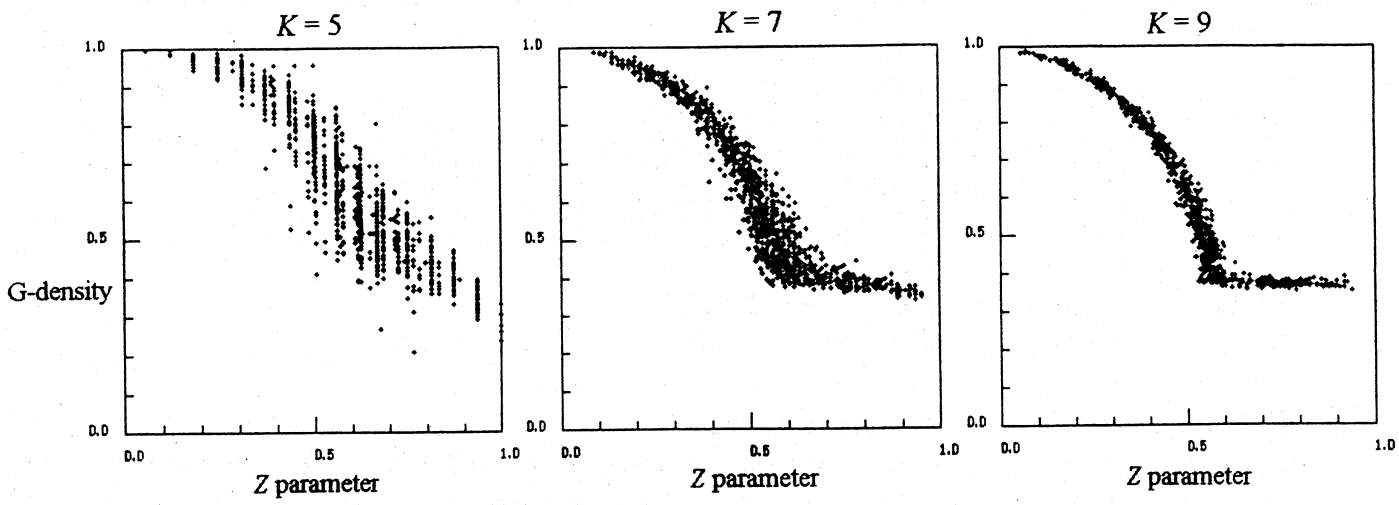

Figure 6.
G-density plotted against the Z parameter for $K5$, $K7$ and $K9$ rules. Each graph shows over 1000 rules chosen at random but biased to include a representative spread of Z values.

The graphs show a cloud of points diverging above the $x=y$ diagonal, closer to it for lower λ_{ratio}, but with $Z \leq \lambda_{ratio}$. The λ_{ratio} - Z relationship is more focused towards the left edge of the cloud for larger K, because higher values of Z are less likely to be thrown up at random in a larger rule-table. For smaller K more points on the graph are superimposed as the values of both Z and λ_{ratio} may take on specific values only, with a smaller range for smaller K.

9. Garden-of-Eden density - variation with system size

The variation of garden-of-Eden density (G-density) against system size, N, as N is increased from 1 to 18 has been plotted for the $K3$ (elementary) rules, the $K5$ totalistic rules, and for the sample of complex rules in appendix 2. For each rule, the complete basin of attraction field was generated for each value of N, and a count made of the number of garden-of-Eden states. These graphs are in appendix 1. A superimposed plot for the sample of complex rules in appendix 2 is shown in figure 5b

The graphs in appendix 1 are presented in order of increasing Z. After an initial unstable phase for low N values, the plot generally stabilises; the G-density increases but to a progressively smaller extent with increased N, possibly to converge asymptotically to a stable value in the limit. Larger systems require testing to confirm this conjecture. Where Z=1 (the limited pre-image rules[21]), the plot behaves exceptionally; generally G-density approaches zero for greater N, or oscillates periodically.

Rules in the same equivalence class have equivalent behaviour and thus identical G-density for a given N. It also appears to be the case that complimentary rules (rule table entries flipped) have identical G-density. Although no proof of this statement is offered, it has been confirmed by many trials. Thus it has been assumed that the same graph showing G-density against N is valid for all rules in a rule cluster[21]. The graphs have therefore been plotted for 48 $K3$ rule clusters and 20 $K5$ totalistic code clusters.

10. Garden-of-Eden Density and the Z parameter

A number of plots of G-density against the Z parameter have been made. Again, for each rule, the whole basin of attraction field was generated. This was plotted against the rule's Z parameter computed from its rule table.

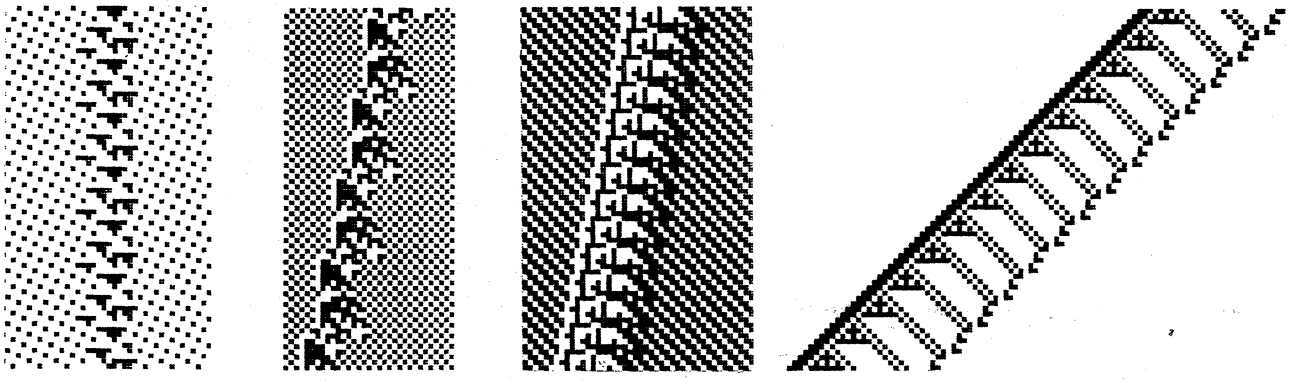

Figure 7.
Gliders with various velocities and their backgrounds. The hex rule numbers and relevant appendix pages are shown.

Appendix 1 shows graphs of G-density against the Z parameter for all $K3$ rules and $K5$ totalistic rules for system size 18. The same plot is shown in figure 5b for the sample of complex rules in appendix 2.

Figure 6 shows three graphs of G-density plotted against the Z parameter for a sample of K=5, 7 and 9 rules. Each sample plots over 1000 rules. The rule sample was biased to include a representative spread of Z values by biasing λ (as described above for the plot of λ_{ratio} against N). However, values in the high ranges of Z had to be evolved. This was done by starting with an unbiased random rule table and flipping (flipping back if necessary) random bits until the required Z parameter threshold was achieved.

The plots produce a characteristic cloud of points with an inverse correlation between G-density and Z, becoming more focused towards the left edge with higher K. The reason for the abrupt change in direction of the cloud at G-density $\approx$ 3.7 and $Z \approx$ 5.5 is unclear. These values probably correspond to the most crowded area of rule-space, at the phase transition between order and chaos. Complex rules are most frequently found in this area.

The intention of these plots was to investigate, for the first time, the characteristic G-density of CA, and how G-density varies with system size. In addition, to what extent Z was able to predict G-density, and thus the convergence of state-space and basin field topology. It is clear that for the vast majority of rules, garden-of-Eden states occupy a high proportion of state-space. Rules with lower Z have higher G-density, increasing with system size at a faster rate. Rules with Z = 0.5 - 0.65, in or near the abrupt change in direction of the cloud of points in the graph, have moderate G-density that increases only slowly with system size, or may even decrease. Rules with high Z have low G-density which decreases with system size, and at a faster rate for higher Z.

How representative these plots are of much larger system sizes is unclear. Although generating the basin field for large systems is impractical, generating a subtree is feasible. The G-density of a subtree may give a good indication of G-density for the field.

11. Complex Rules and Gliders

Whether or not a rule is described as complex has depended to a certain extent on a subjective appraisal of its dynamical behaviour evident in typical space-time patterns. For $K \leq 5$ rules there is a characteristic structure to the pattern, which is recognisable even when space-time patterns appear chaotic. This becomes less obvious for larger K.

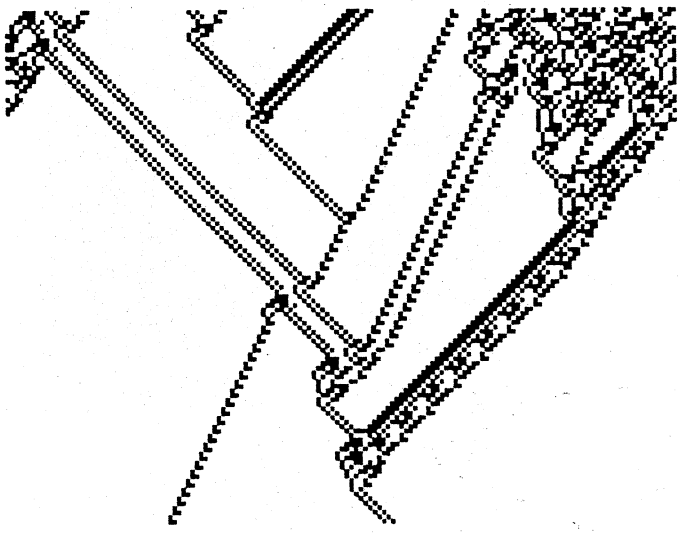

Figure 8.
Glider collisions against a background of all 0s. *K*5 rule 5c 6a 4d 98.
(appendix 2.4).

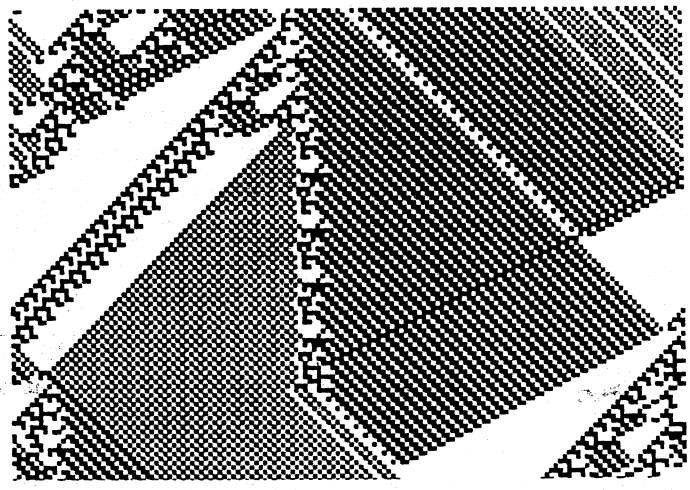

Figure 9.
A glider forming the boundary between two different backgrounds. *K*5 rule bc 82 27 1c.
(appendix 2.9).

Appendix 2 and 3 presents a sample of about 60 complex 1-D rules with glider-like characteristics. These rules where evolved by the method already described, or found by accident. Several are borrowed from other sources[1,10,17,21], or are well-known examples from the literature. Although there are countless such complex rules, they are buried in an even vaster rule-space, and relatively few have been available for study.

Appendix 2 presents 36 rules, each with a typical space-time pattern, 200 cells × 480 time-steps, a detail showing glider collisions, and the basin of attraction field including significant data for a system size 16. Appendix 3 presents 26 further rules, each with a typical space-time pattern, 150 cells × 460 time-steps, showing the lookup frequency histogram and entropy plot along side (described below). The space-time patterns shown were, to a limited extent, selected for an interesting view of glider interactions, by varying the initial random seed. The complex rules in this paper show gliders emerging rapidly in small systems, but other rules that might appear chaotic at this scale may be complex at a larger scale, requiring a longer time for wider gliders to emerge.

What are the essential features of complex one-D CA behaviour based on our sample? Complex dynamics occurs if a limited set of self-sustaining configurations emerge from random initial states, and if the interactions between configurations persist for an extended time before settling into a relatively short

attractor. The configurations are static, or propagate at various velocities up to a maximum, the system's *speed of light*. They exist against a uniform or periodic space-time background which of necessity has simultaneously emerged. The background may be simple such as a checkerboard, or a more complex pattern. For simplicity, I will use the name *gliders* for such self-sustaining configurations, even if the glider has zero velocity.

Although there are borderline cases, complex space-time patterns are generally easily recognised in contrast to patterns that stabilise rapidly to fixed points or short periods on the one hand, or where chaotic patterns persist on the other. The borderline cases verge either on stable or chaotic behaviour. Chaotic behaviour may also contain distinct chaotic backgrounds or domains[3], where *filtering* is required to uncover domain walls analogous to gliders.

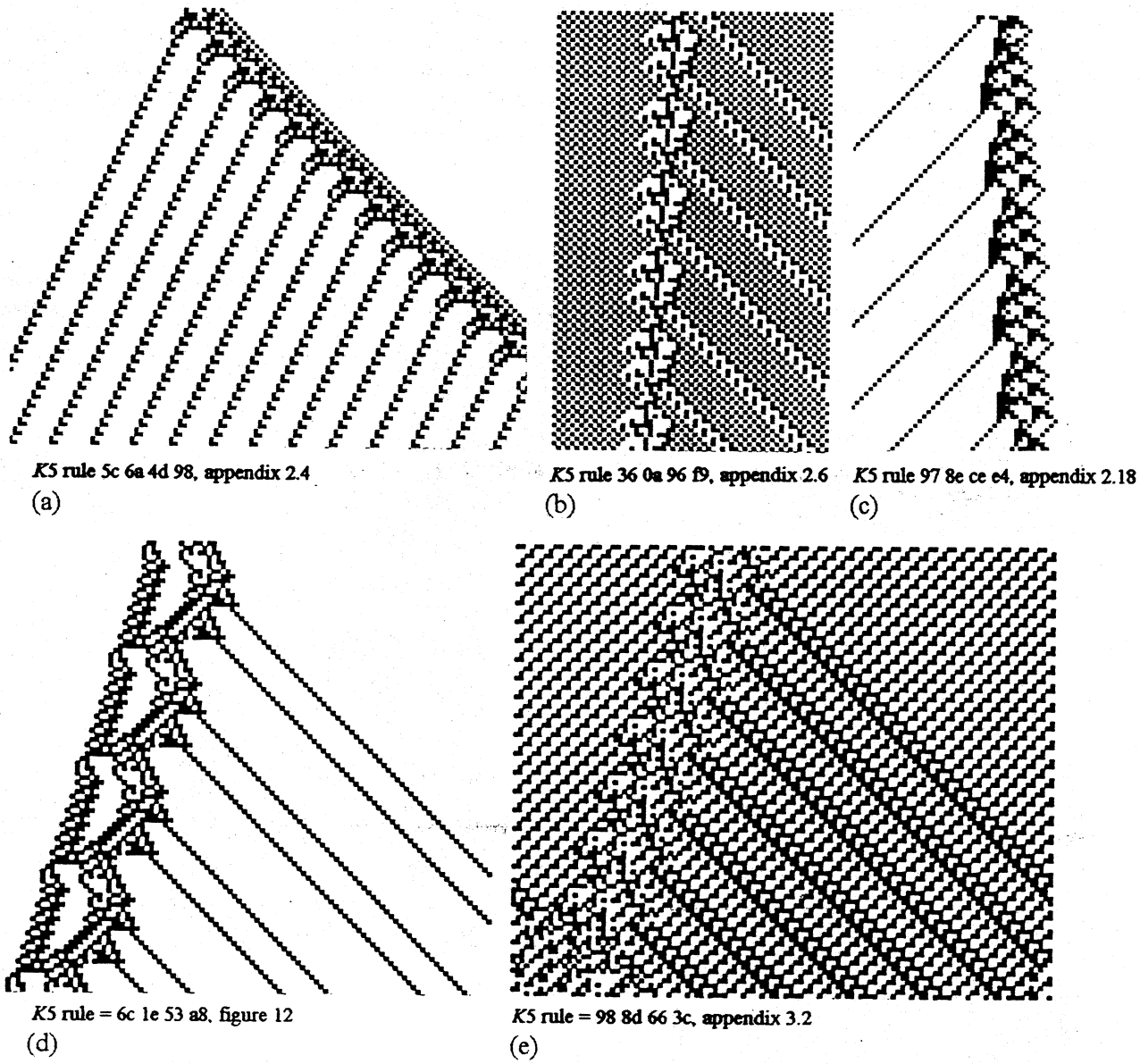

Figure 10.
Examples of glider-guns. The hex rule numbers and relevant appendix pages are shown.

The complex rules (and some borderline cases) in our sample are illustrated in descending order of their Z parameter in appendix 2. As Z increases, the basin of attraction field tends to include larger basins with longer transients, with a lesser degree of pre-imaging and thus smaller G-density. A plot of Z against G-density for system size 18, for all the rules in appendix 2 is shown in figure 5b.

The space-time patterns in appendix 2 and 3 (and extensive simulations) show many examples of gliders within a periodic space-time background or a uniform background. Some examples are given in figure 7. A uniform background (all white or black) has a period of one in both space and time. Gliders my be regarded as solitary waves within the background. Gliders may have the special property of *solitons*[1], preserving their shape after interacting with other solitons. For a neighbourhood radius r, glider velocity varies from 0 to a maximum of r cells per time step towards the left or right. A glider configuration that repeats at each time-step, i.e. with period one, is limited to velocities of $0,1,2,...,r$ per time-step. Gliders with periods greater than one may have intermediate fractional velocities. A glider's attributes are the background pattern and period (on both sides of the glider), the glider's period and velocity, its changing diameter, and the list of its repeating configurations. The same description might be applied recursively to each sub-glider component of a *compound* glider.

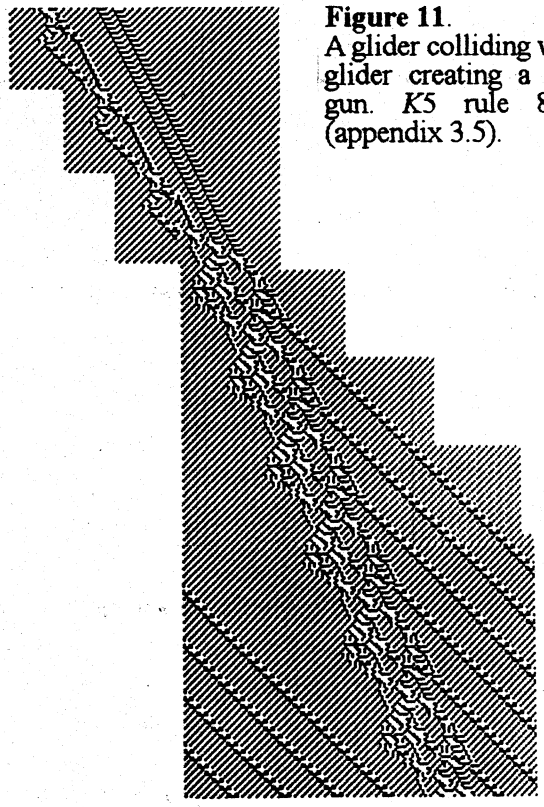

Figure 11.
A glider colliding with a compound glider creating a complex glider-gun. *K*5 rule 89 ed 71 06. (appendix 3.5).

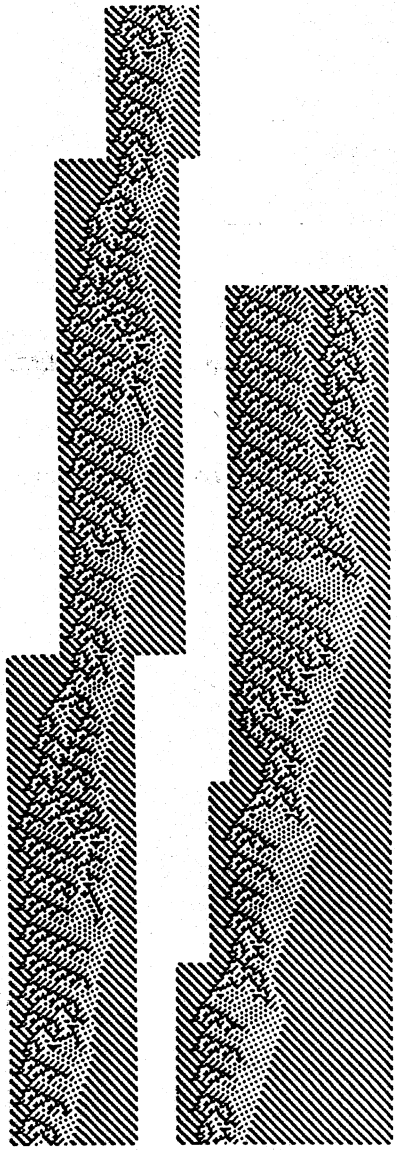

Figure 12.
Far left: a glider with a large diameter and period. The diameter varies between 22 and 42 cells, the period is 402 time-steps. *Left*: a collision between two large gliders creating a third large glider. *K*5 rule 82 26 dc 23 (appendix 3.2).

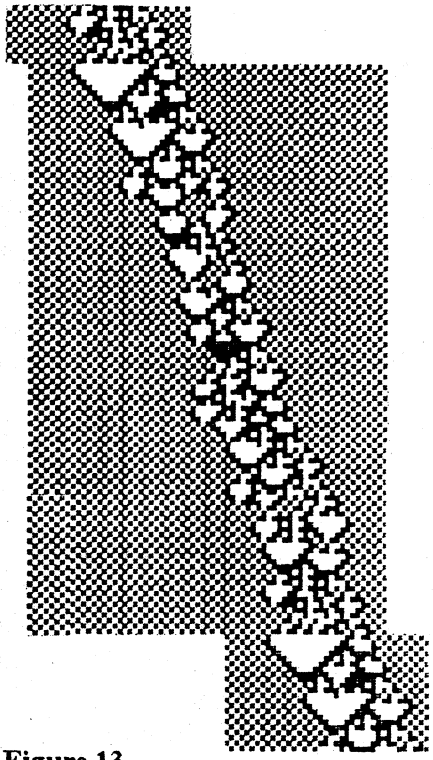

Figure 13.
A glider with a period of 106 time-steps.
*K*5 rule b5 1e 9c e8 (also figure 15)

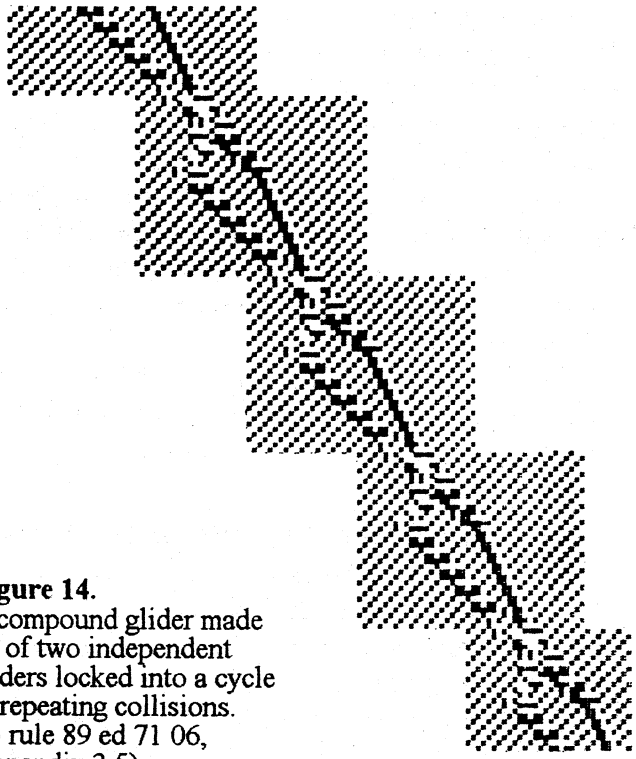

Figure 14.
A compound glider made up of two independent gliders locked into a cycle of repeating collisions.
*K*5 rule 89 ed 71 06, (appendix 3.5).

From an random seed, a limited number of different glider types emerge after an initial *sorting out* phase and continue to interact by collisions for an extended time, for example figure 1. Collisions between two glider types often result in a third glider type (or more). One or both of the gliders may survive a collision with a possible shift in trajectory, or both gliders may be extinguished. Often a collision initially results in a complex interaction phase, before the final outcome emerges. The outcome of a collision is sensitive to the point of impact relative to the space-time period of each glider.

The emergence of gliders implies the emergence of one or more periodic backgrounds. A glider generally represents a dislocation of varying width in the background, which is often out of phase on either side of the glider, analogous to fracture planes in a crystal lattice. Alternatively, a glider may be seen as the zone that reconciles the two areas of out-of-phase background. A glider may separate two entirely different backgrounds, acting as the boundary. The example in figure 9 has three different backgrounds. Gliders that eject a stream more or less complex sub-gliders at regular intervals, as in figure 10, and gliders that survive by absorbing a regular glider stream, as in figure 7d, are relatively common in our sample. They are analogous to *glider-guns* and *eaters* in the *game of life*[2]. Because a regular glider stream is essentially the same as a regular periodic background, a glider-gun creates a background, and a glider-eater absorbs a background. Glider-guns/eaters are thus equivalent to a glider forming the boundary between two backgrounds.

Both the period and diameter of a glider may be considerable. The diameter may show a large variation within the period. The example in figure 13 shows a glider with a period of 106 time-steps. The example in figure 12, shows a the glider with a period of 402 time steps; its diameter varies between 22 and 42 cells. A further example in figure 12 (the same rule) shows a collision between two large gliders creating a third large glider. Obviously such gliders and interactions can only emerge in a large enough system.

The existence of *compound* gliders made up of sub-gliders colliding periodically may be expected in large enough systems. Compound gliders could combine into yet *higher order*[7] gliders, and the process could unfold hierarchically without limit. The example in figure 7d shows a compound glider made from a glider-gun and a parallel glider-eater which absorbs the sub-glider stream; the compound glider can have an arbitrary diameter. A compound glider-gun is shown in figure 10d. Figure 11 shows a compound glider colliding with two simple gliders creating a compound glider-gun. The compound glider is made of two independent gliders locked into a cycle of repeating collisions, a detail is shown in figure 14.

Compound gliders are analogous to the complex glider/gun/eater interactions engineered by Conway to make logical gates and an external memory in his demonstration that the *game of life*[2] is a *universal Turing machine*.

An example of a kind of self-reproduction is seen in rule 3a 48 b5 c4 (appendix 2.6), where gliders eject close mirror image copies of themselves with opposite velocity. A third glider kills off the reproducing gliders, thus checking overcrowding.

12. Neighbourhood lookup frequency and entropy

Gliders and backgrounds are built from a set of self sustaining configurations that emerge from an initial chaotic phase, crowding out all the other many possible configurations, to dominate the CA's future space. An initial random seed contains all 2^K K-neighbour configurations with equal probability. It is likely to be a garden-of-Eden state, because as has been shown experimentally, garden-of-Eden states usually make up a large proportion of state space.

As the CA evolves through the initial sorting out phase, some neighbourhoods will feature more frequently, others less. The frequency that each of the neighbourhoods in the rule-table is "looked up" at a given time-step can be represented by a histogram, or lookup spectrum, as in figure 15, which distributes the total of N lookups among the 2^K neighbourhoods (shown as the fraction of maximum lookups N, where N=system size, K=neighbourhood size). The entropy of the lookup histogram, S, at time-step t is given by,

$$S^{(t)} = -\sum_{i=1}^{2^K} \left(Q_i^{(t)} / N \times \log \left(Q_i^{(t)} / N \right) \right)$$

Where $Q_i^{(t)}$ is the lookup frequency of neighbourhood i at time t.

Figure 15 shows two complex rules as set out in appendix 3. This illustrates a typical lookup frequency histogram of the very last time-step A *superimposed* frequency spectrum (2^K points corresponding to the histogram values) is plotted alongside each time-step in the space-time pattern. The entropy of the lookup frequency spectrum is also shown for each time step on the same graph.

Because the initial state is set at random, the 2^K points in the lookup frequency histogram will be distributed close together at low values, corresponding to an equal probability of all neighbourhoods; the entropy will be correspondingly high. The evolution of the frequency spectrum for successive iterations of the CA, and the frequency spectrum entropy, is characteristic of the quality of the dynamics.

In simple behaviour the frequency spectrum will rapidly become highly unbalanced, with most neighbourhoods never looked at (their lookup frequency = 0); the few remaining high frequencies settle on constant or periodic values; the entropy will settle at a low constant or periodic value, corresponding to a fixed point or short cycle attractor. Simple behaviour produces extremely short and bushy transient trees with a high G-density.

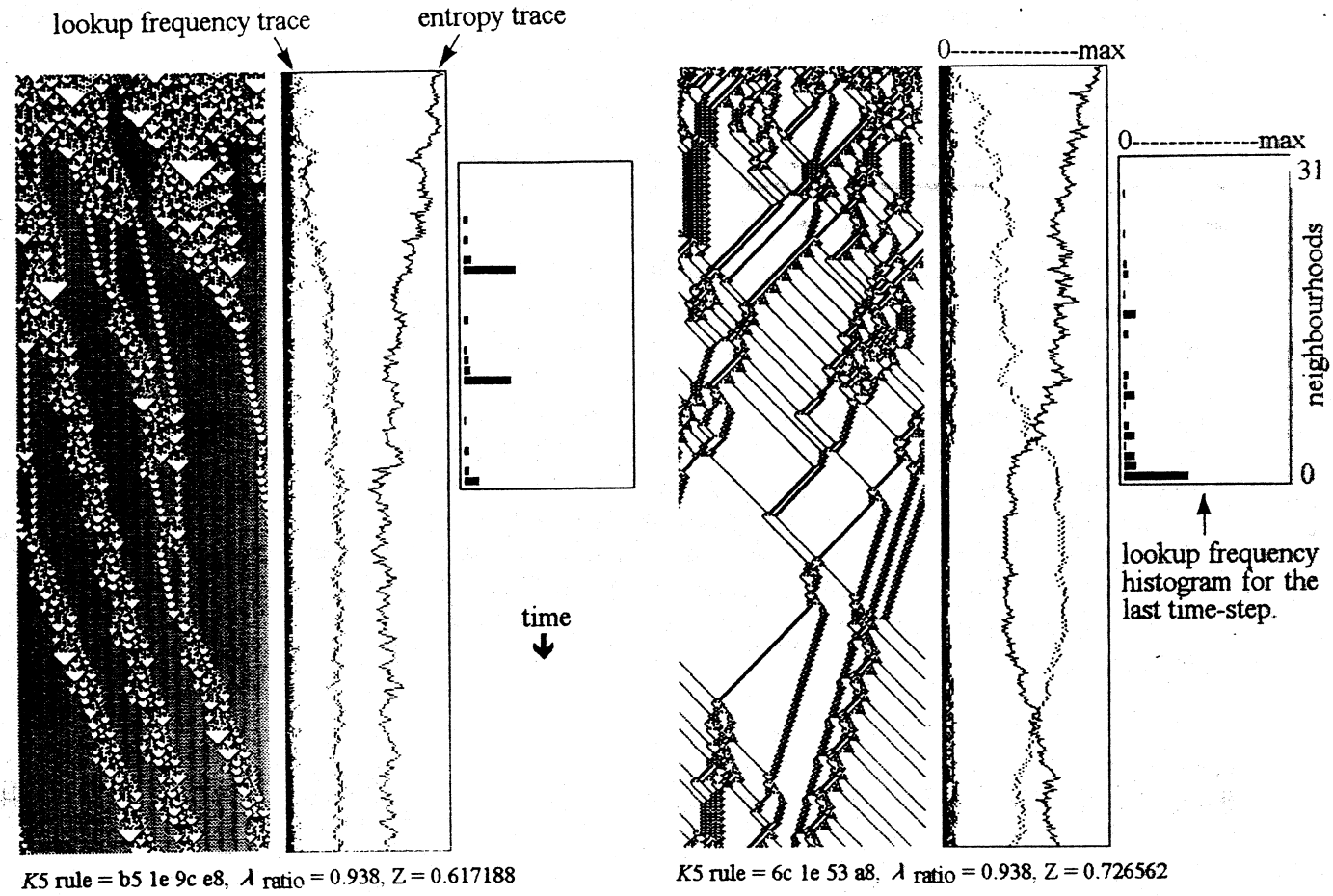

Figure 15.
Two examples of complex space-time patterns as presented in appendix 3. System size 150 with periodic boundary conditions. 460 time-steps from a random seed. An example of the lookup frequency histogram is shown for the last time-step. A *superimposed* frequency spectrum is plotted alongside each time-step, with 2^K points corresponding to the histogram values; the entropy at each time-step is also shown on the same plot. Rule numbers are shown in hex.

In chaotic behaviour, the frequency spectrum will fluctuate chaotically at low values, and the entropy will fluctuate chaotically within a narrow high band, corresponding to dynamics on very long transients or cycles, analogous to strange attractors in continuous dynamical systems. The very long and sparse transient trees have a low branching incidence and low G-density.

In complex behaviour, the frequency spectrum becomes unbalanced, breaking up into high and low strands that exhibit large chaotic fluctuations, reflected in large chaotic fluctuations in entropy. The distinct characteristics of these measures could form the basis of an automatic procedure for identifying complex rules. As in simple behaviour, a proportion of neighbourhoods is never looked at again after the initial sorting out phase; these neighbourhoods are, in a sense, leached out of the system. After an

extended time, (100s or 1000s of time-steps) the system settles onto a short attractor cycle. The high strands in the superimposed frequency spectrum are the frequencies of the emergent background (or multiple high strands for multiple backgrounds). The low strands are the frequencies of interacting gliders. Glider interactions sometimes produce a short-lived chaotic phase after which glider dominance is re-established.

In the sample of complex rules in appendix 3, the entropy of the lookup frequency histogram is shown alongside each time-step. The entropy starts off high for the random seed and the initial sorting out phase. It then fluctuates erratically at a lower level during the glider interaction phase, and settles at a periodic or constant minimum level at the attractor cycle.

13. Glider interactions and basins of attraction

It is possible to identify classes of configurations that make up different components of the basin of attraction field in complex CA. In states chosen at random, all configuration occur with equal probability, including potential background and glider configurations. Such randomly chosen states make up the majority of state space, and correspond to garden-of-Eden states, or states just a few steps forward in time from garden of Eden states. They occur in the initial sorting out phase of the dynamics and appear as short bushy dead end side branches along the length of long transients, as well as at their tips.

States dominated by glider and background configurations are special cases, thus a small subcategory of state-space. They constitute the glider interaction phase, making up the main lines of flow within the long transients. Gliders in the interaction phase can be regarded as competing sub-attractors, with the final survivors persisting in the attractor cycle. A detail of a typical transient tree of a complex rule is shown in figure 16.

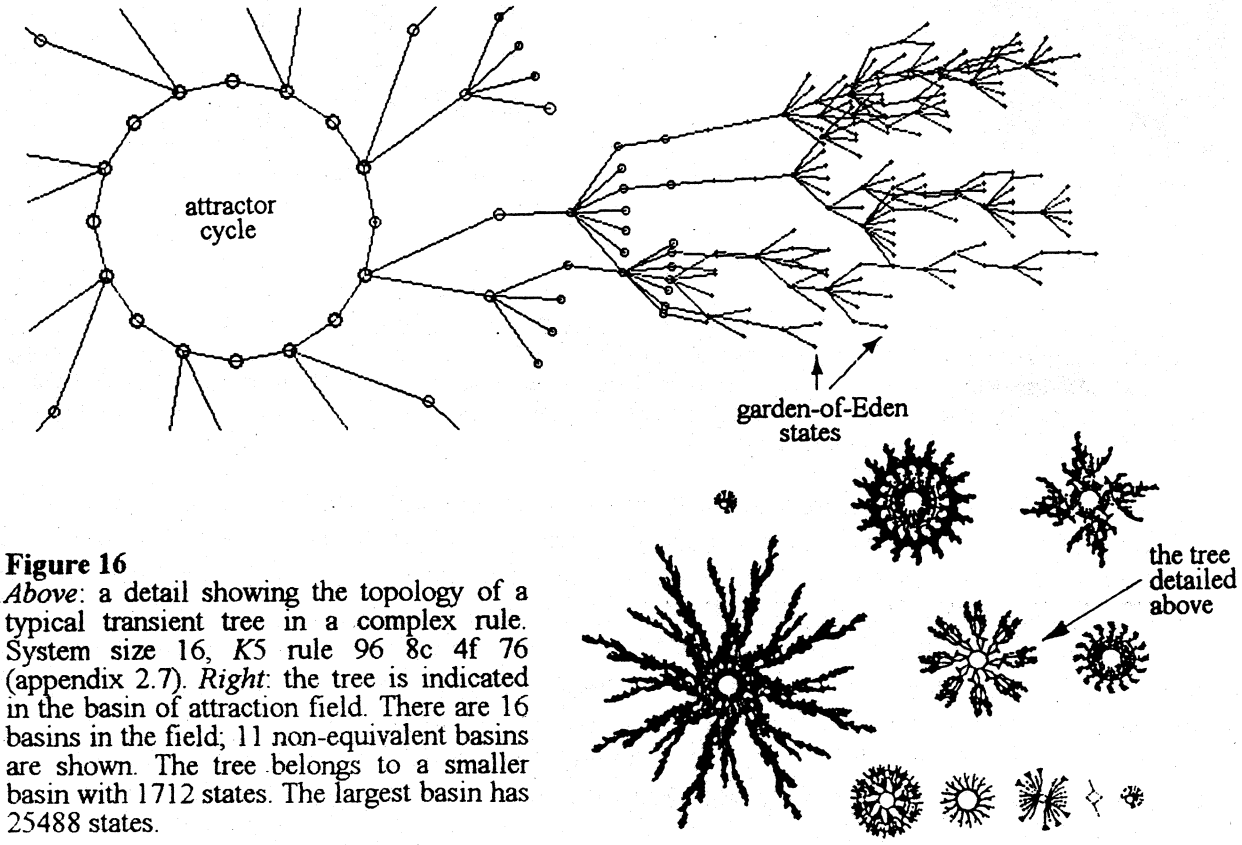

Figure 16
Above: a detail showing the topology of a typical transient tree in a complex rule. System size 16, *K*5 rule 96 8c 4f 76 (appendix 2.7). *Right*: the tree is indicated in the basin of attraction field. There are 16 basins in the field; 11 non-equivalent basins are shown. The tree belongs to a smaller basin with 1712 states. The largest basin has 25488 states.

Finally, states made up solely of non-interacting gliders configurations (i.e. having equal velocity), or backgrounds free of gliders, must cycle and therefore constitute the relatively short period attractors. Attractor states themselves are a small subcategory of possible glider/background configurations, and thus form a tiny subcategory of state-space. By simply looking at the space-time patterns of a complex rule from a number of different seeds, most gliders in its glider repertoire (relative to the system size) may be identified. A complete list would allow a complete description of all the attractors in state-space, by finding all possible permutation of non-interacting gliders.

14. Summary and Discussion

This paper describes the emergence and interactions of gliders in one-D CA on the basis of a relatively large sample of so called complex rules. Gliders propagate and collide against a uniform or periodic background; new gliders may emerge from glider collisions. Gliders may eject and/or absorb regular streams of sub-gliders, or spontaneously combine to form compound gliders.

Gliders may be viewed from many perspectives: as dislocations in the background analogous to fracture planes in a crystal lattice, as solitary waves, as particles, as structures that convey information, or as periodic sub-attractors analogous to auto-catalytic sets. Gliders forming the boundary between different backgrounds are equivalent to glider-guns, or glider-eaters. For a set of gliders to emerge and interact for an extended time, a rule must be finely balanced between order and chaos. This is reflected in the evolution of the lookup frequency spectrum, and its entropy.

A global perspective on CA dynamics and rule-space is provided by the notion of the basin of attraction field. The topology of basins of attraction and sub-trees, and the degree of convergence of state-space, ties in with the quality of CA dynamics, simple-complex-chaotic, seen in space-time patterns. Complex dynamics achieves a fine balance between high and low convergence. The Z parameter predicts the degree of convergence, which is measured by the garden-of-Eden density. The basin of attraction fields of complex rules are typically composed of a small number of basins with long, moderately bushy, transients trees rooted on short attractor cycles. Glider interactions belong to the main lines of flow within the transient trees. Configurations where gliders have ceased to interact make up the attractor cycles.

Gliders seem to be central to our perception of complexity in CA. We perceive gliders as having a distinct identity. Their interactions are predictable. A collision-table could be formulated empirically, without knowing the underlying rule-table mechanism. The collision-table would probably need to hold much more information than the rule-table. It would need to describe all possible permutations of collisions at different points of impact between gliders in a given complex CA rule. However, compared to the rule-table, the collision table would provide a far more useful description of *established* behaviour, enabling some prediction of future evolution. On the other hand only the rule-table can account for the *origins* of gliders, their emergence by a process of self-organisation from random patterns.

Interacting gliders may combine to create compound gliders, interacting at yet higher levels of description. A collision table of compound gliders might provide a useful description of established *higher* level behaviour with scant knowledge of the underlying sub-glider collisions rules. Compound gliders could combine into yet higher order gliders, and the process could unfold hierarchically without limit in large enough systems. This is analogous to describing matter in terms of chemistry as opposed to the underlying sub-atomic particles, or in terms of biology as opposed to the underlying chemistry. There are any number of further analogies that might be drawn from nature or society. However, the *origins* of the higher level entities must refer to the lower level. A system's complexity may be the extent to which it is able to support such a hierarchy of levels of description. One-D CA provide the simplest possible system supporting such complexity.

15. Acknowledgements

My thank to Chris Langton, Joshua Smith, Phil Husbands and Guillaume Barreau for suggestions and comments.

16. The Software

The software used for the examples, figures and data in this paper was based partly on developments of software included with *The Global Dynamics of Cellular Automata*[21], and on new software. The software runs on PCs, a version for the Sun is under development. Those interested in obtaining the latest version of the software should contact the author.

17. References

1. Aizawa,Y., I.Nishikawa and K.Kaneko, (1990) "Soliton Turbulence in One-Dimensional CellularAutomata", *Physica D* 45, 307-327.
2. Conway,J.H., (1982) "What is Life?" in *Winning ways for your mathematical plays*, Berlekamp,E, J.H.Conway and R.Guy, Vol.2, chap.25, Academic Press, New York.
3. Crutchfield,J.P and J.E.Hanson, (1993) "Turbulent Pattern Bases for Cellular Automata", Santa Fe Instiute Technical Report SFI 93-03-010, to appear in *Physica D*.
4. Gutovitz,H.A, (1991) "Transients, cycles, and complexity in cellular automata", *Physical Review A*, Vol.44, No.12.
5. Gutovitz,H.A, Ed., (1991) *Cellular Automata, Theory and Experiment*, MIT press.
6. Kauffman,S.A., (1993) *The Origins of Order, Self-Organization and Selection in Evolution*, Oxford University Press.
7. Langton,C.G, (1986) "Studying Artificial Life with Cellular Automata", *Physica D*, 22, 120-149.
8. Langton,C.G, (1990) "Computation at the Edge of Chaos: Phase Transitions and Emergent Computation", *Physica D*, 42, 12-37.
9. Li,W., and M.G.Nordahl, (1992) "Transient Behaviour of Cellular Automata Rule 110". Santa Fe Institute Working Paper 92-03-016.
10. Li,W., (1989) "Complex Patterns Generated by Next Nearest Neighbors Cellular Automata", *Comput.& Graphics* Vol.13, No.4, 531-537.
11. Lindgren,K., and M.G.Nordahl, (1990) "Universal Computation in Simple One-Dimensional Cellular Automata". *Complex Systems*, 4, 298-318.
12. Vichniac,G.Y. (1990) "Boolean derivatives on Cellular Automata", *Physica D* 45, 63-74.
13. Walker,C.C., and W.R.Ashby, (1966) "On the temporal characteristics of behavior in certain complex systems", *Kybernetik* 3 , 100-108
14. Walker,C.C., (1971) "Behavior of a class of complex systems: the effect of system size on properties of terminal cycle", *Cybernetics*, 55-67
15. Wolfram,S., "Statistical mechanics of cellular automata", *Reviews of Modern Physics*. vol 55, no.3 (1983) 601-64.
16. Wolfram,S., "Universality and complexity in cellular automata", *Physica D*,vol 10D (1984), 1-35.
17. Wolfram,S., ed. (1986a) *Theory and Application of Cellular Automata"*, World Scientific, 1986.
18. Wolfram,S., ed. (1986b) Random sequence generation by cellular automata", *Adv. Applied Math.* 7, 123-169.
19. Wolfram,S., (1985) "Twenty problems in the theory of cellular automata", *Physica Scripta*. Vol.T9, 170-183.
20. Wooters,W.K., and C.Langton, (1990) "Is there a sharp Phase transition for deterministic cellular automata?", in: *Proceedings of the 1989 Cellular Automata Workshop, Santa Fe Institute, Physica D*.
21. Wuensche,A., and M.J.Lesser. *"The Global Dynamics of Cellular Automata; An Atlas of Basin of Attraction Fields of One-Dimensional Cellular Automata"*, (diskette included), Santa Fe Institute Studies in the Sciences of Complexity, Reference Vol.I, Addison-Wesley, (1992).
22. Wuensche,A. "The Ghost in the Machine; Basin of Attraction Fields of Random Boolean Networks", in *Artificial Life III*, ed C.G.Langton, Santa Fe Institute Studies in the Sciences of Complexity, Addison-Wesley, (1993)

Appendix 1 - Garden-of-Eden density/ System size graphs

K=3 rules. (*K*=5 totalistic rules, page 1.4)

The garden of Eden density (G-density) is plotted against system size, *N*, as *N* is increased from 1 to 18. The rules in a rule cluster[21] have equivalent G-density, so the graphs have therefore been plotted for 48 *K*3 rule clusters. The clusters are ordered by the Z parameter (which is indicated) and secondly by the lowest rule number, in the top left hand corner of each cluster. The plots are based on the complete basin of attraction field for each value of *N*.

Below right are graphs of G-density against the *Z* parameter for all *K*3 rules and *K*5 totalistic rules for *N*=18. The rules in a rule clusters have equivalent *Z*.

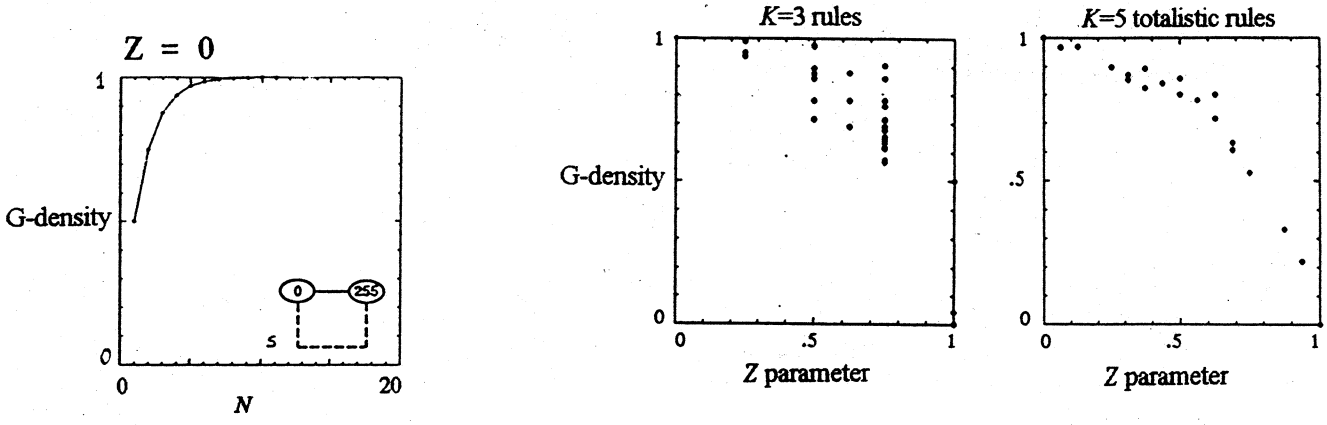

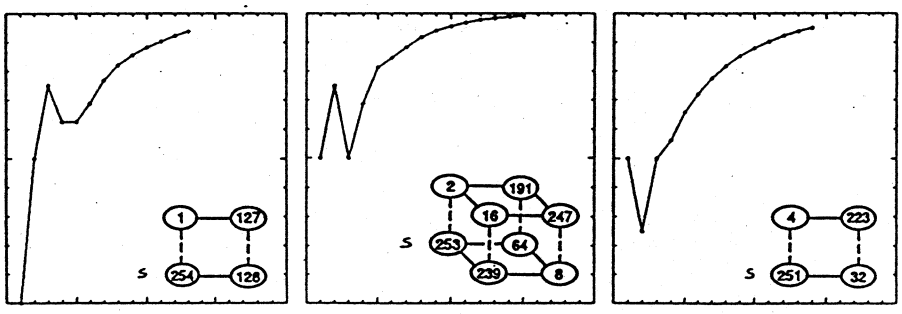

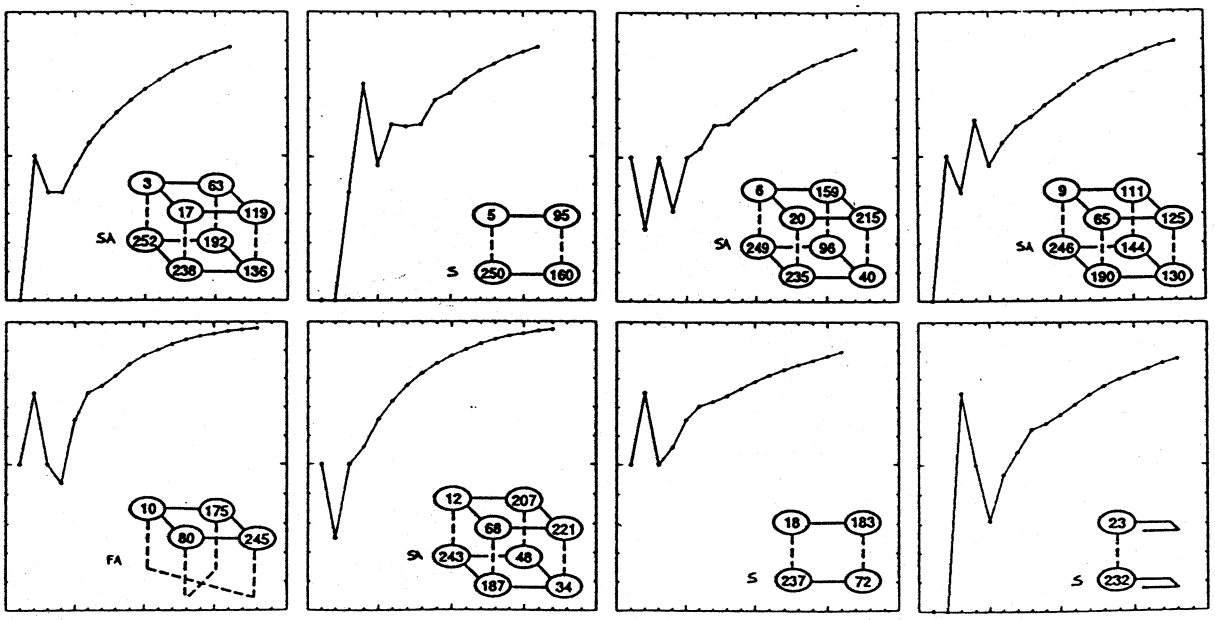

K=3 rules. G-density plotted against system size, N, for N=1 to 18 continued...

Z = 0.5 *continued*

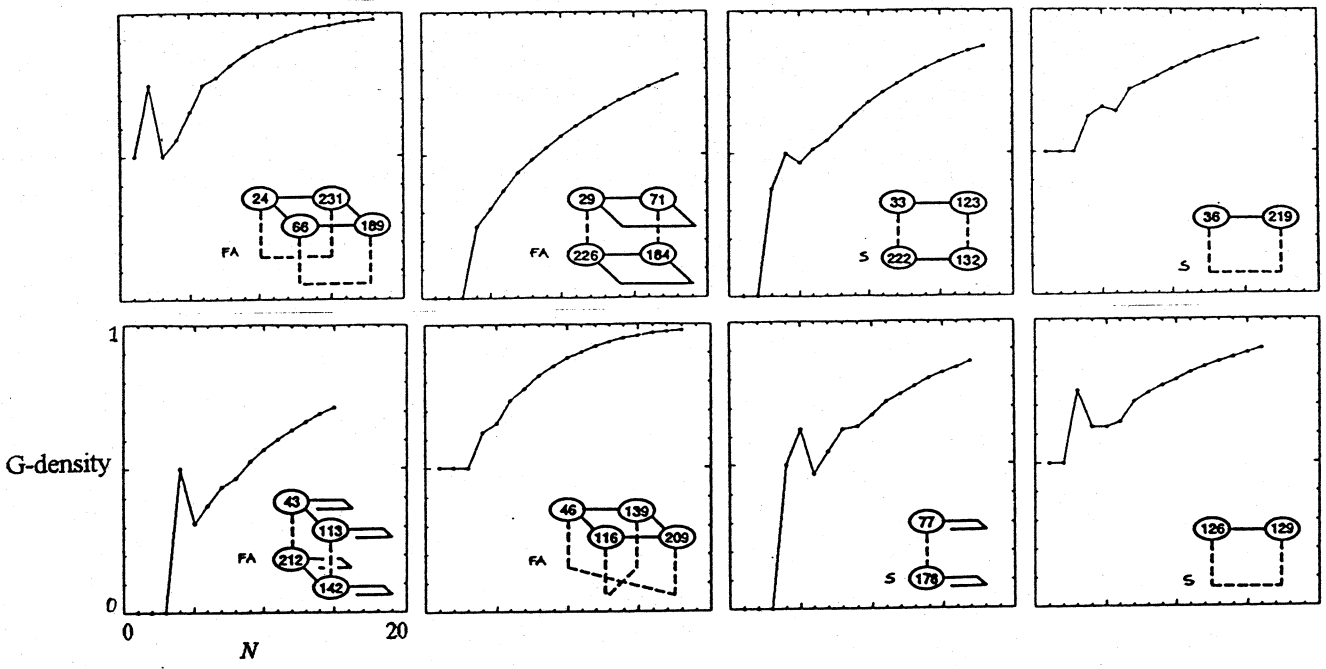

Z = 0.625

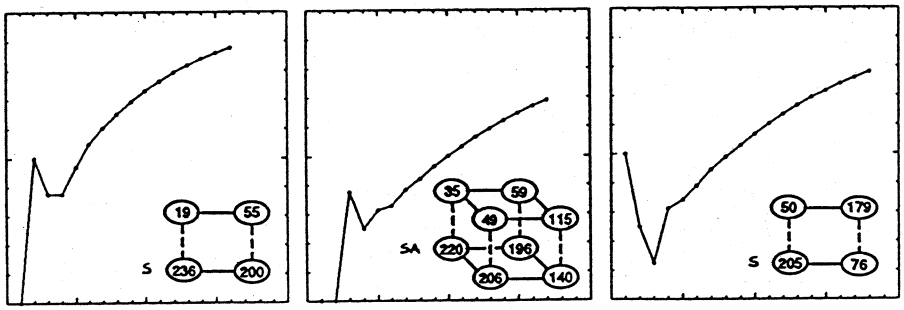

Z = 0.75

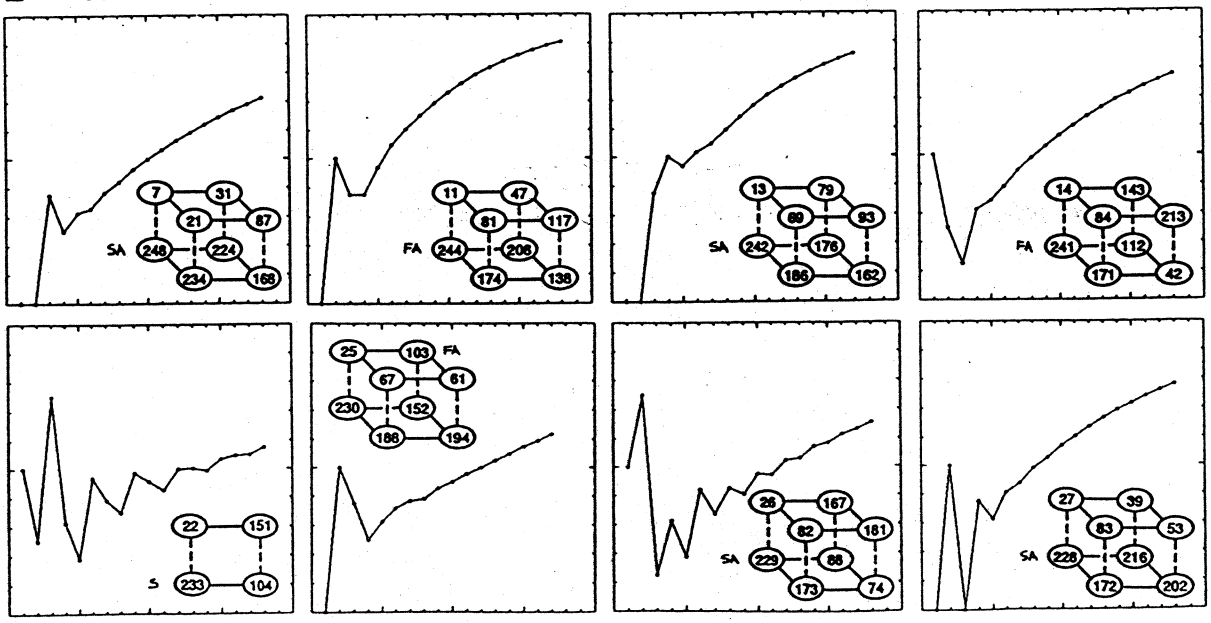

G-density plotted against system size, N, for N=1 to 18 continued...

Z = 0.75 *continued*

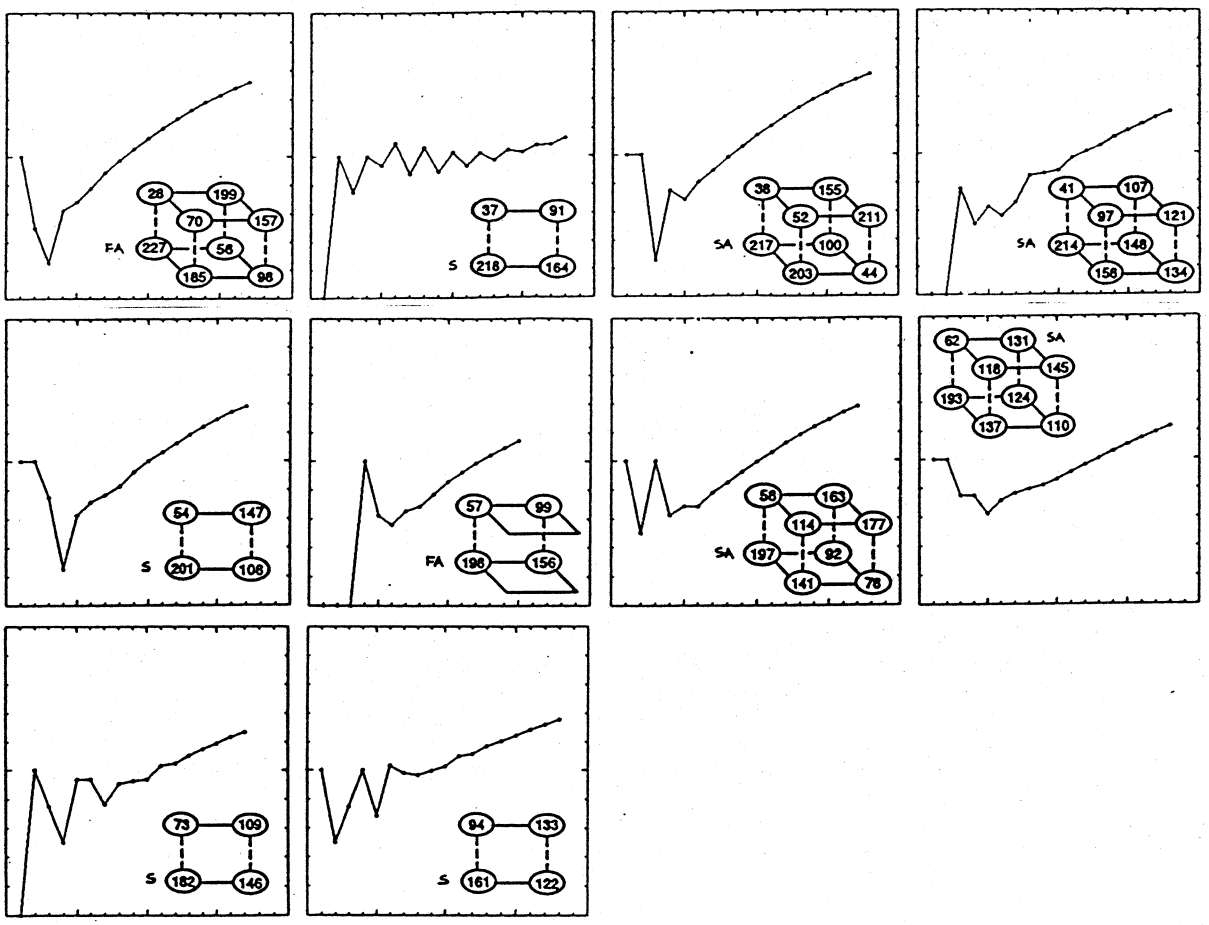

Z = 1

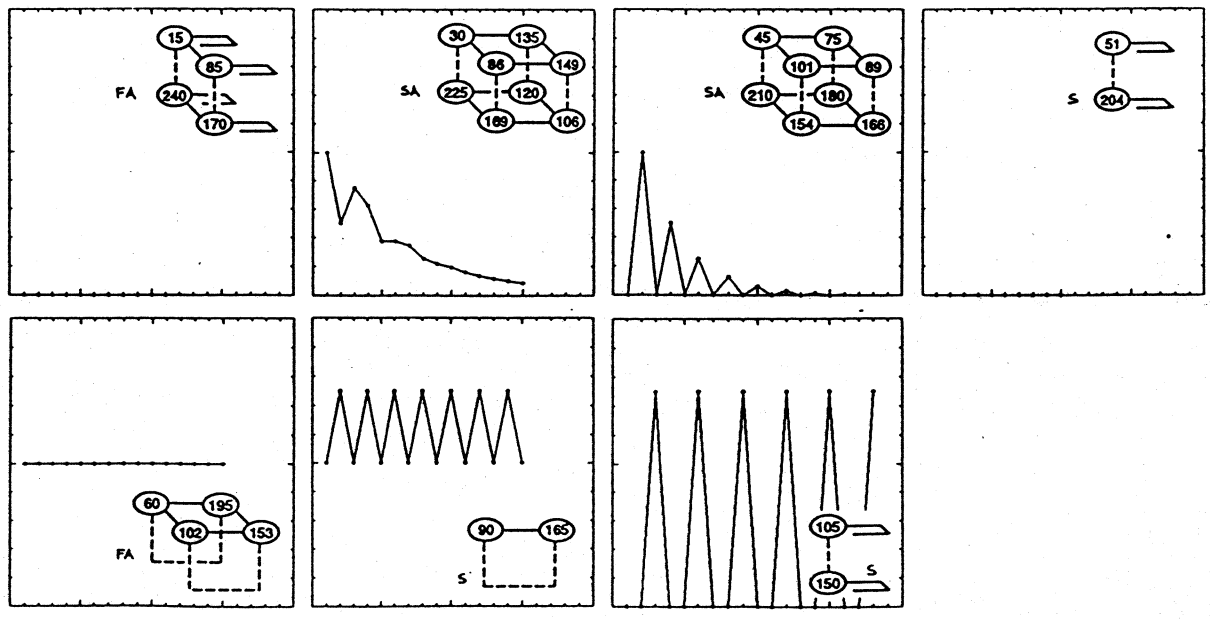

K=5 totalistic rules.

The garden of Eden density (G-density) is plotted against system size, *N*, as *N* is increased from 1 to 18. The rules in a rule cluster[21] have equivalent G-density, so the graphs have therefore been plotted for 20 *K*5 totalistic rule clusters. Totalistic rules are identified by their totalistic code[16,21]. The clusters are ordered by the Z parameter (which is indicated) and secondly by the lowest code number, in the top left hand corner of each cluster. The plots are based on the complete basin of attraction field for each value of *N*.

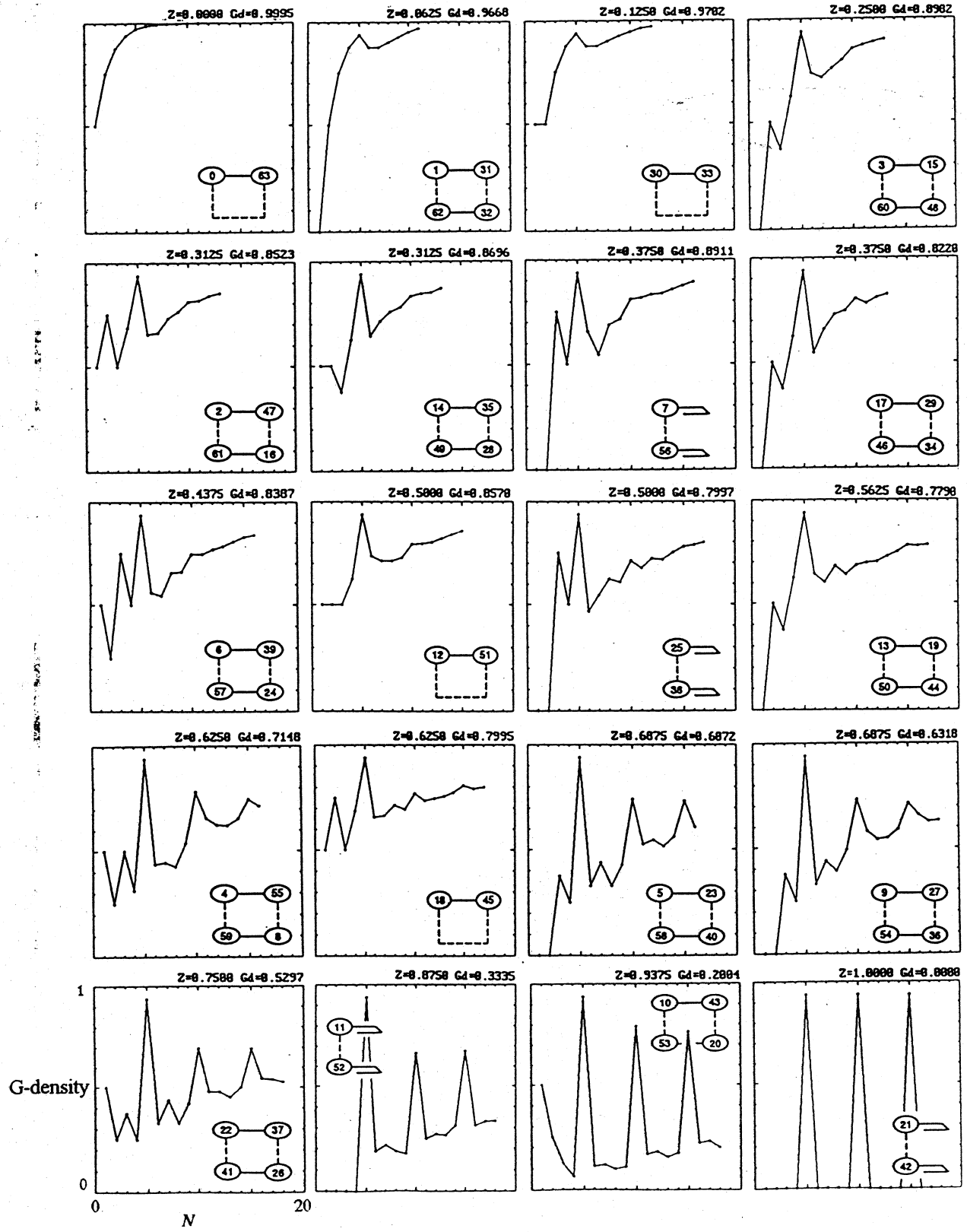

Appendix 2 - Sample of complex rules, K=5,

Space-time patterns and the basin of attraction field.

The following characteristics of behaviour are illustrated in appendix 2 for each rule in the sample. A typical space-time pattern, a detail showing glider interactions, the basin of attraction field, data relating to the field, and a graph of G-density against increasing system size. A typical layout from appendix 2 is annotated below.

1. A typical space-time pattern form a random seed, system size 200 with periodic boundary conditions, 480 time-steps from the top down.

2. The basin of attraction field[21] for system size 16. Only one example of each equivalent basin is shown.

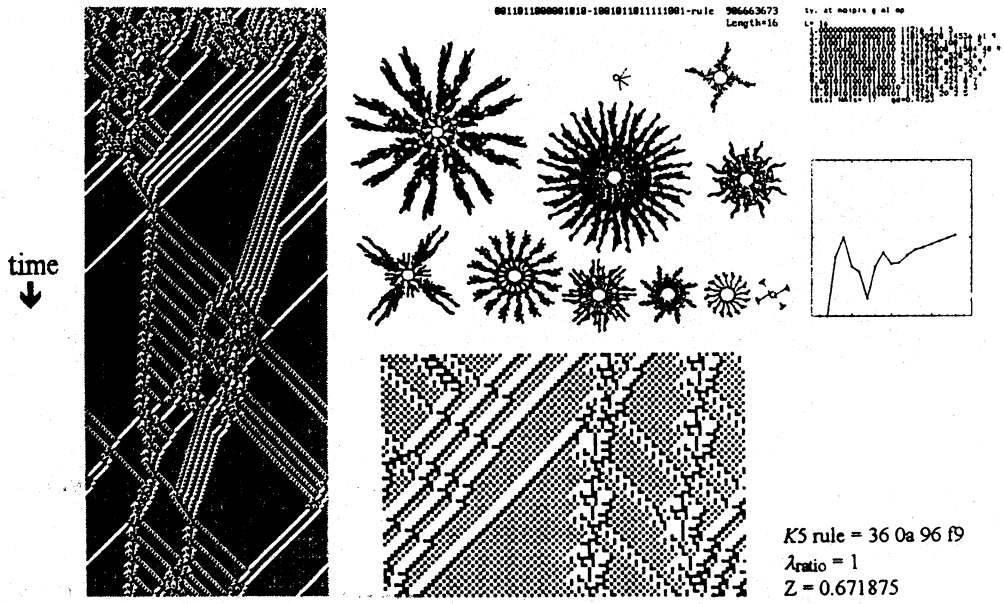

3. Data on the basin of attraction field[21] Key to data below.

4. Graph of G-density (y-axis, 0-1) against system size from 1 to 18. The x-axis is scaled 0-20.

*K*5 rule = 36 0a 96 f9
λ_{ratio} = 1
Z = 0.671875

5. The rule number in hex, the λ_{ratio} and Z parameter.

6. An evolved space-time pattern, (3 times the scale of 1) showing a detail of typical glider interactions. System size 100, periodic boundary conditions.

Key to data

```
!  ty. at no(p)s g ml mp
L= 16
1.0000000000000000 1(2)6 4 1 5
2.1000011010000110 1(8)30928 14536 61 9
3.0100110010110100 4(16)220 108 11 5
4.1010000110101010 1(16)23808 11584 48 9
5.0101010010110101 2(16)1136 528 16 7
6.0010101000101010 2(8)1972 892 30 9
7.0101101010001010 1(16)2064 992 20 6
8.1001100010011000 1(16)568 232 12 4
9.0010101001011010 2(16)448 224 8 7
10.0111110101100010 1(32)144 64 4 3
11.0101010101010101 1(2)26 20 2 5
total NATs= 17   gd=0.4753
```

system size, 16 cells →

reminder of data order relating to each equivalent basin of attraction type.

ty. - equivalent basin type.
at. - an attractor state.
no. - number of equivalent basins.
(p) - attractor period
s - total states in the basin
g - total garden-of Eden states in the basin.
ml - maximum length of longest transient.
mp - maximum pre-imaging.

total number of basins in the basin of attraction field.

gd - garden-of Eden density of the basin of attraction field.

Appendix 2.2 *Andrew Wuensche*

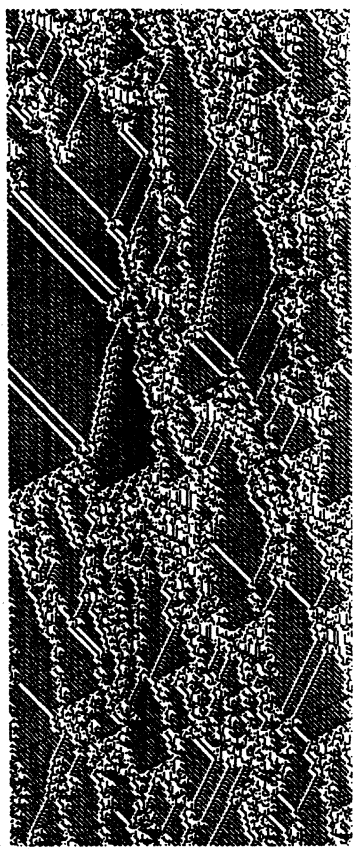

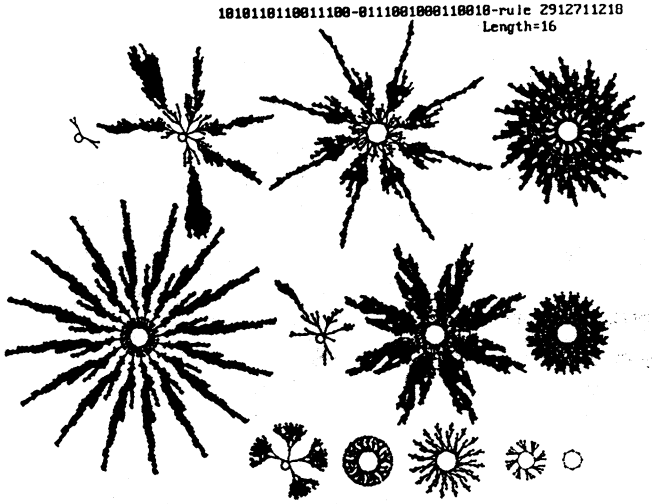

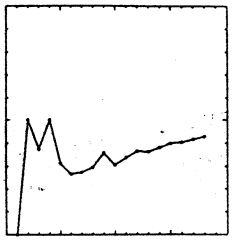

*K*5 rule = ad 9c 72 32
λ_{ratio} = 1
Z = 0.75

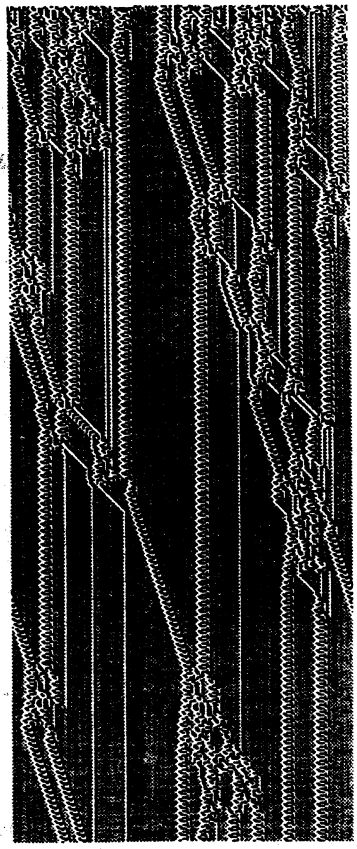

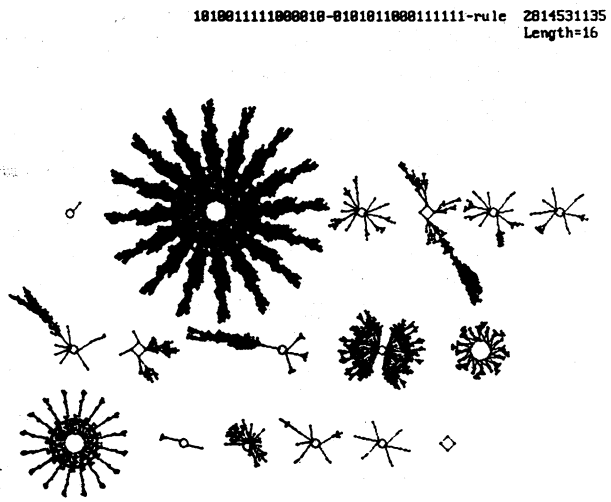

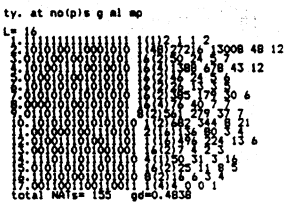

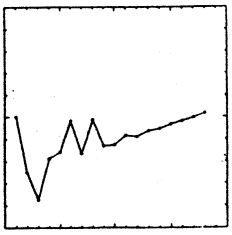

*K*5 rule = a7 c2 56 3f
λ_{ratio} = 0.875
Z = 0.75

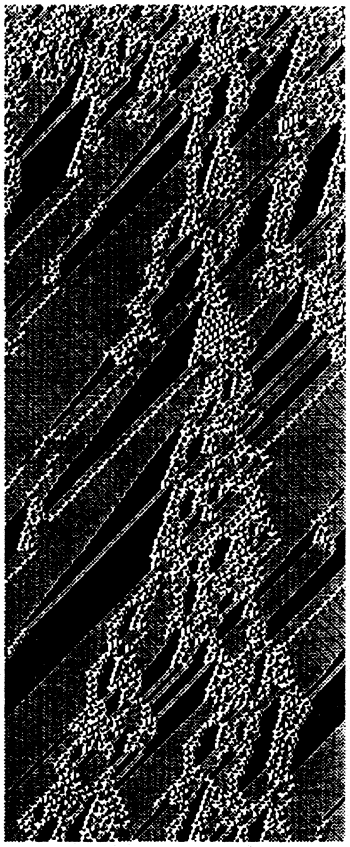

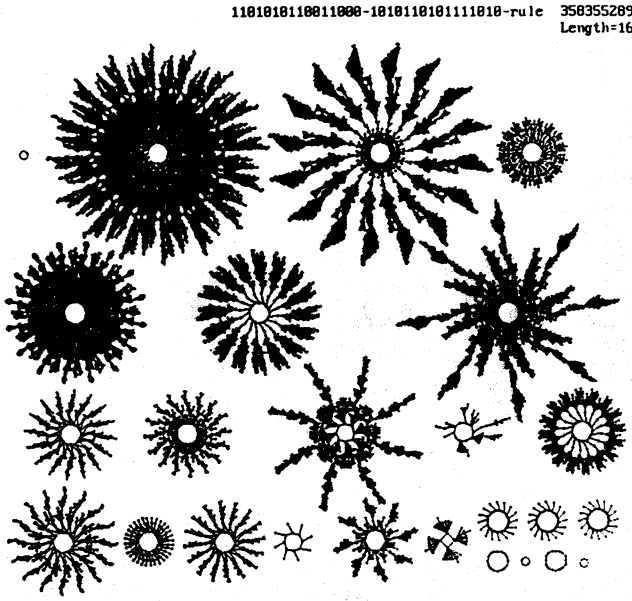

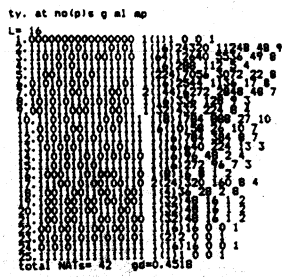

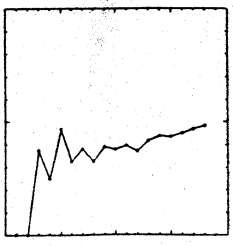

$K5$ rule = d5 98 ad 7a
λ_{ratio} = 0.875
Z = 0.75

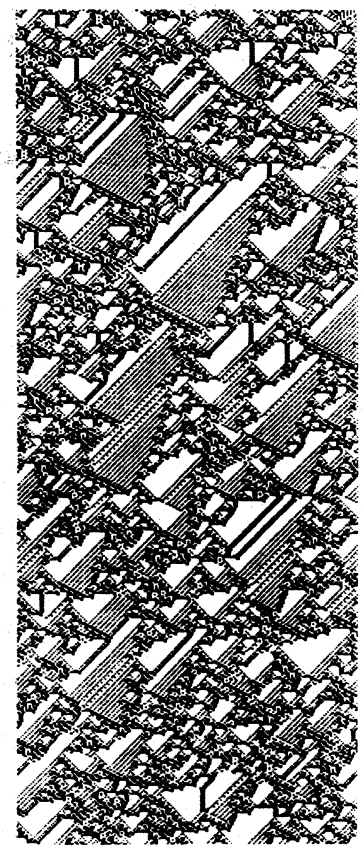

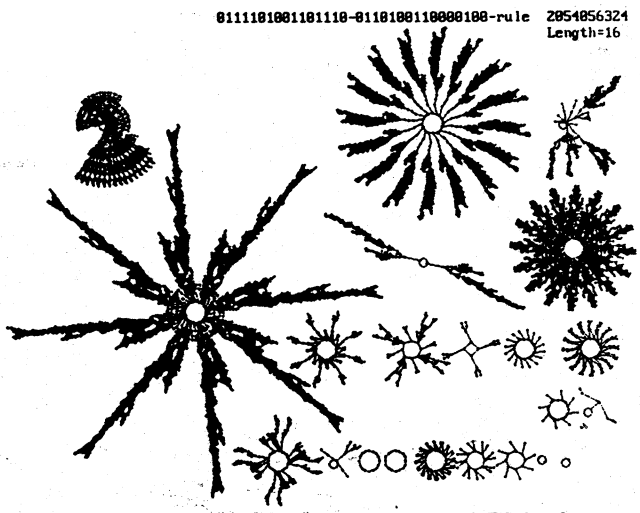

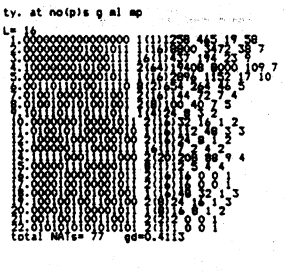

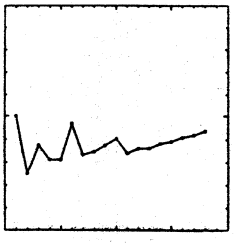

$K5$ rule = 7a 6e 69 84
λ_{ratio} = 1
Z = 0.75

Appendix 2.4 *Andrew Wuensche*

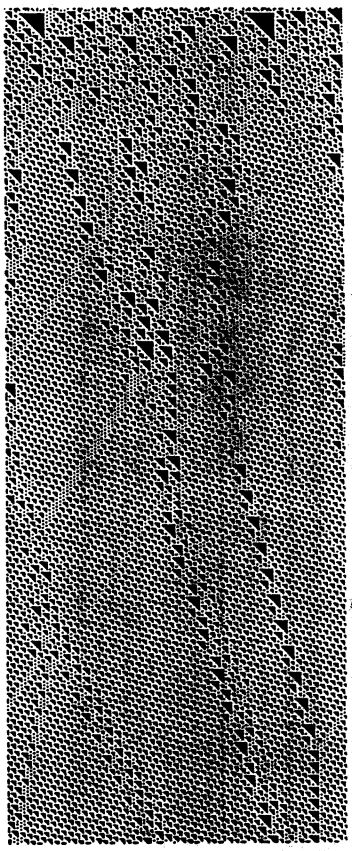

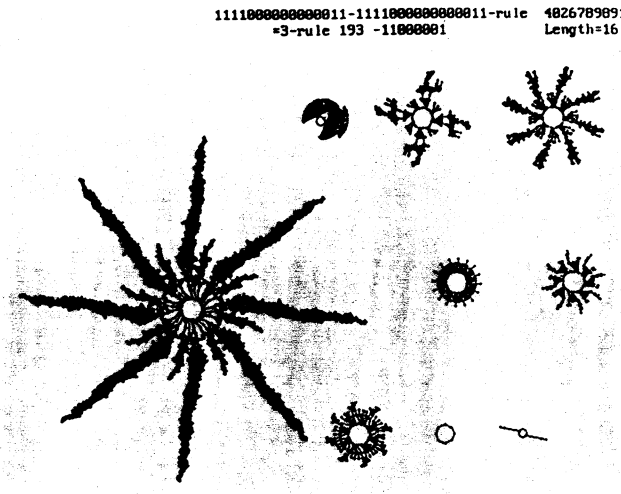

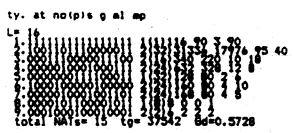

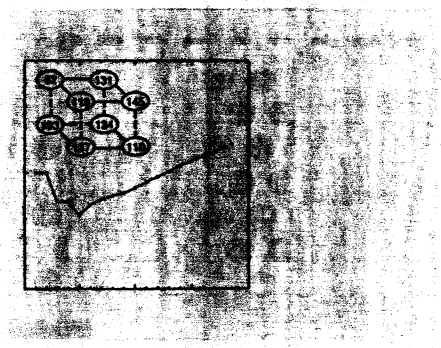

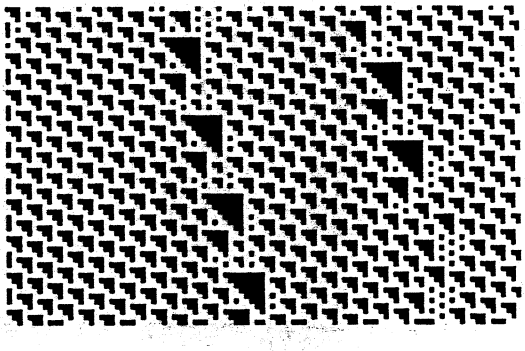

Acknowledgements to Wolfram [17]

*K*3 rule = c1 (dec 193)
λ_{ratio} = 0.75
Z = 0.75

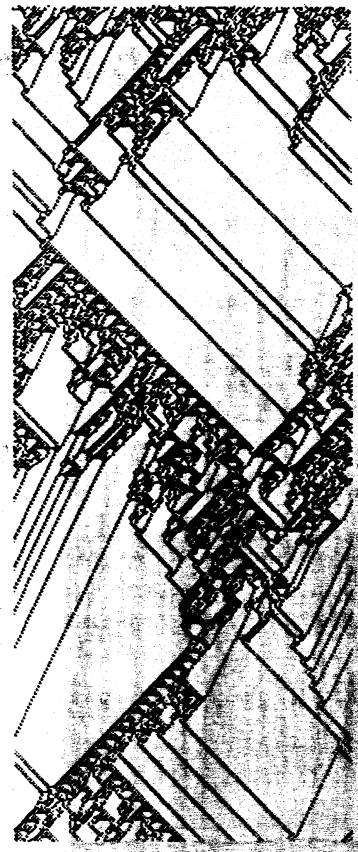

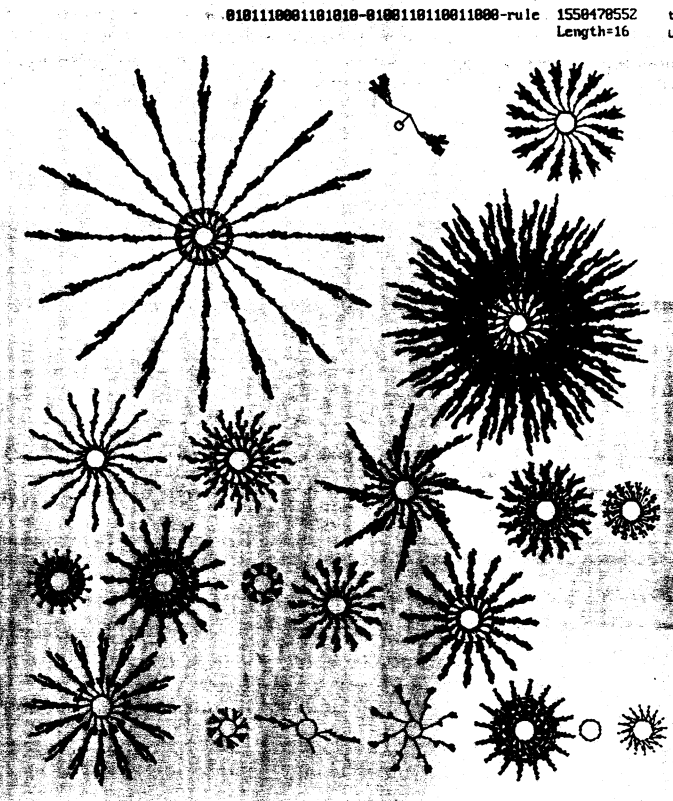

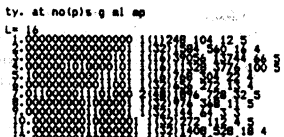

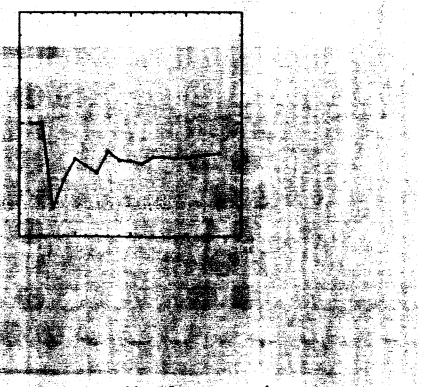

for detail of space-time pattern see figure

*K*5 rule = 5c 6a 4d 98
λ_{ratio} = 0.9375,
Z = 0.7265625

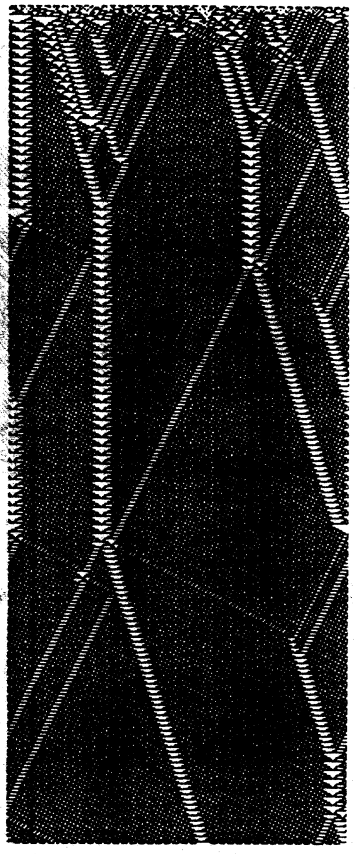

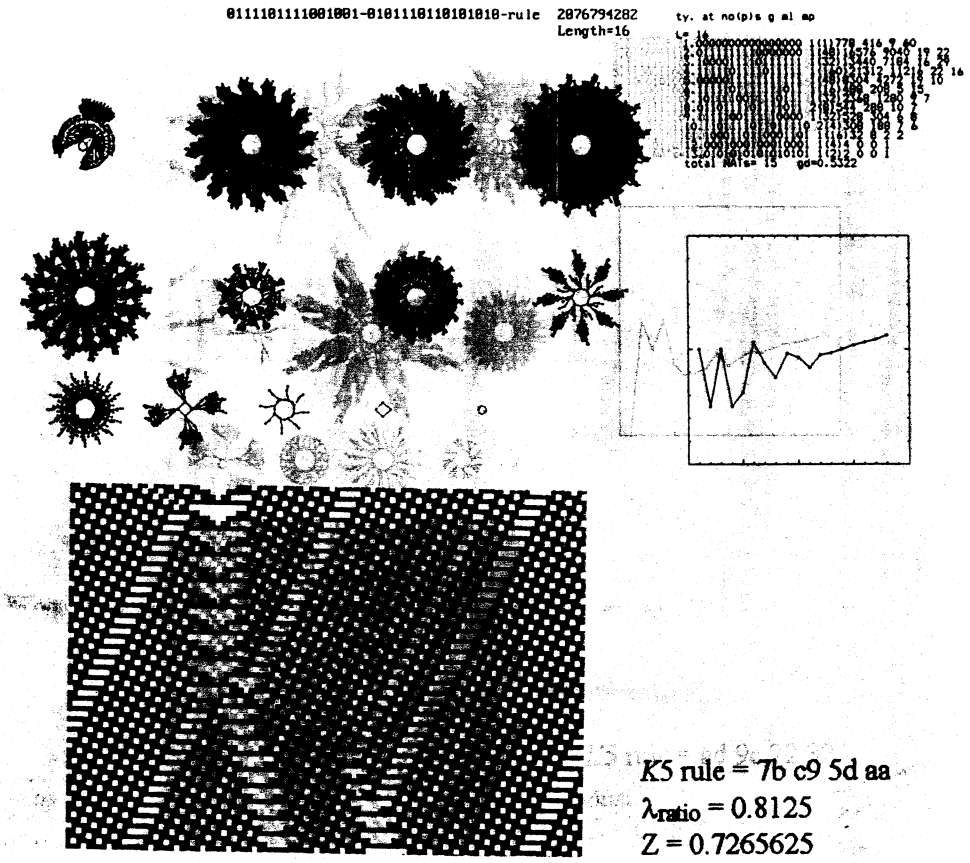

*K*5 rule = 7b c9 5d aa
λ_{ratio} = 0.8125
Z = 0.7265625

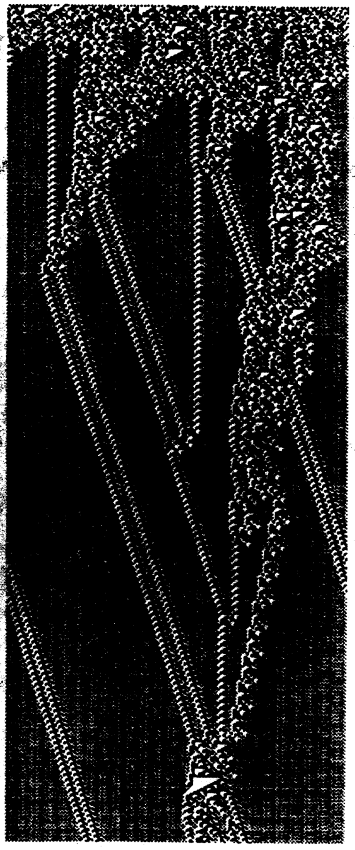

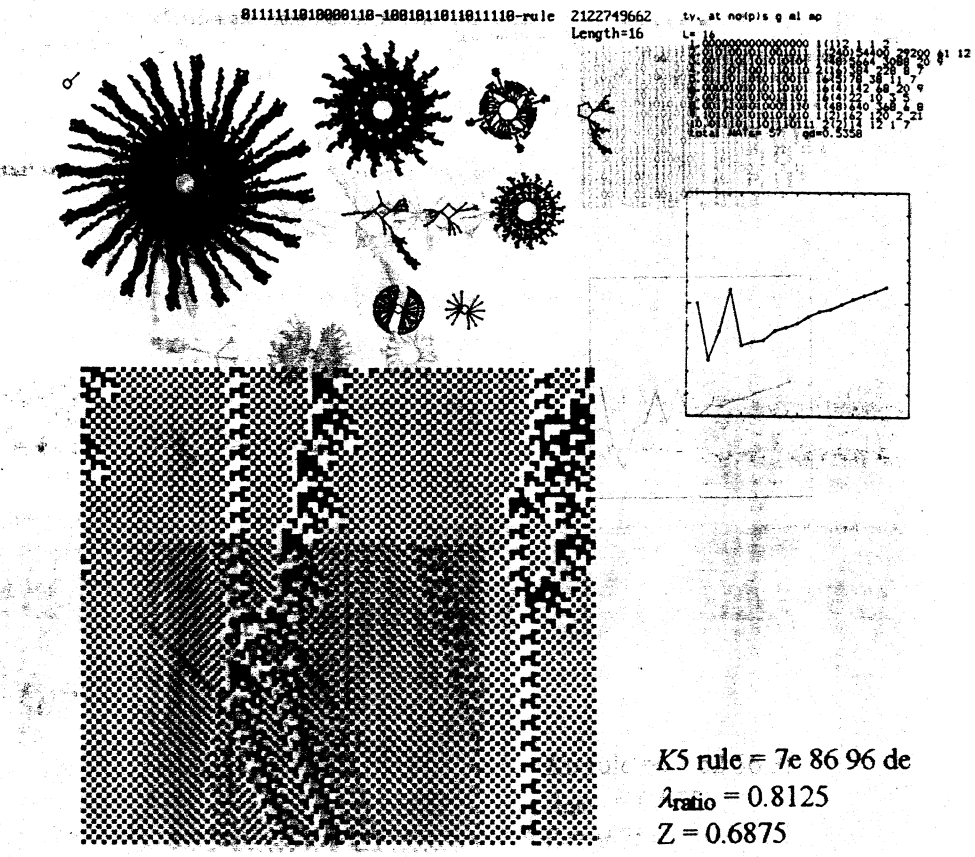

*K*5 rule = 7e 86 96 de
λ_{ratio} = 0.8125
Z = 0.6875

Appendix 2.6 *Andrew Wuensche*

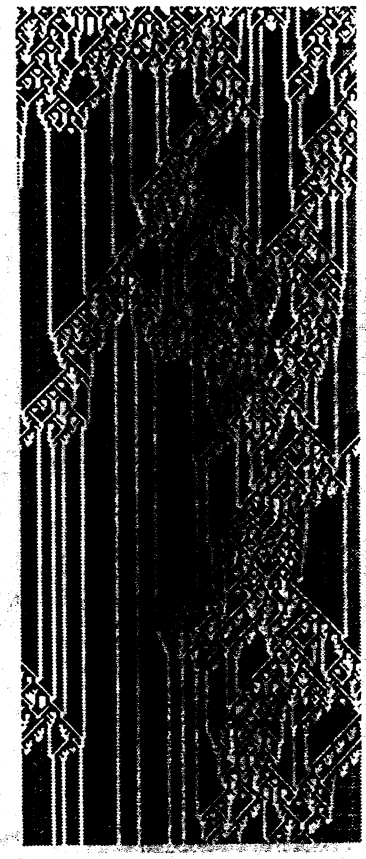

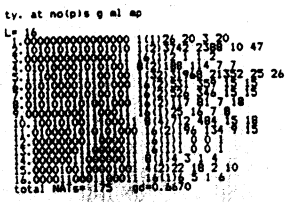

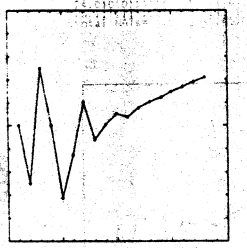

*K*5 rule = 3a 48 b5 c4
λ_{ratio} = 0.875
Z = 0.6875

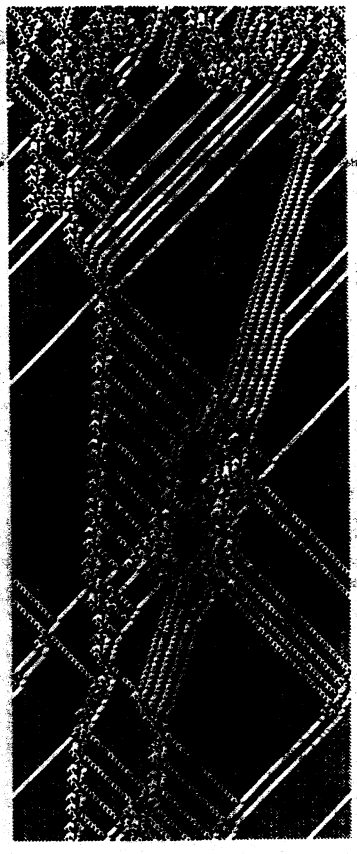

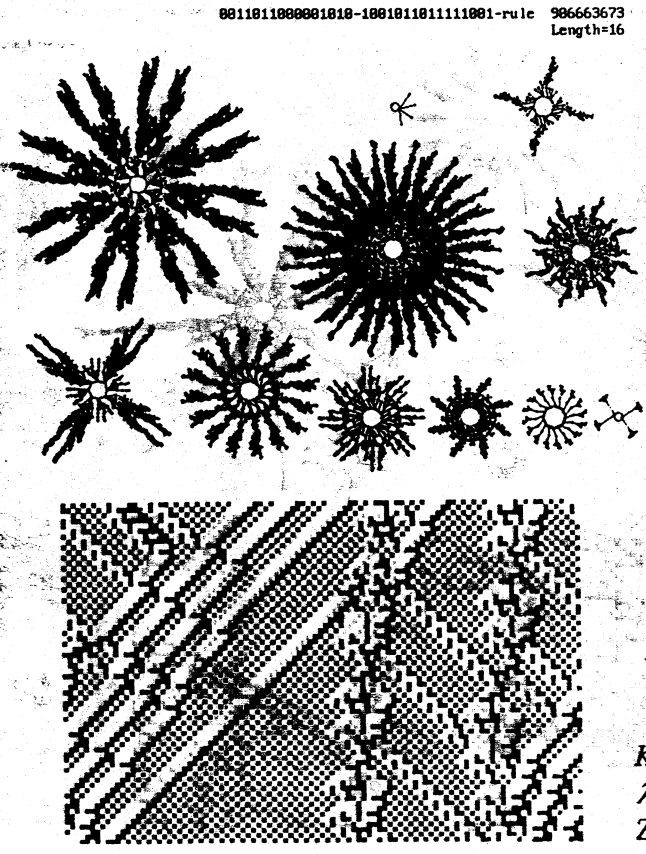

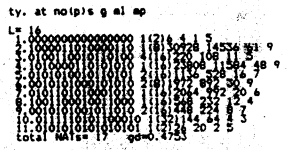

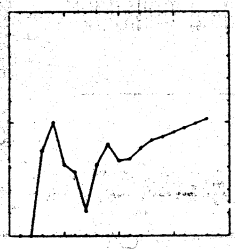

*K*5 rule = 36 0a 96 f9
λ_{ratio} = 1
Z = 0.671875

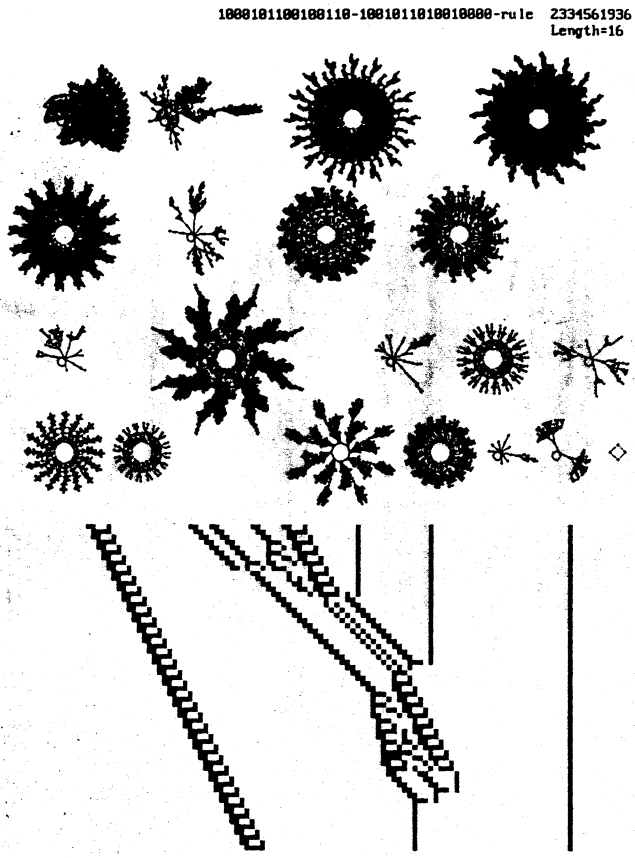

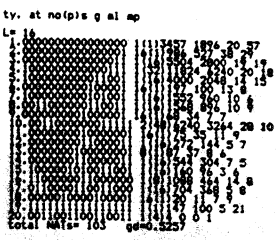

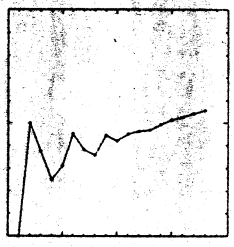

*K*5 rule = 8b 26 96 90
λ_{ratio} = 0.8125
Z = 0.6875

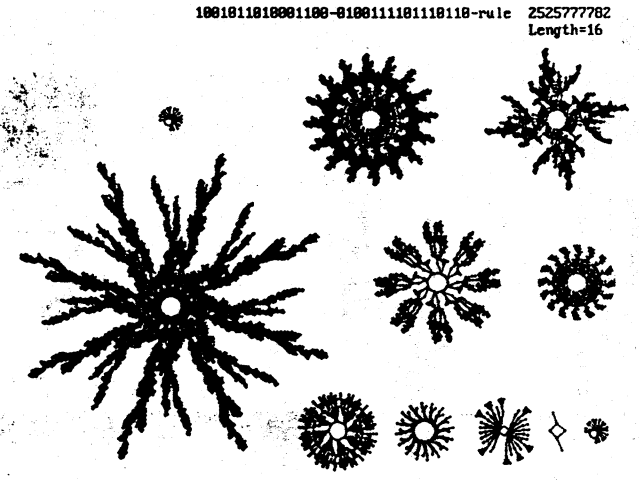

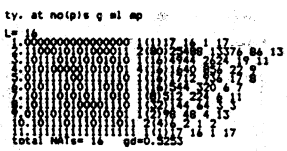

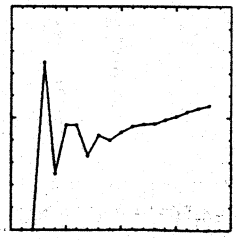

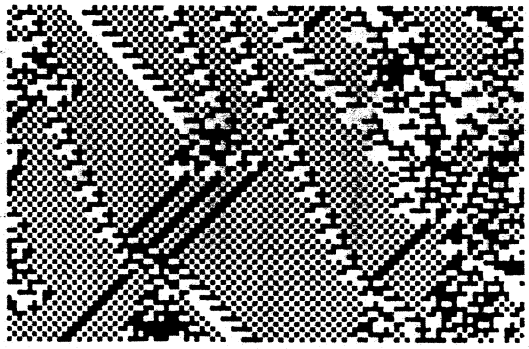

*K*5 rule = 96 8c 4f 76
λ_{ratio} = 0.9375
Z = 0.6875

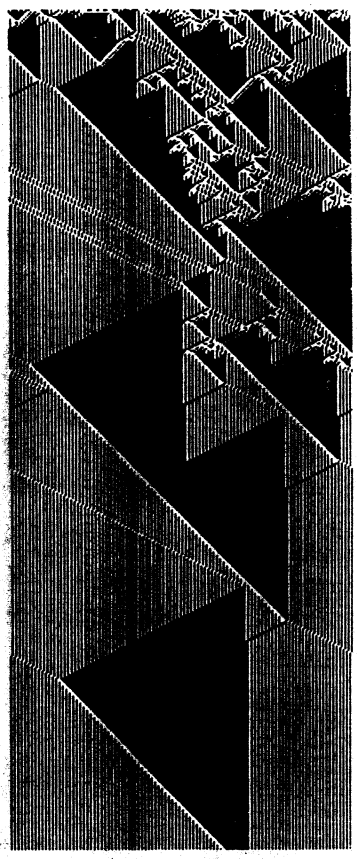

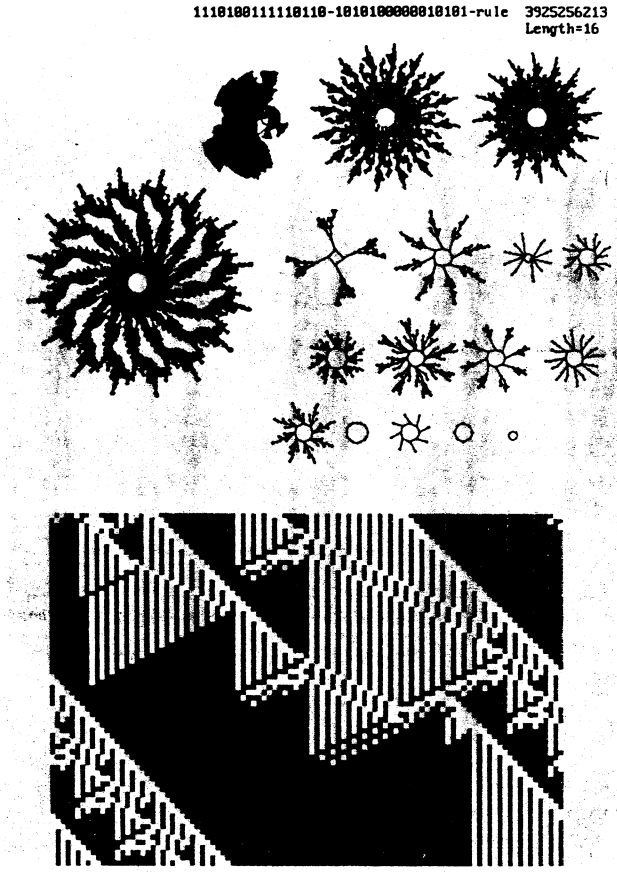

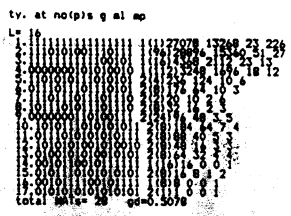

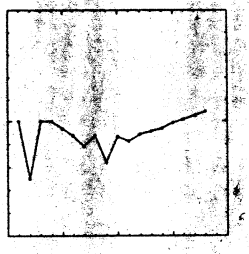

*K*5 rule = e9 f6 a8 15
λ_{ratio} = 0.9375
Z = 0.6875

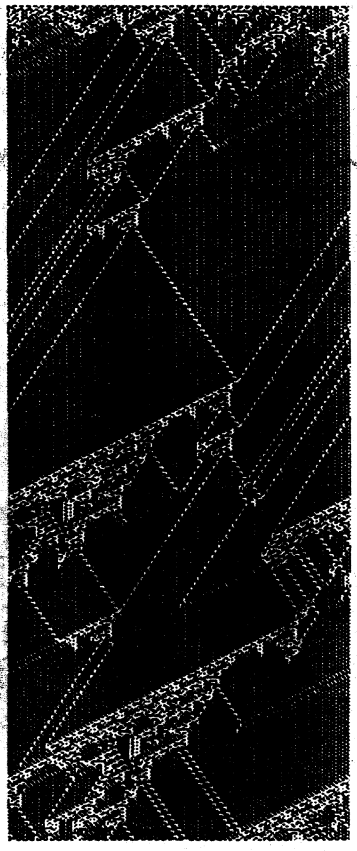

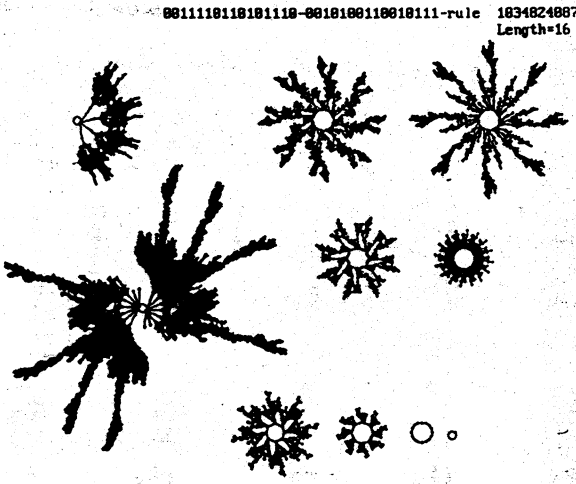

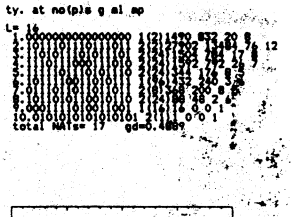

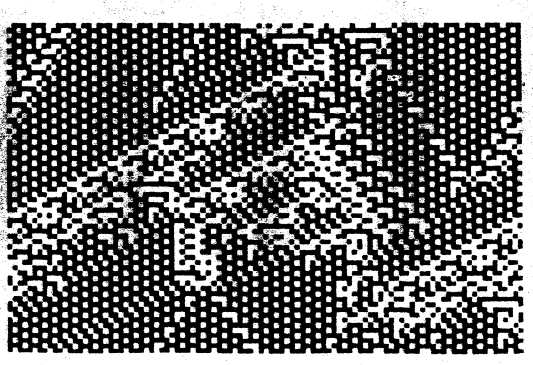

*K*5 rule = 3d ae 29 97
λ_{ratio} = 0.875
Z = 0.671875

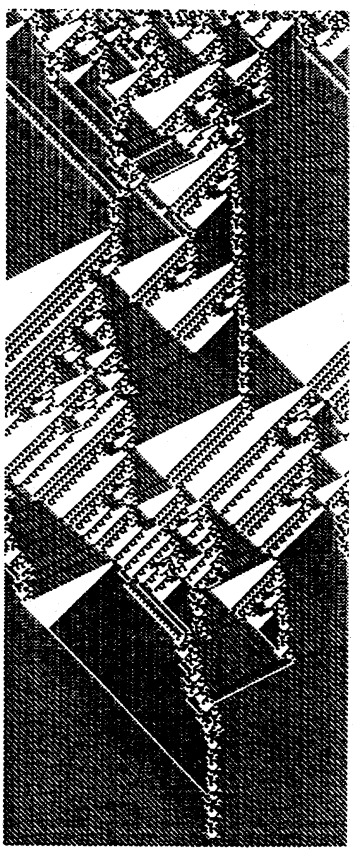

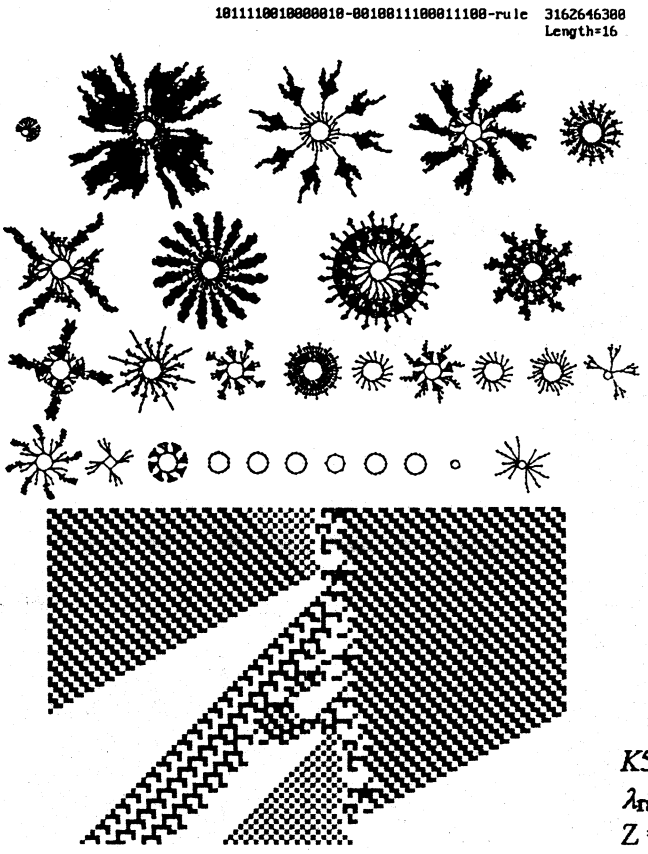

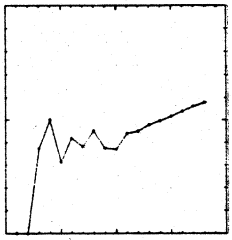

*K*5 rule = bc 82 27 1c
λ_{ratio} = 0.875
Z = 0.671875

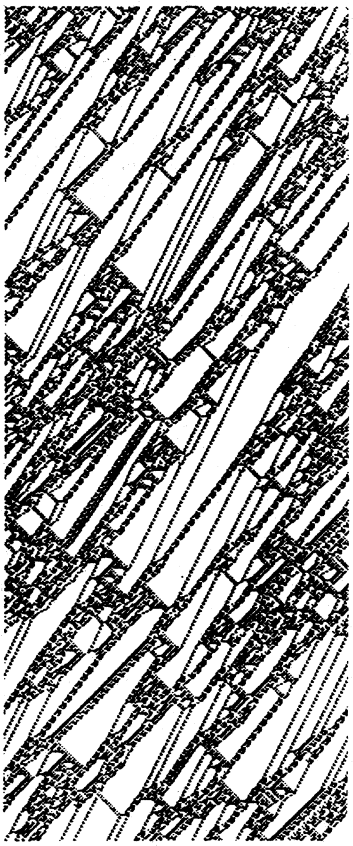

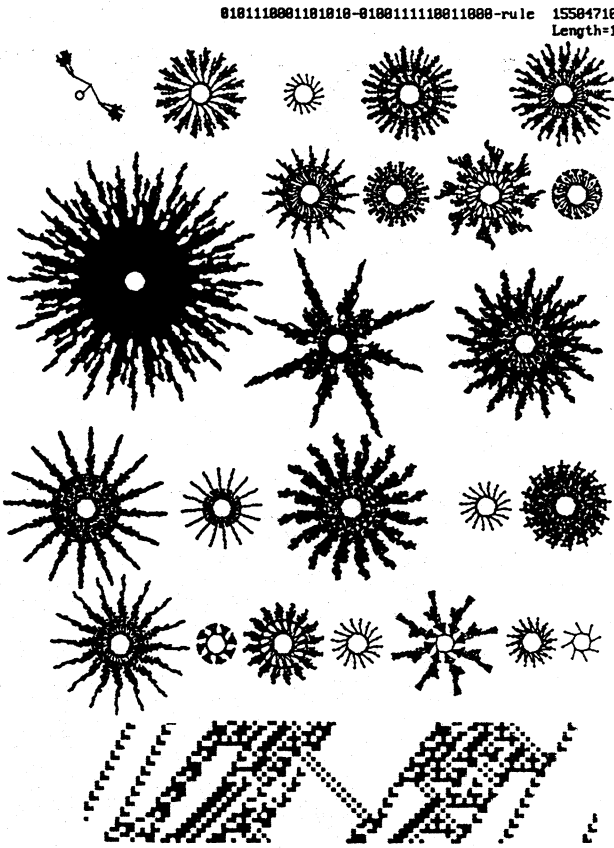

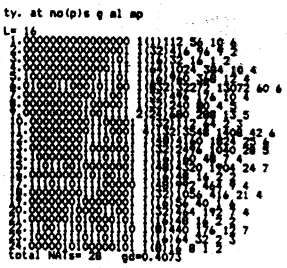

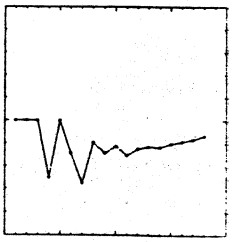

*K*5 rule = 5c 6a 4f 98
λ_{ratio} = 1
Z = 0.671875

Appendix 2.10 *Andrew Wuensche*

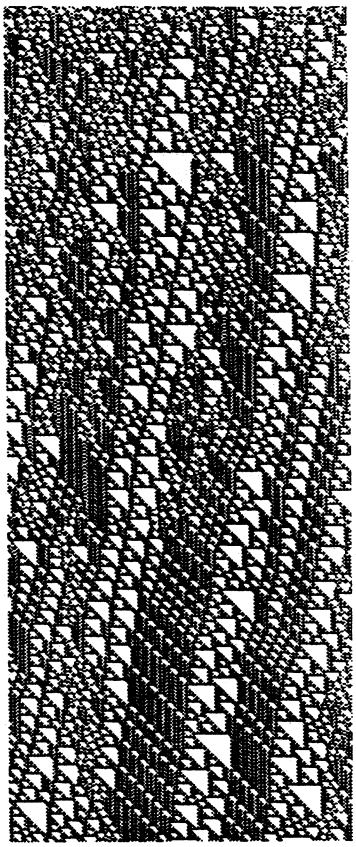

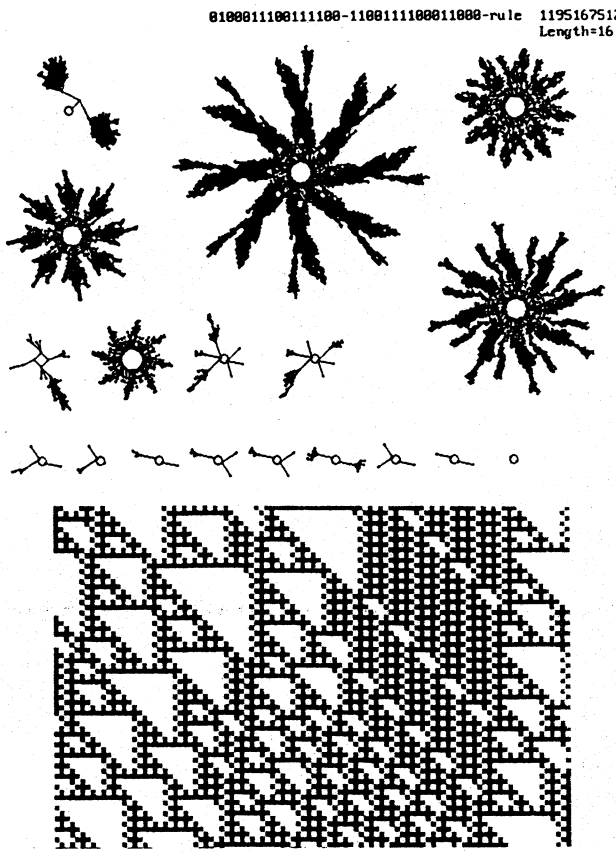

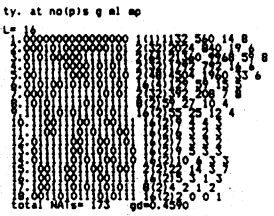

*K*5 rule = 47 3c cf 18
$\lambda_{ratio} = 1$
Z = 0.625

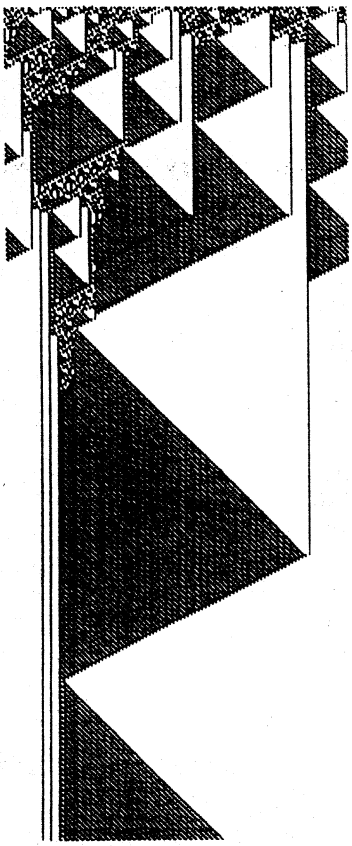

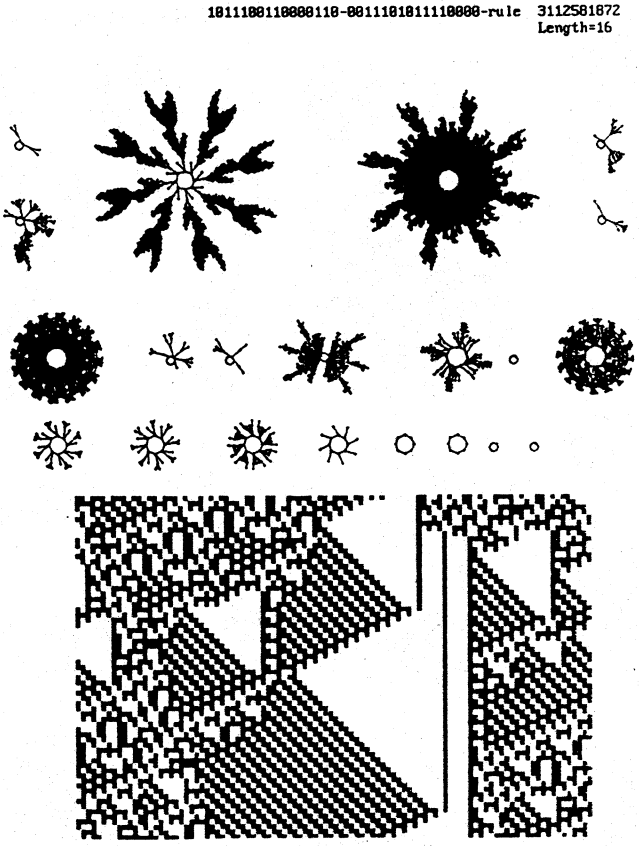

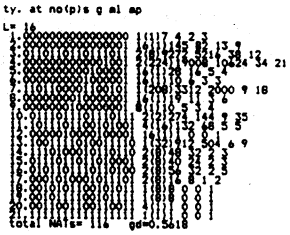

*K*5 rule = b9 86 3a f0
$\lambda_{ratio} = 1$
Z = 0.671875

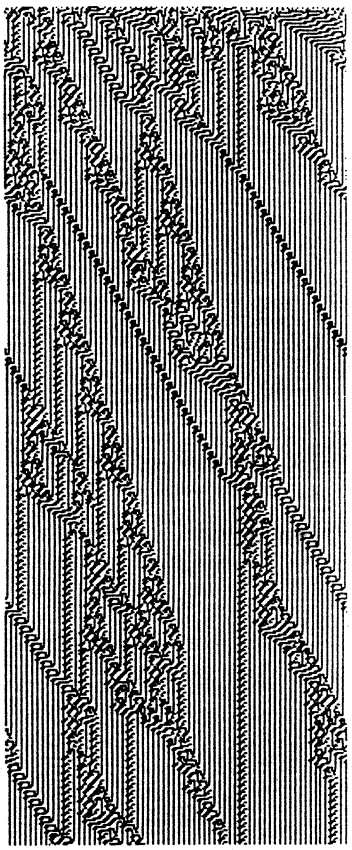

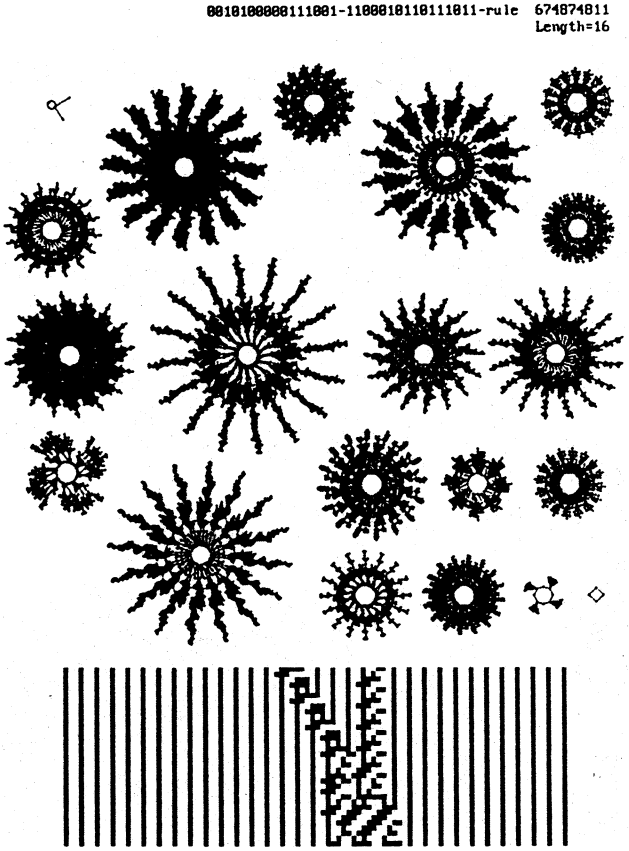

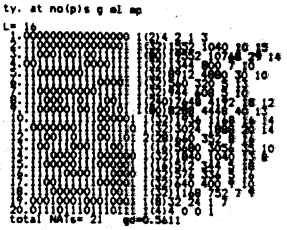

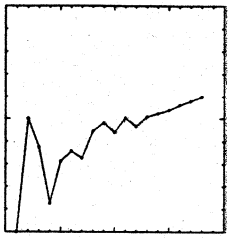

*K*5 rule = 28 39 c5 bb
$\lambda_{ratio} = 1$
Z = 0.625

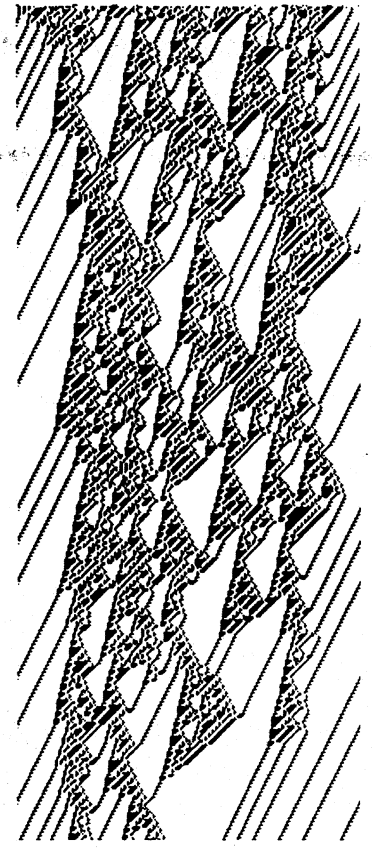

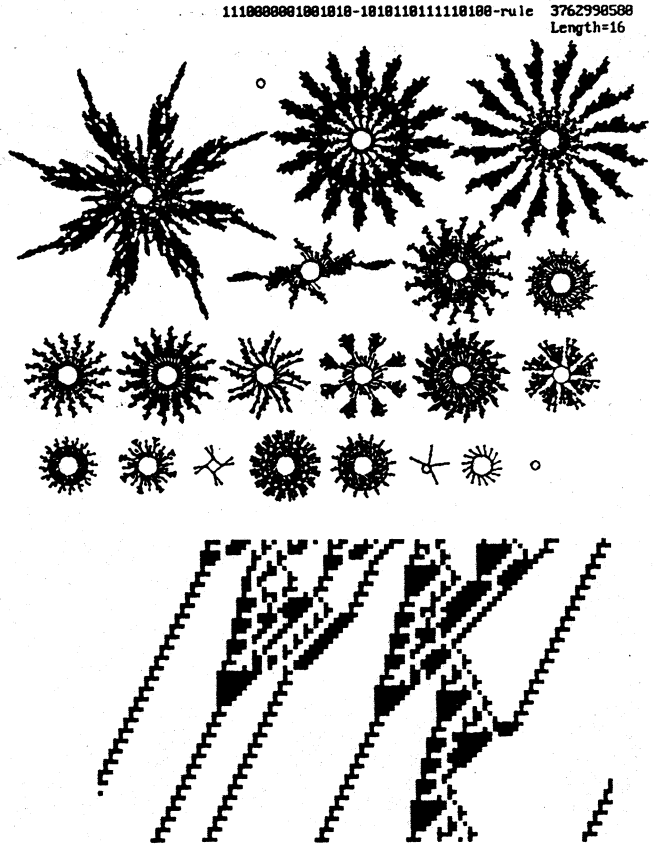

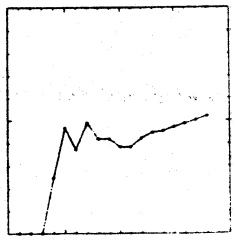

*K*5 rule = e0 4a ad f4
$\lambda_{ratio} = 1$
Z = 0.625

Appendix 2.12 *Andrew Wuensche*

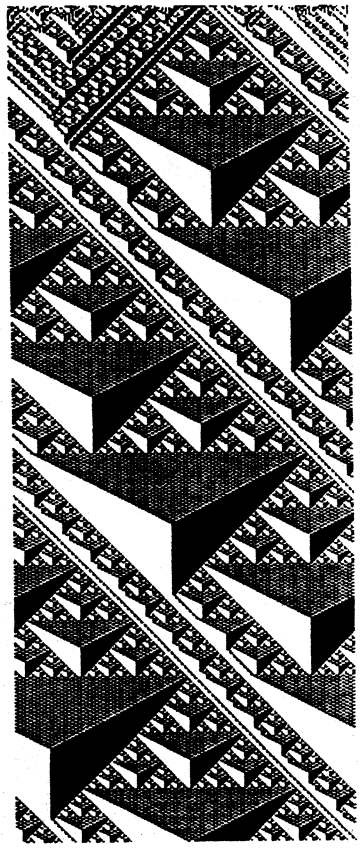

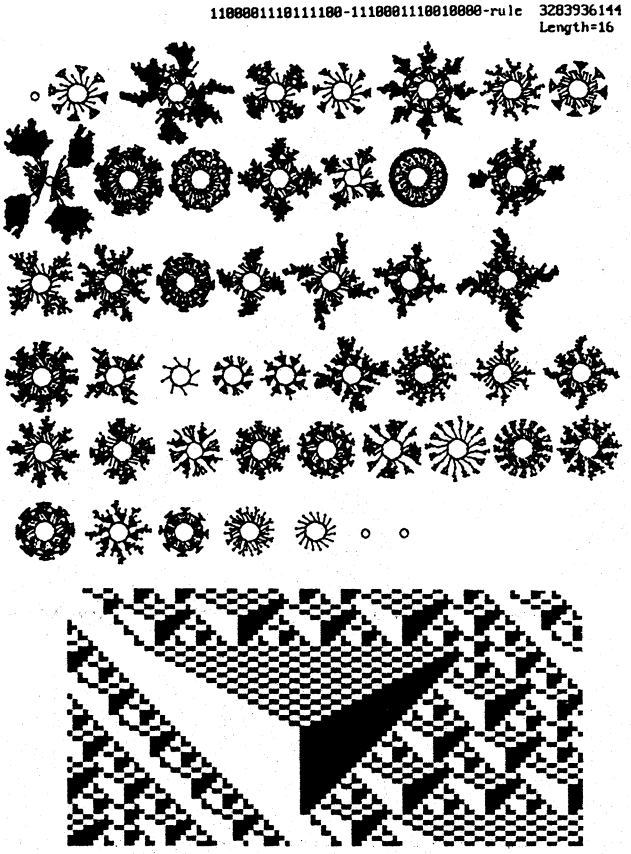

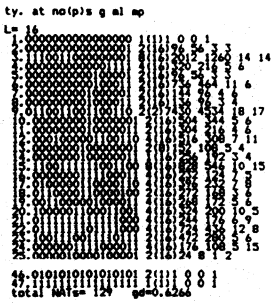

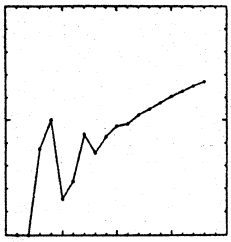

Acknowledgements to Wentian Li[10]

*K*5 rule = c3 bc e3 90
$\lambda_{ratio} = 1$
Z = 0.625

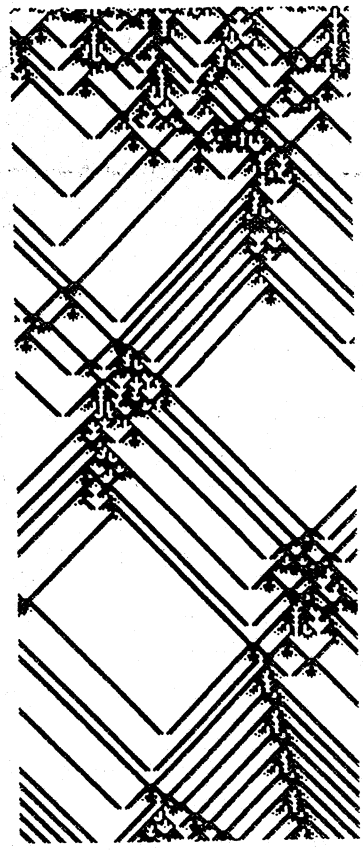

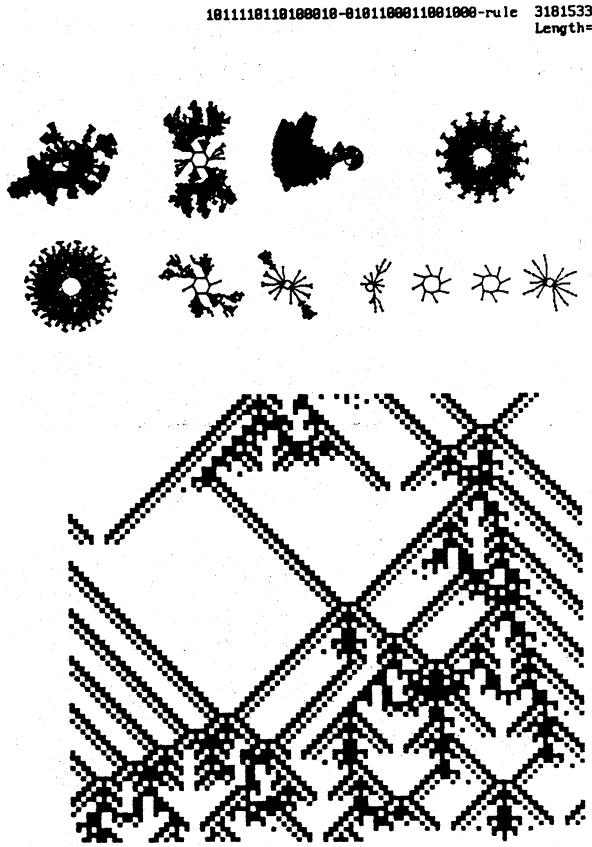

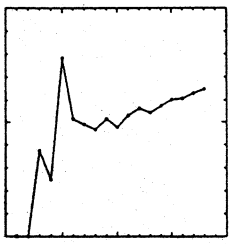

Acknowledgements to Aizawa *et al*[1]

*K*5 rule = bd a2 58 c8
$\lambda_{ratio} = 0.9375$
Z = 0.6171875

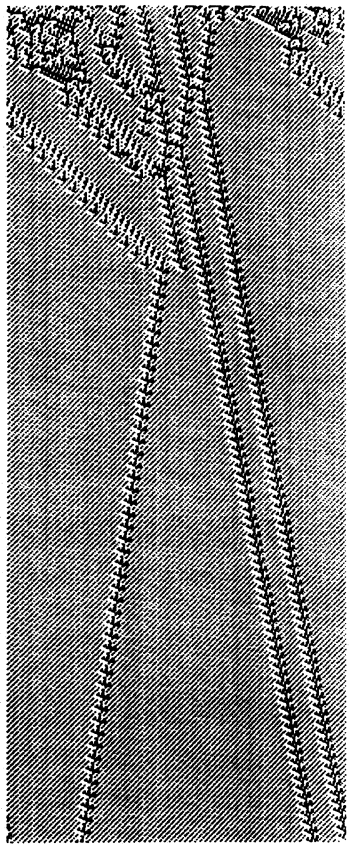

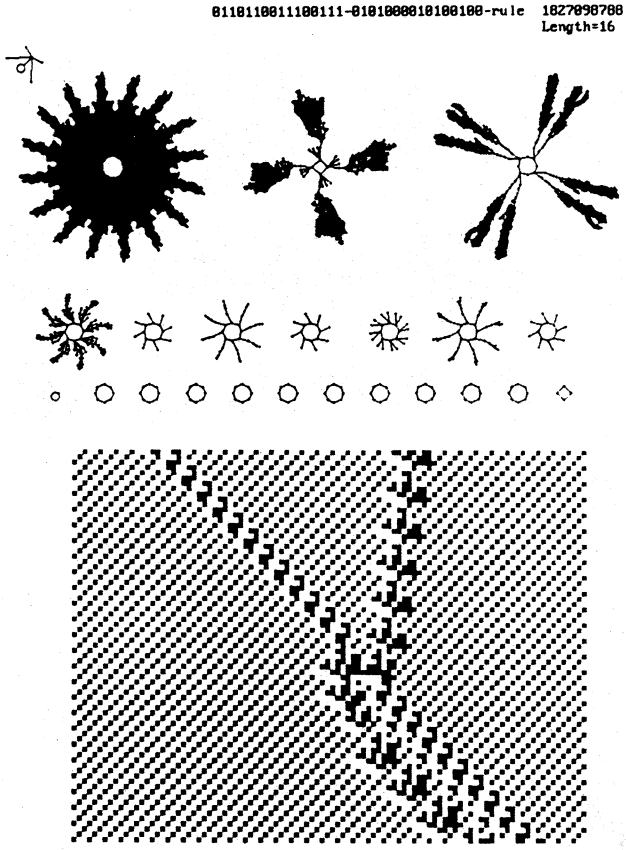

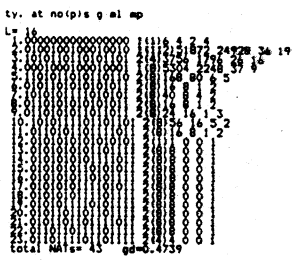

$K5$ rule = 6c e7 50 a4
λ_{ratio} = 0.9375
Z = 0.6171875

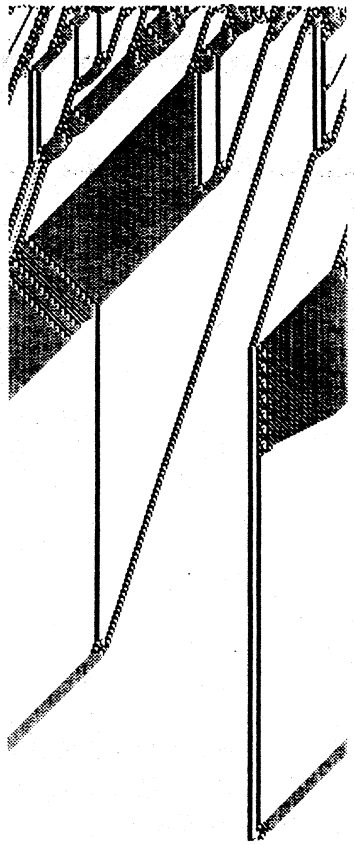

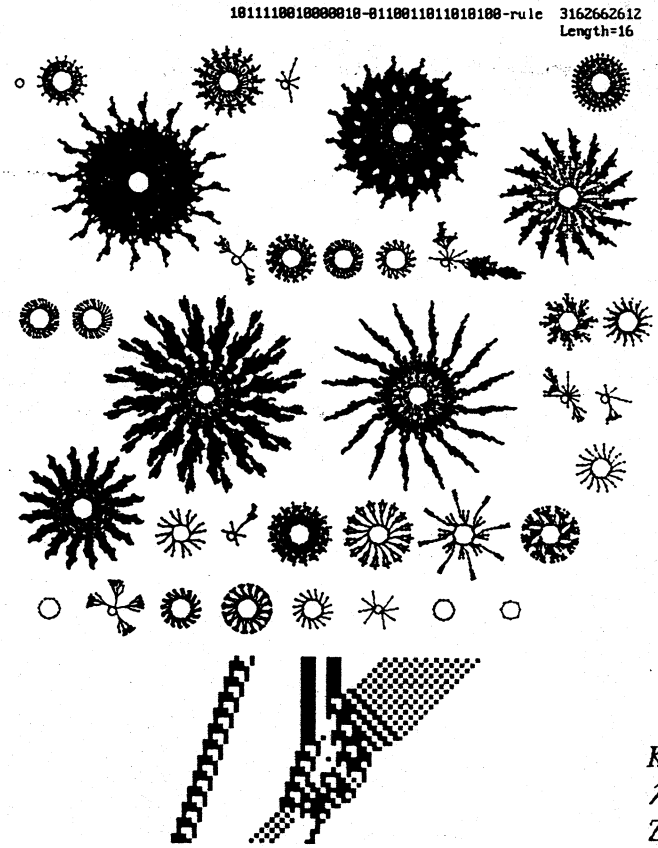

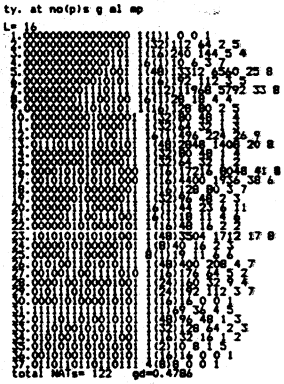

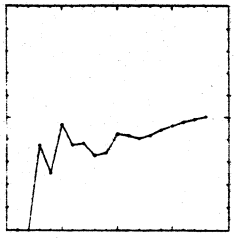

$K5$ rule = bc 82 66 d4
λ_{ratio} = 0.9375
Z = 0.6171875

Appendix 2.14 *Andrew Wuensche*

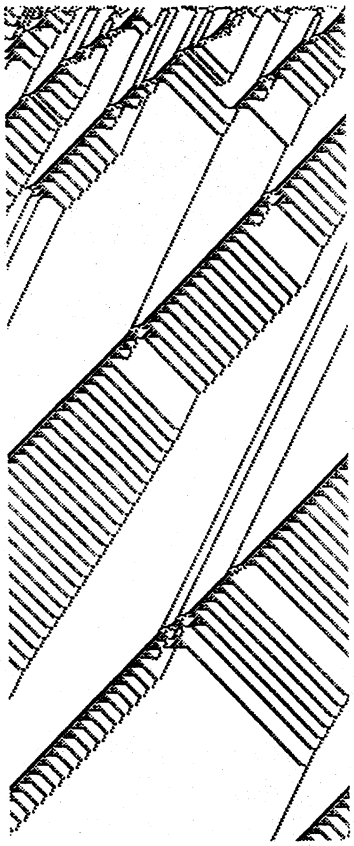

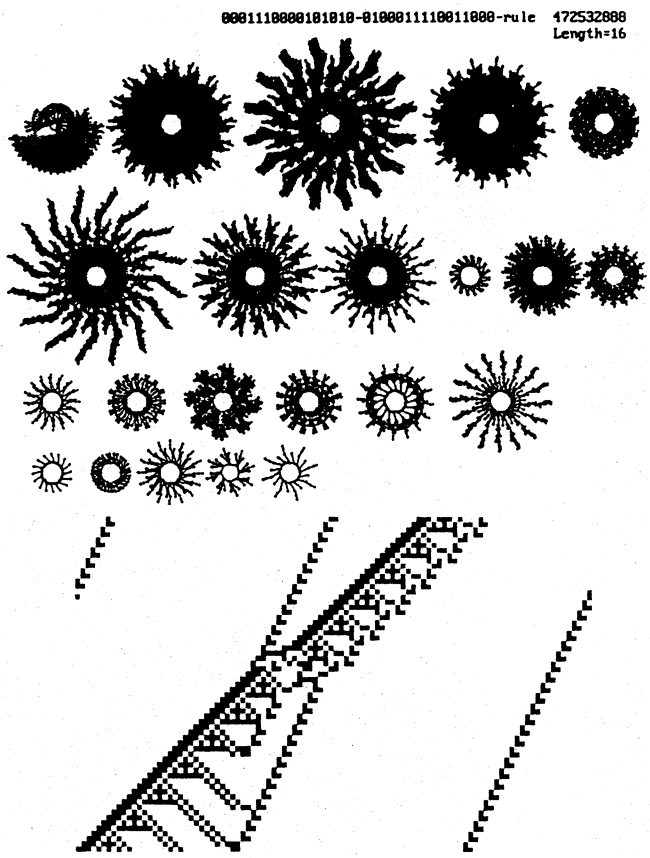

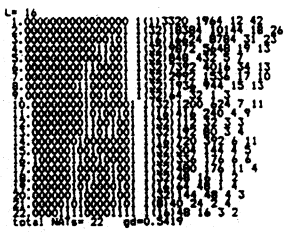

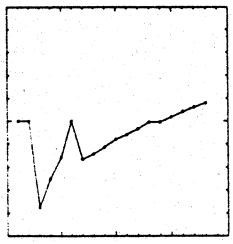

*K*5 rule = 1c 2a 47 98
λ_{ratio} = 0.8125
Z = 0.6171875

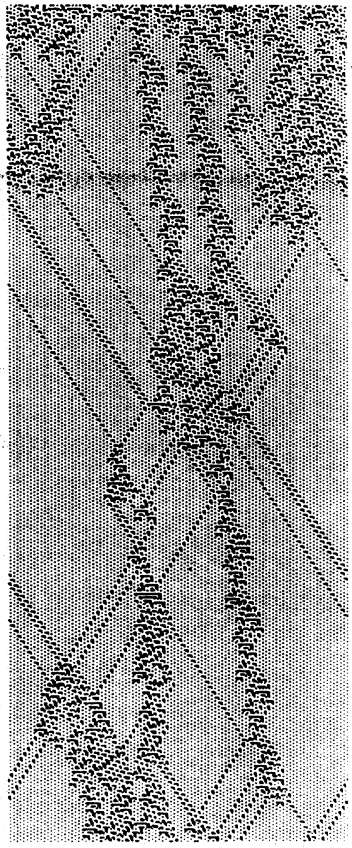

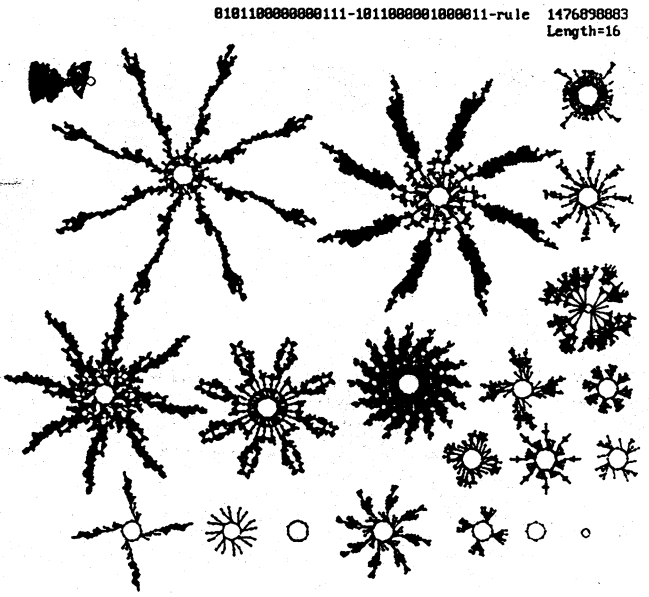

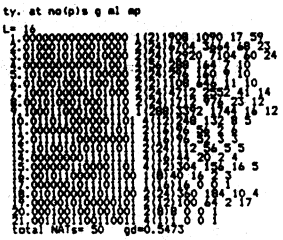

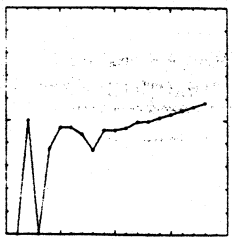

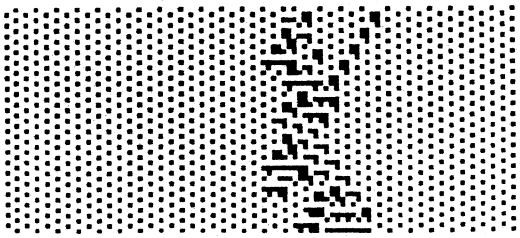

*K*5 rule = 58 07 b0 43
λ_{ratio} = 0.75
Z = 0.609375

Appendix 2.16 *Andrew Wuensche*

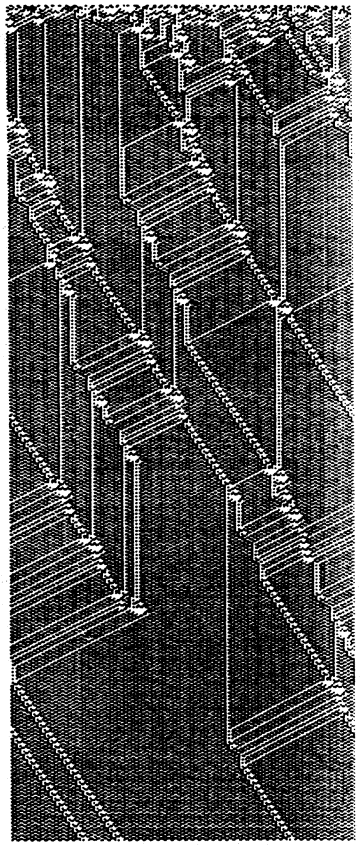

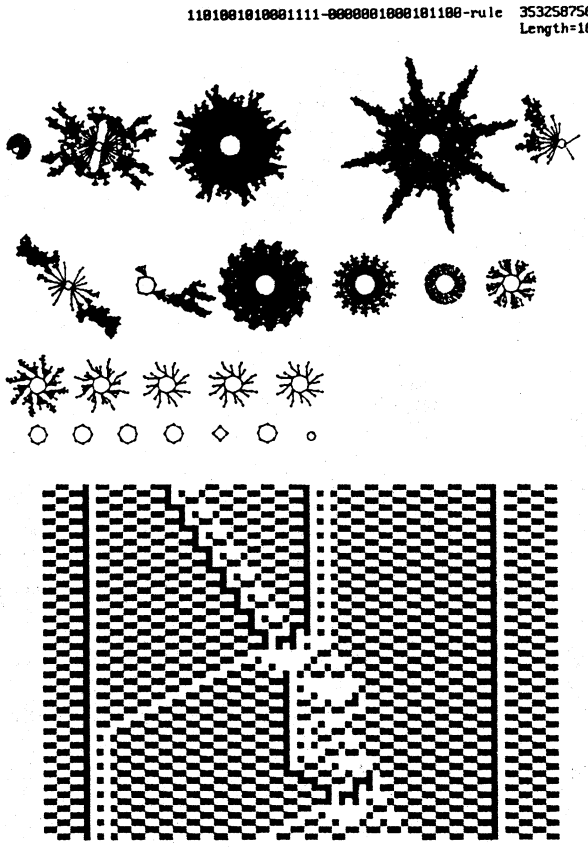

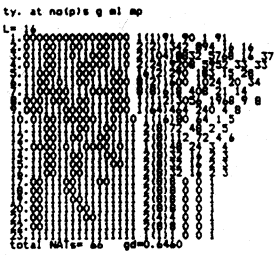

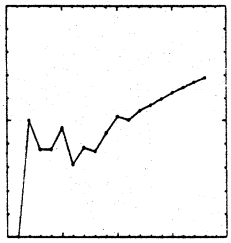

*K*5 rule = d2 8f 02 2c
λ_{ratio} = 0.8125
Z = 0.578125

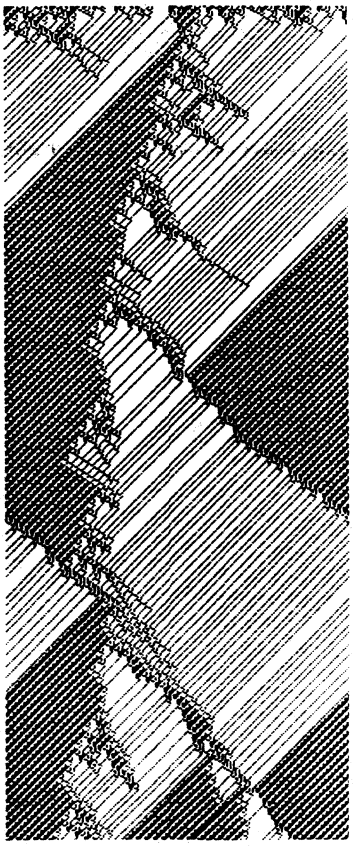

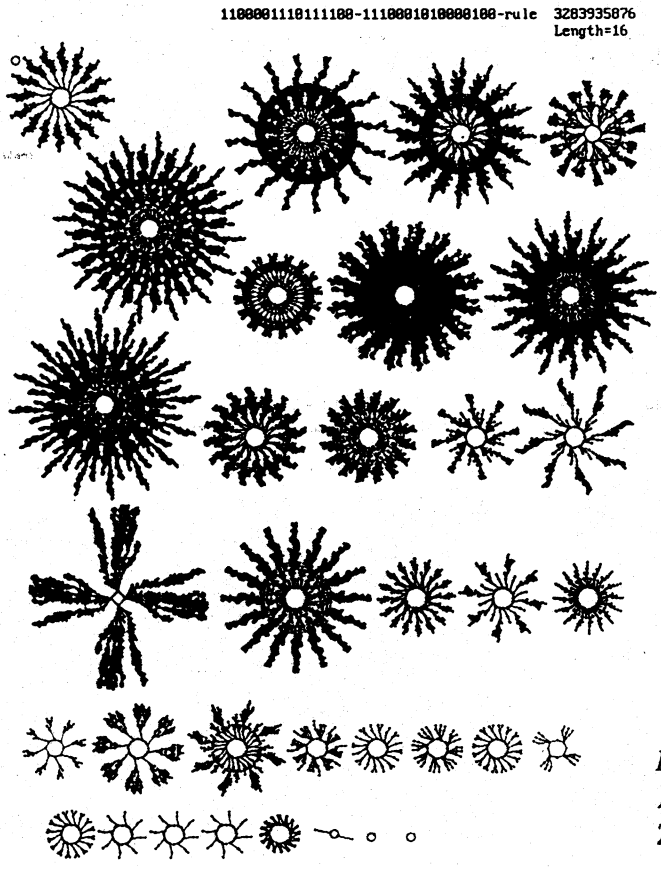

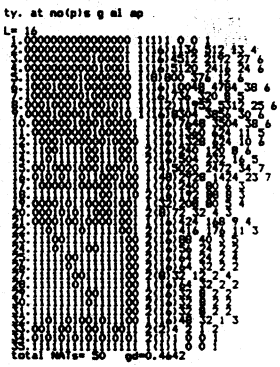

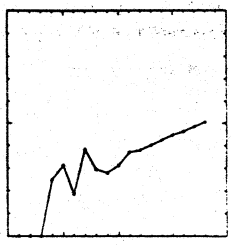

*K*5 rule = c3 bc e2 84
λ_{ratio} = 0.9375
Z = 0.5703125

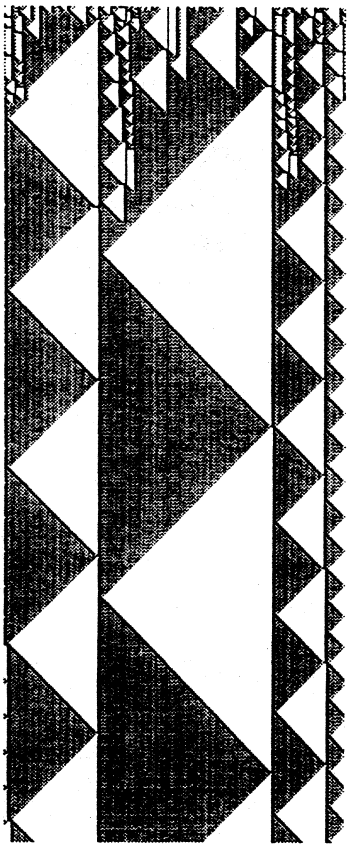

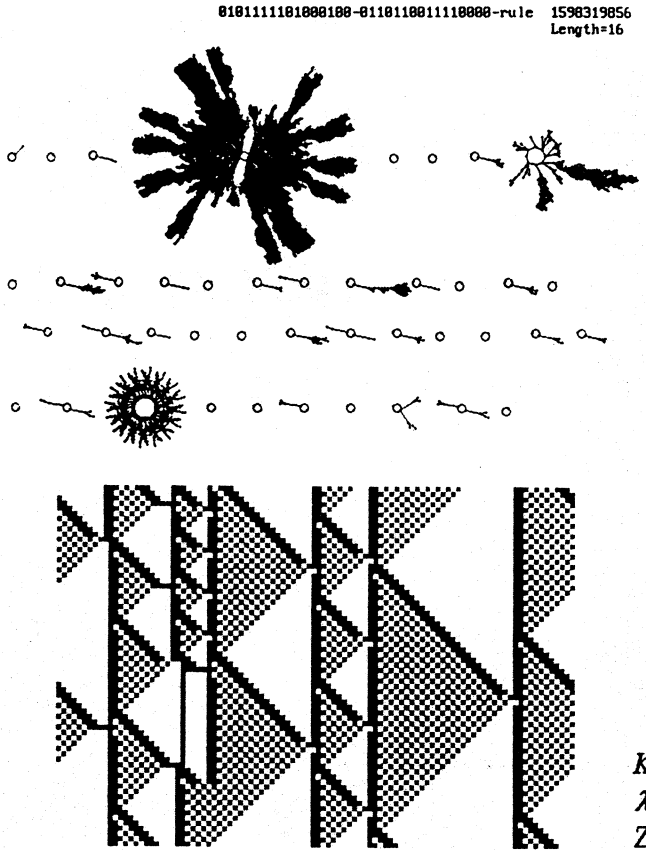

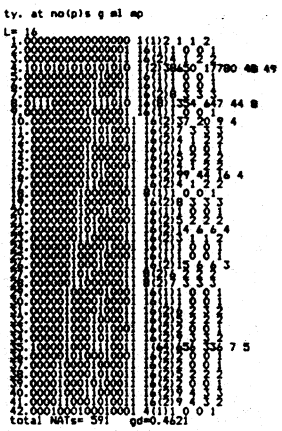

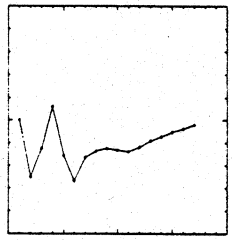

$K5$ rule = 5f 44 6c f0
$\lambda_{ratio} = 1$
$Z = 0.58984375$

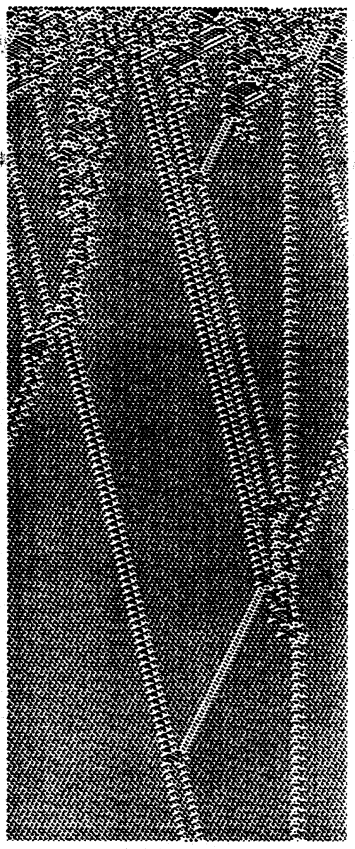

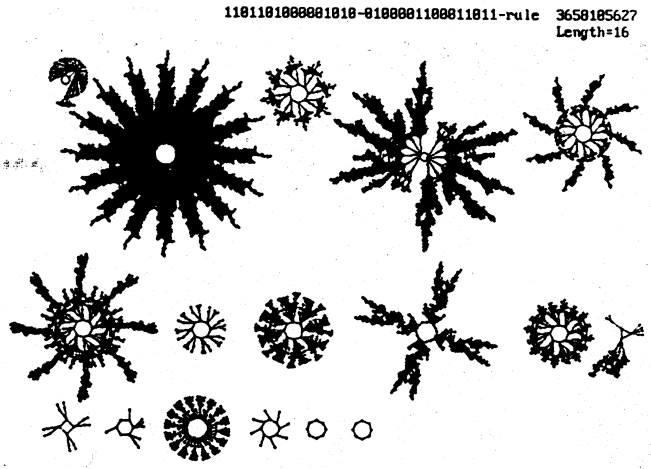

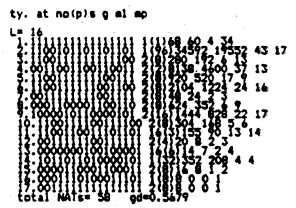

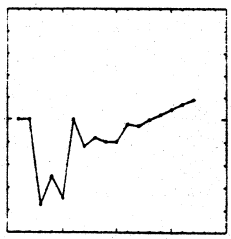

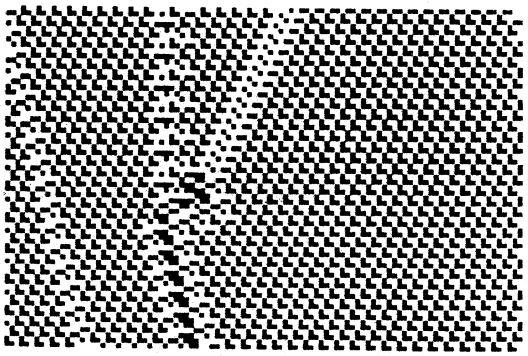

$K5$ rule = da 0a 43 1b
$\lambda_{ratio} = 0.875$
$Z = 0.58984375$

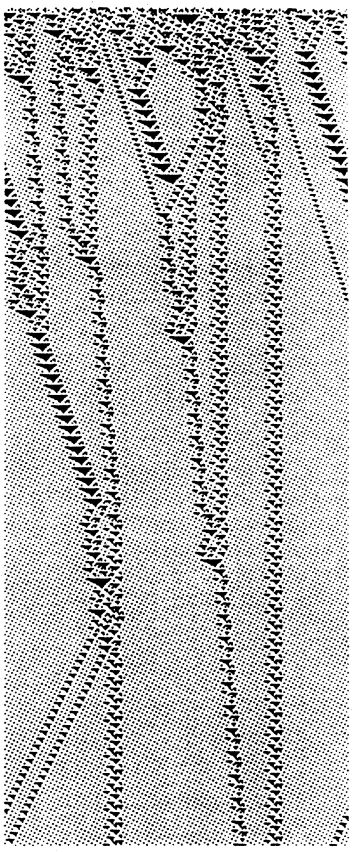

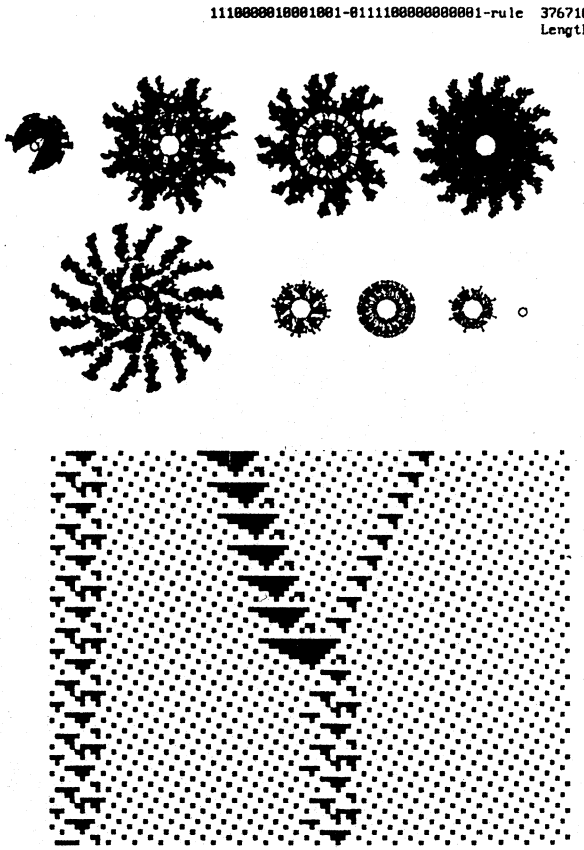

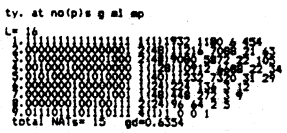

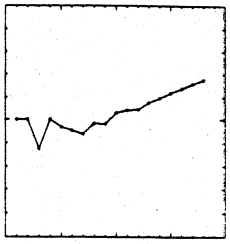

*K*5 rule = e0 89 78 01
λ_{ratio} = 0.6875
Z = 0.5703125

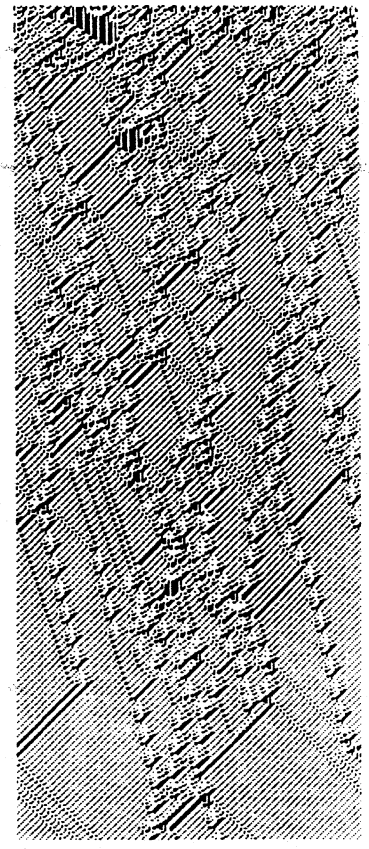

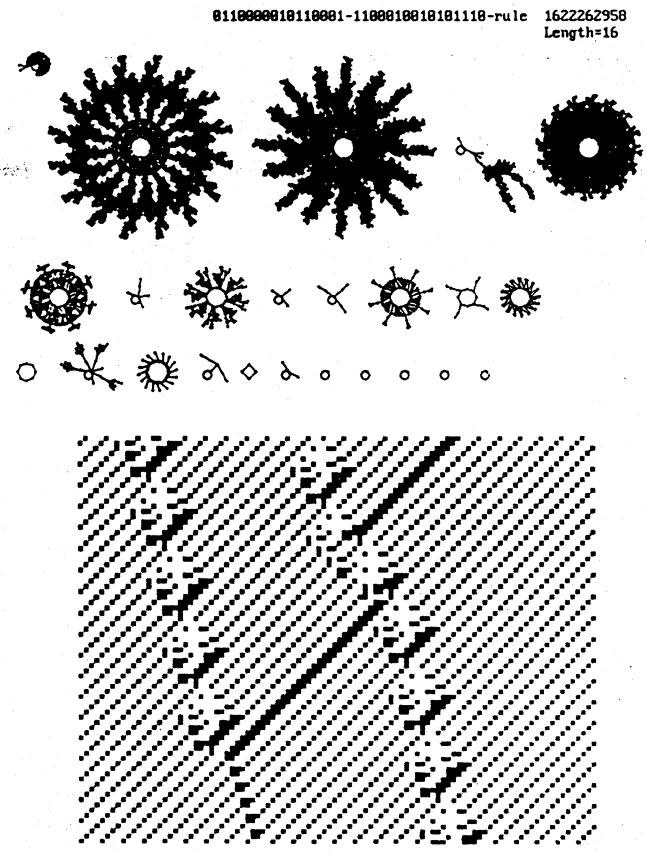

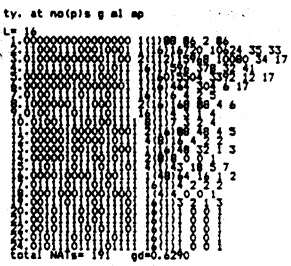

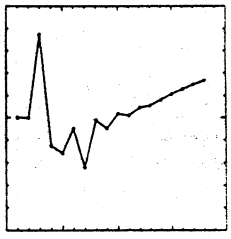

*K*5 rule = 60 b1 c4 ae
λ_{ratio} = 0.875
Z = 0.5625

Appendix 2.18 *Andrew Wuensche*

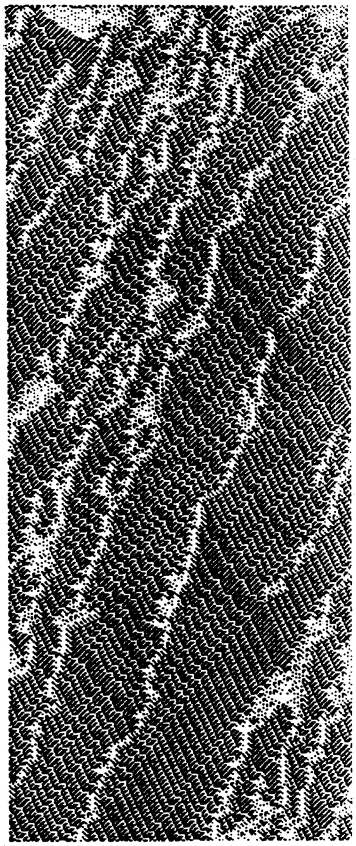

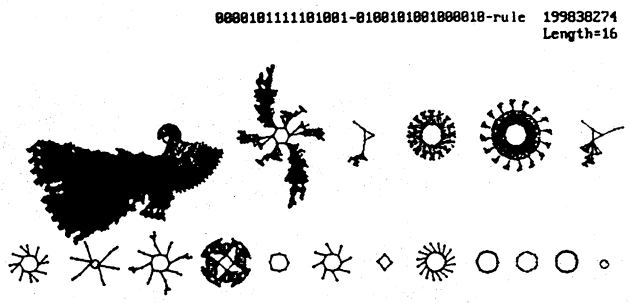

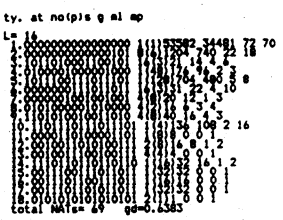

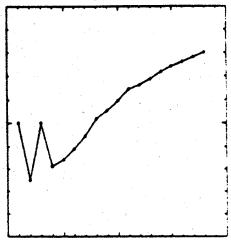

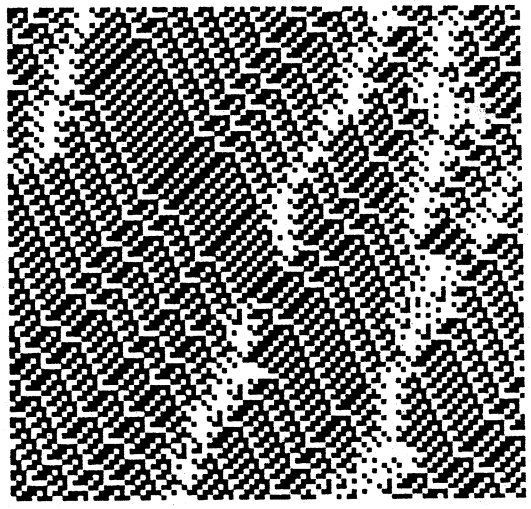

*K*5 rule = 0b e9 4a 42
λ_{ratio} = 0.8125
Z = 0.5625

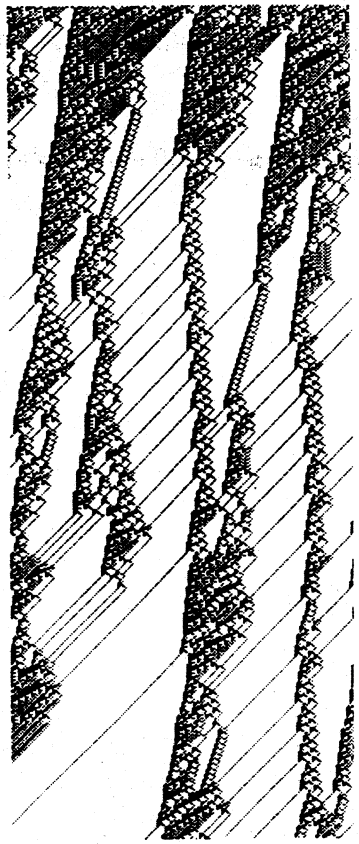

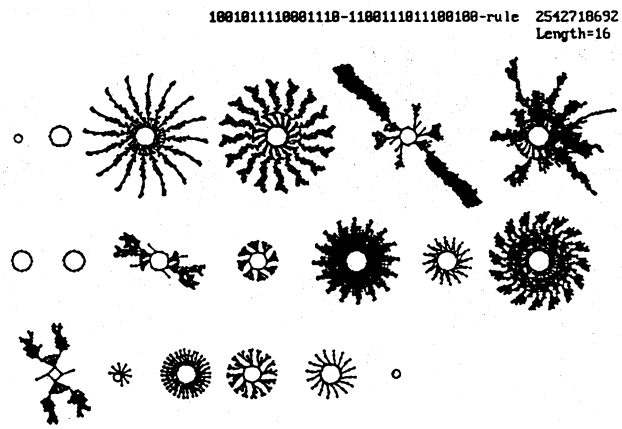

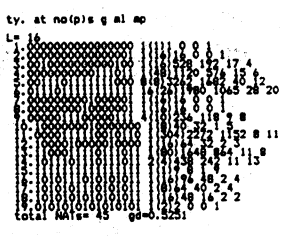

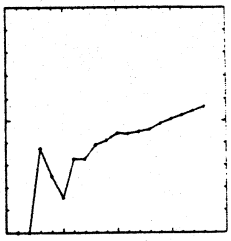

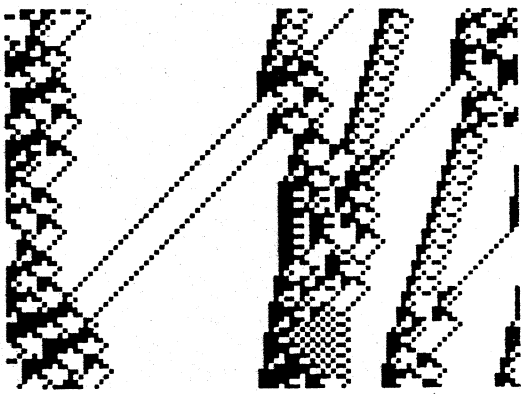

*K*5 rule = 97 8e ce e4
λ_{ratio} = 0.875
Z = 0.5625

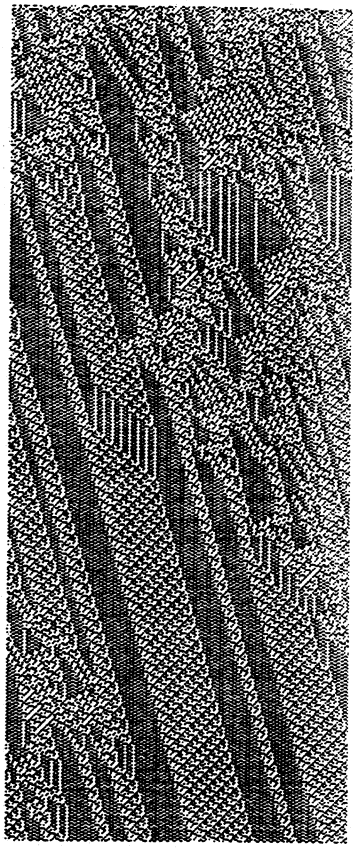

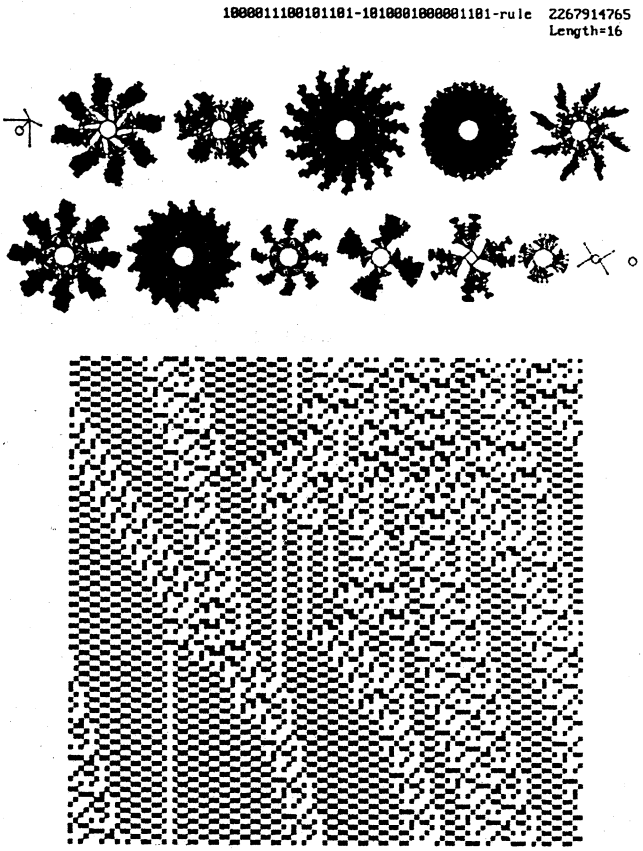

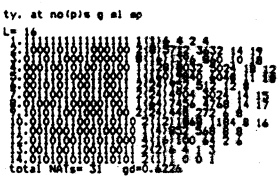

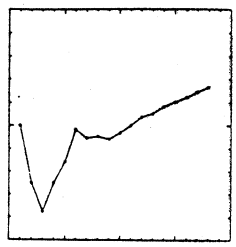

*K*5 rule = 97 2d a2 0d
λ_{ratio} = 0.875
Z = 0.53125

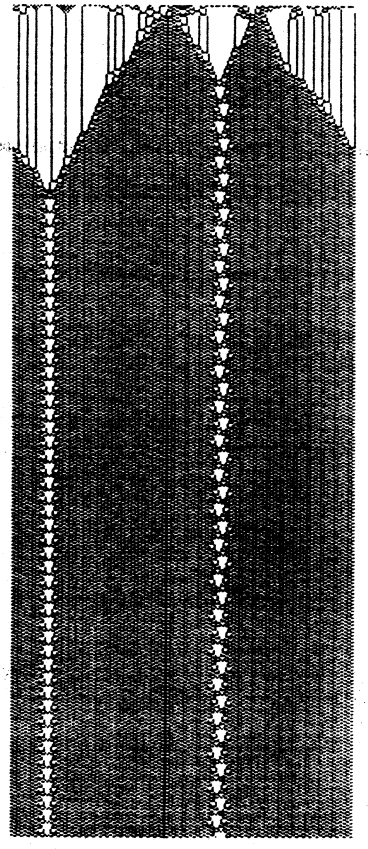

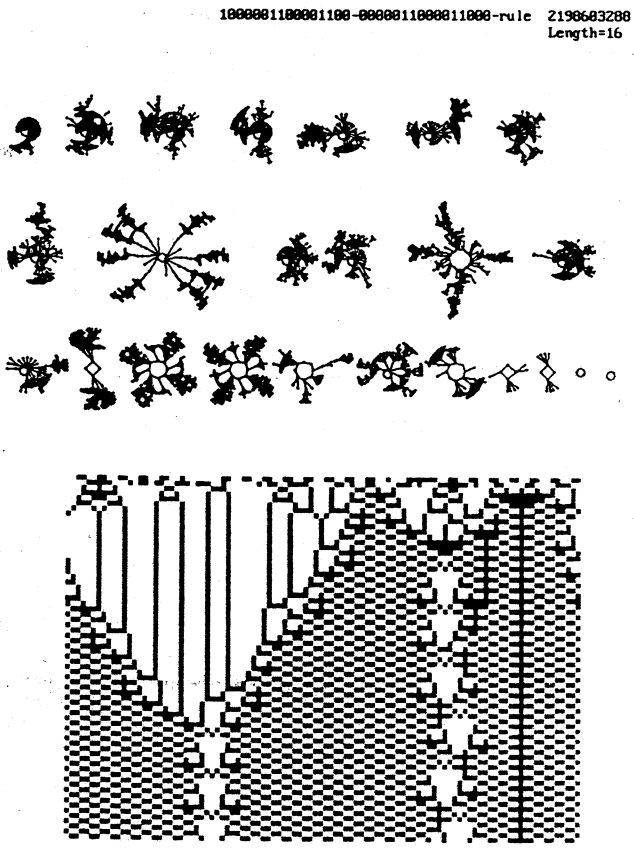

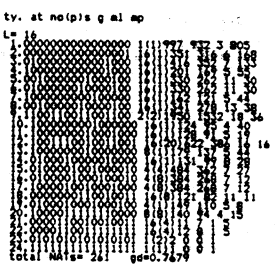

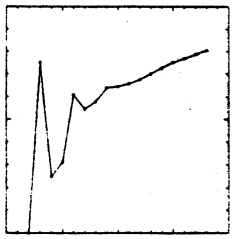

*K*5 rule = 83 0c 06 18
λ_{ratio} = 0.5625
Z = 0.484375

Appendix 3 - Sample of complex rules, *K*=5,6,7.

Space-time patterns, neighbourhood lookup frequency and entropy

The frequency that each of the K neighbourhoods in the rule-table is "looked up" at a given time-step can be represented by a histogram, or lookup spectrum. A typical lookup histogram (of the very last time-step) is shown, which distributes the total of N lookups among the 2^K neighbourhoods, (where N=system size). For each rule in the sample, appendix 3 shows a typical space-time pattern, with a *superimposed* frequency spectrum (2^K points corresponding to the histogram values) plotted alongside each time-step. The entropy of the lookup frequency spectrum is also shown for each time step on the same plot.

A typical layout from appendix 3 is annotated below.

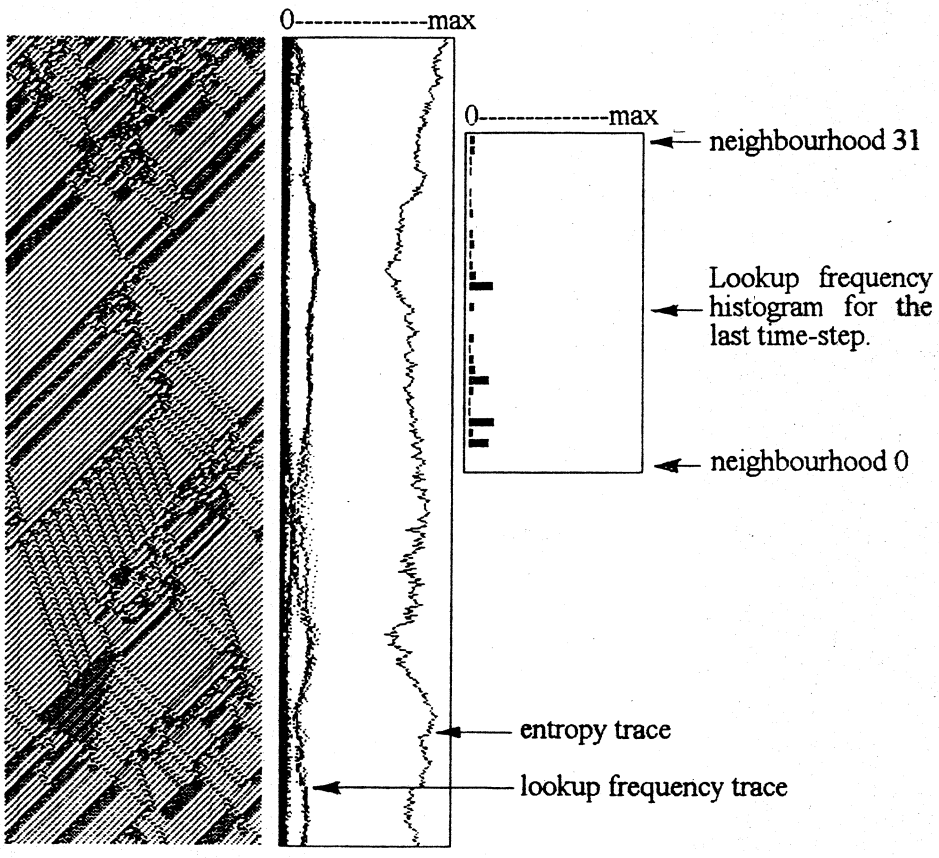

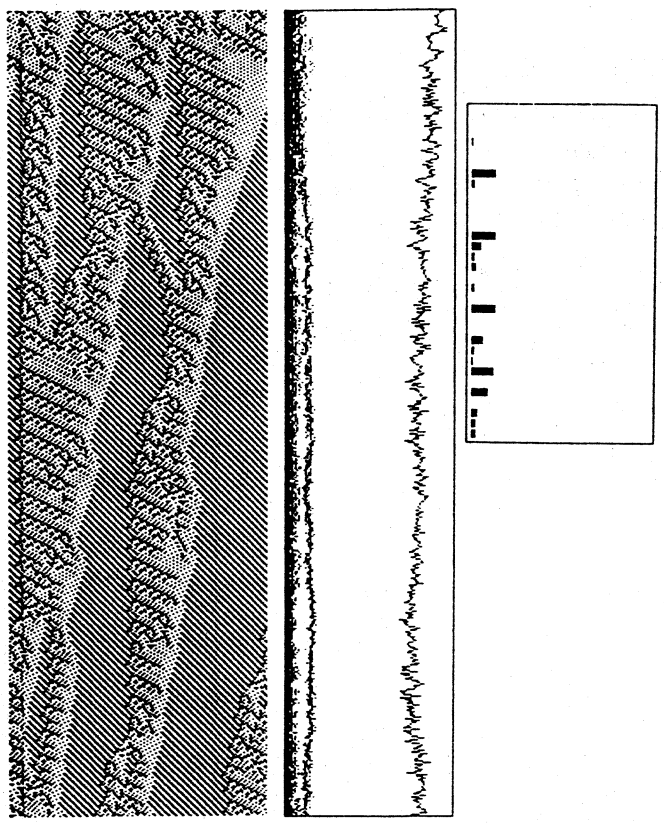

*K*5 rule = 82 26 dc 23, λ ratio = 0.812, Z = 0.578125

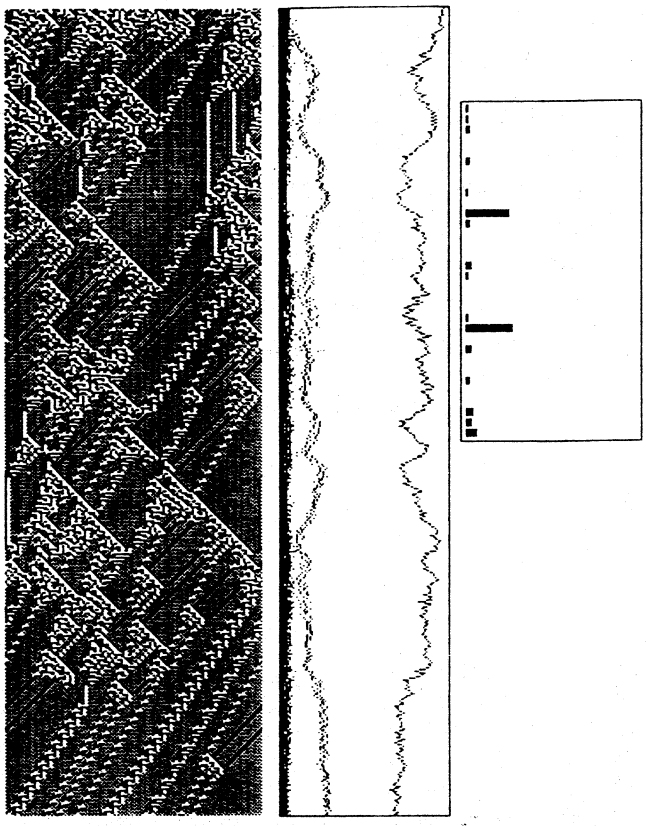

*K*5 rule = 5d 91 ac 17, λ ratio = 1, Z = 0.671875

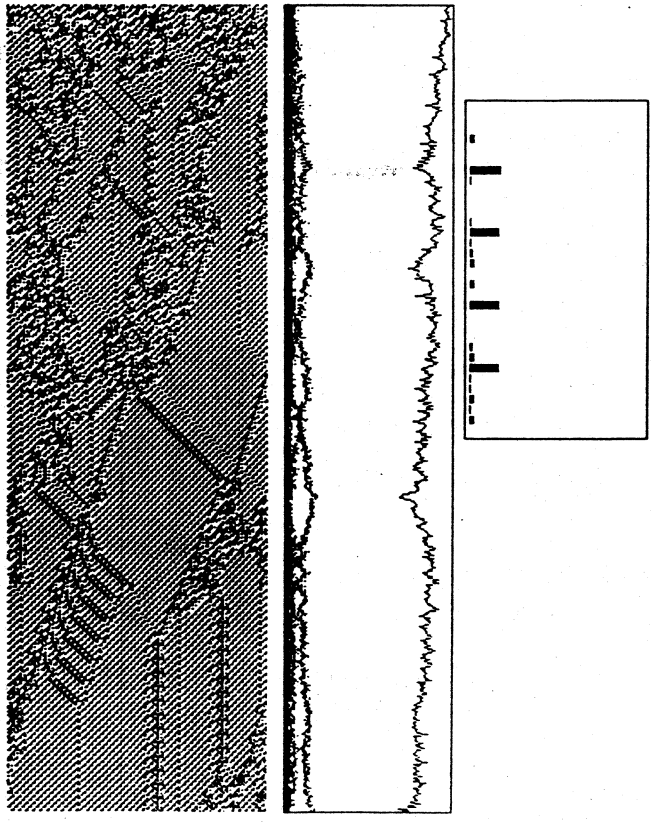

*K*5 rule = 98 8d 66 3c, λ ratio = 0.938, Z = 0.6875

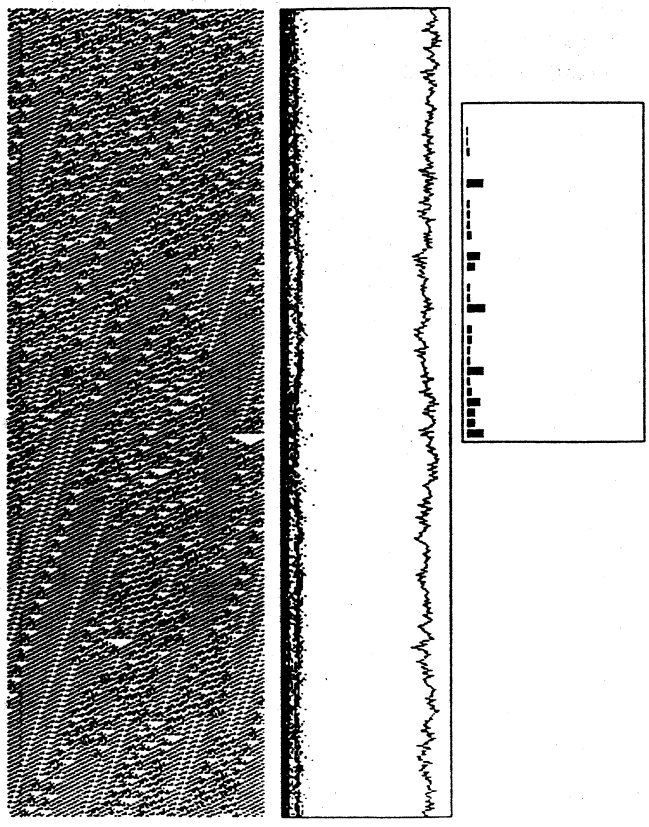

*K*5 rule = 44 2b 8a 3e, λ ratio = 0.875, Z = 0.5625

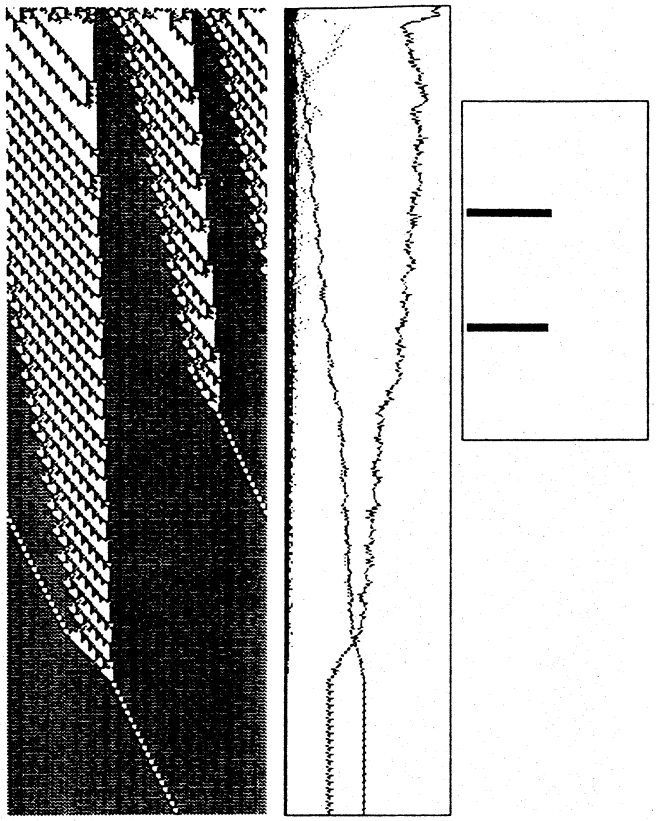

*K*5 rule = 07 1c dc e0, λ ratio = 0.875, Z = 0.75

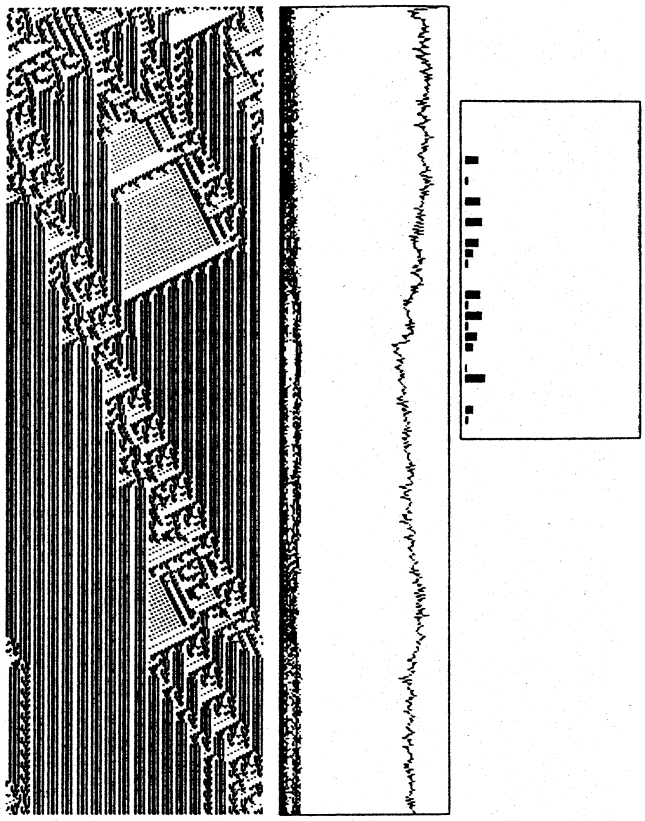

*K*5 rule = c1 d0 64 22, λ ratio = 0.688, Z = 0.5625

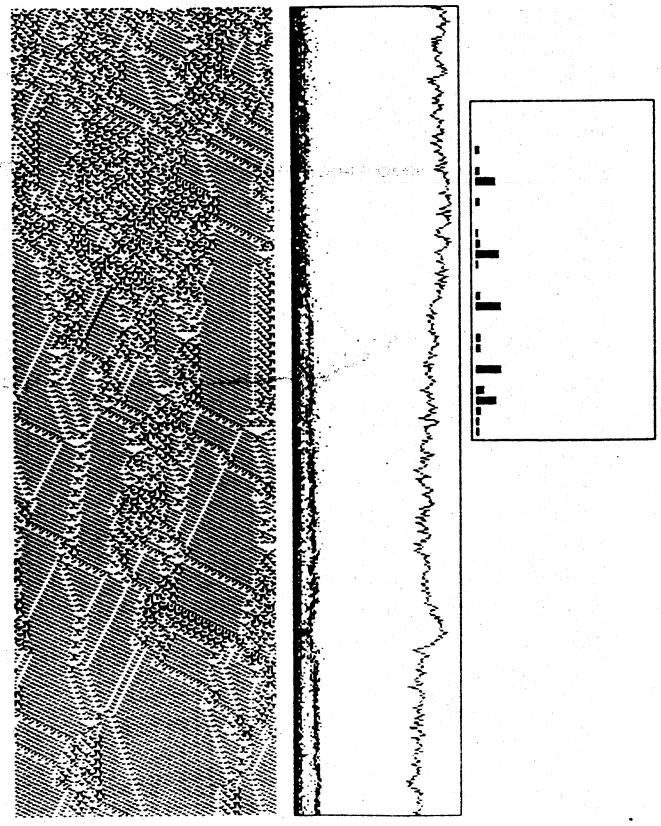

*K*5 rule = a1 1b c1 26, λ ratio = 0.812, Z = 0.617188

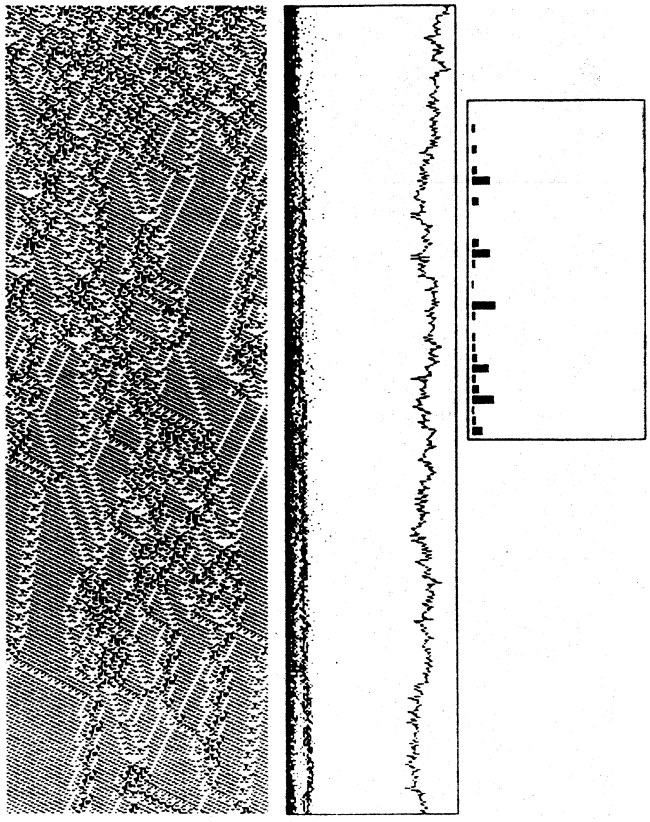

*K*5 rule = a1 9b c1 26, λ ratio = 0.875, Z = 0.671675

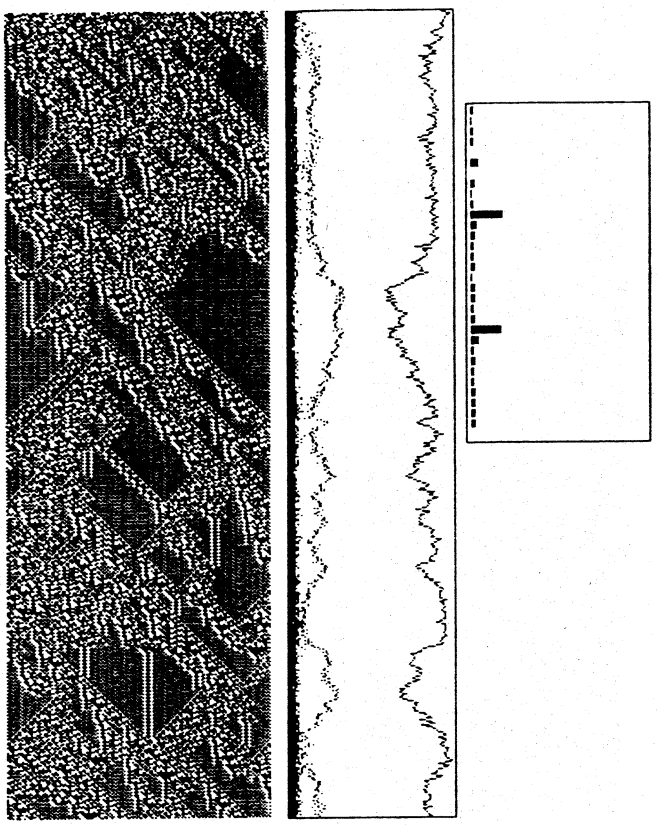

*K*5 rule = 9a 4c f7 17, λ ratio = 0.875, Z = 0.671875

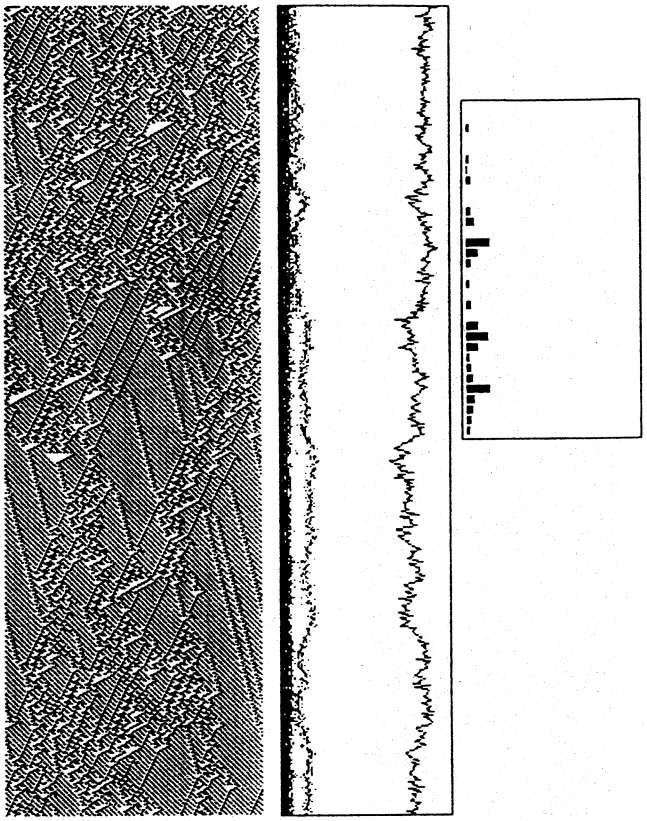

*K*5 rule = 0e d0 83 0e, λ ratio = 0.75, Z = 0.625

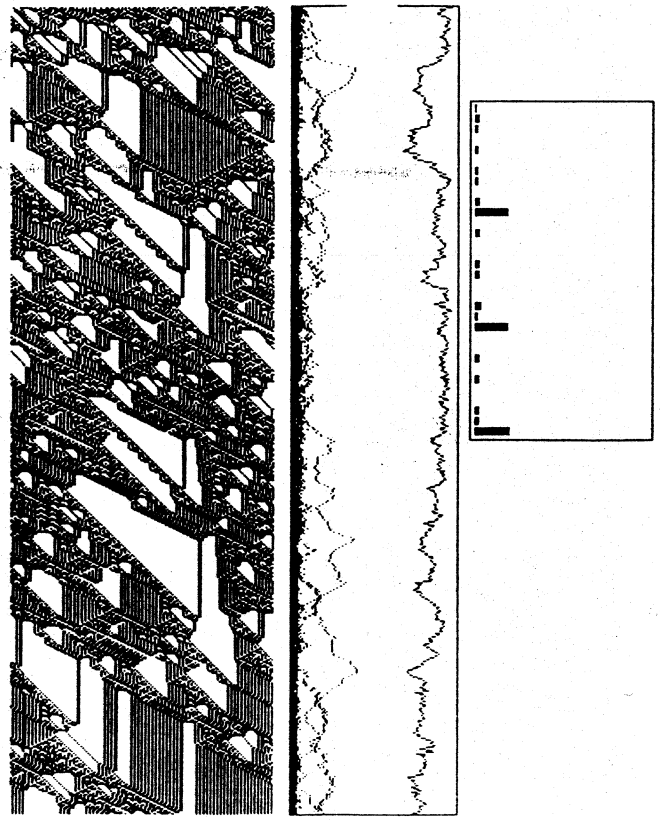

*K*5 rule = 6e ee 93 60, λ ratio = 0.938, Z = 0.6875

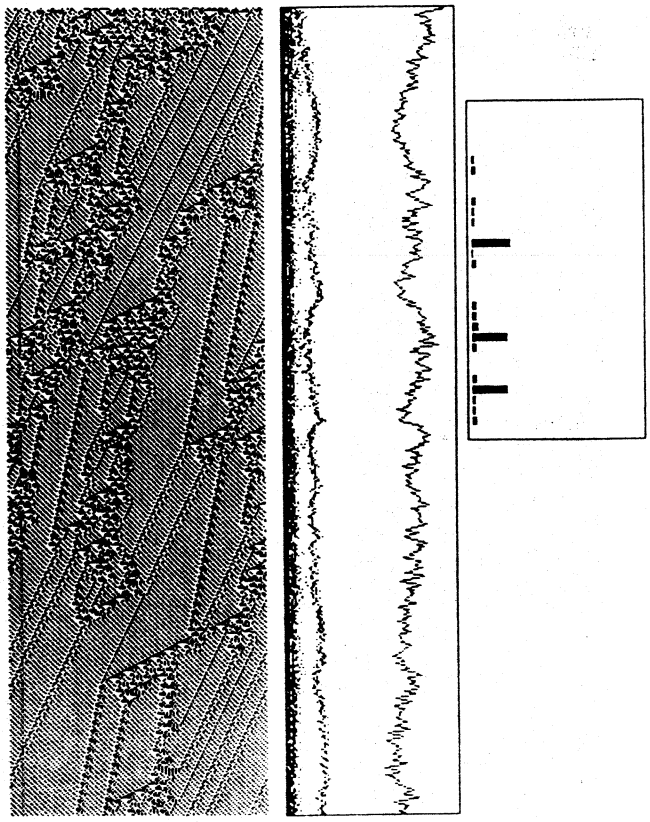

*K*5 rule = 0f 68 63 46, λ ratio = 0.875, Z = 0.671875

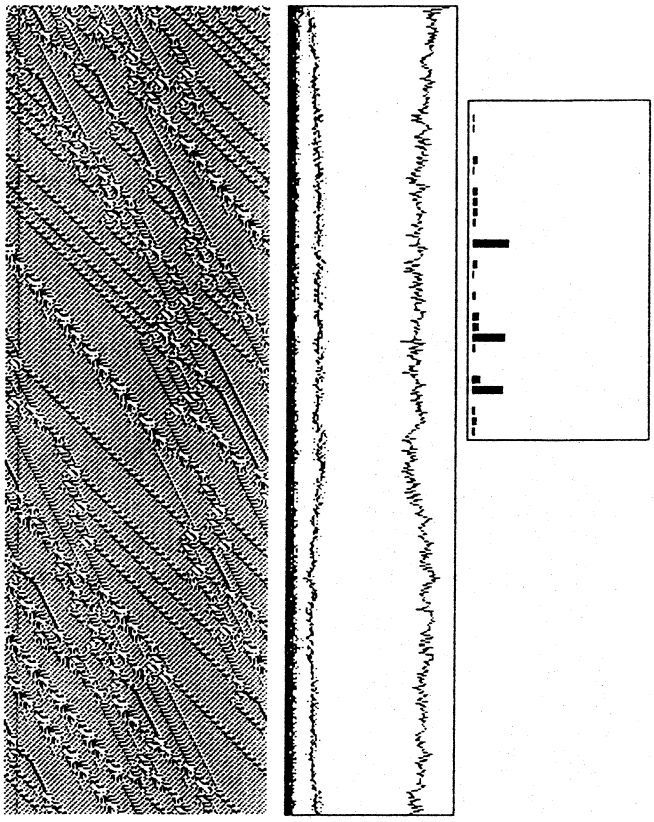

*K*5 rule = 89 ed 71 06, λ ratio = 0.938, Z = 0.726562

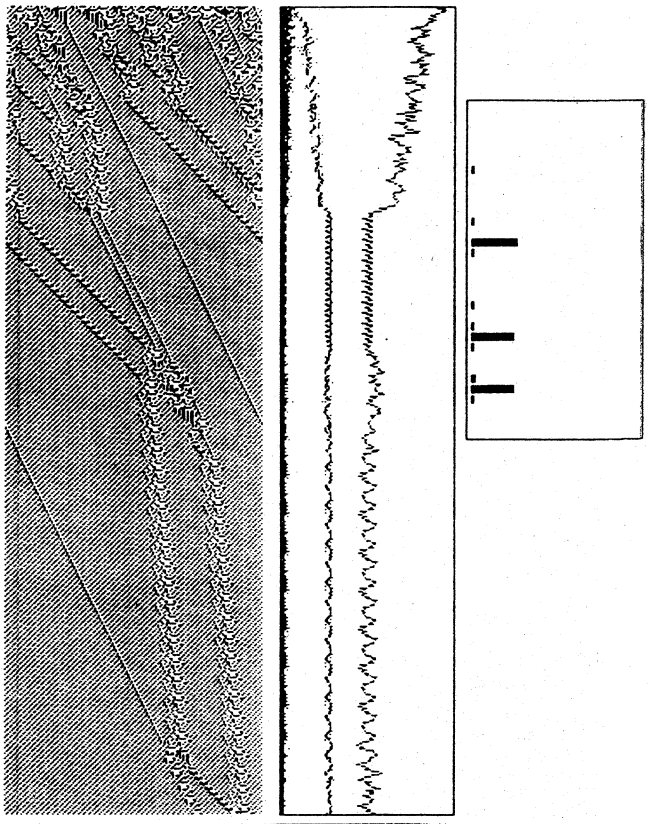

*K*5 rule = 88 6d 71 06, λ ratio = 0.812, Z = 0.726562

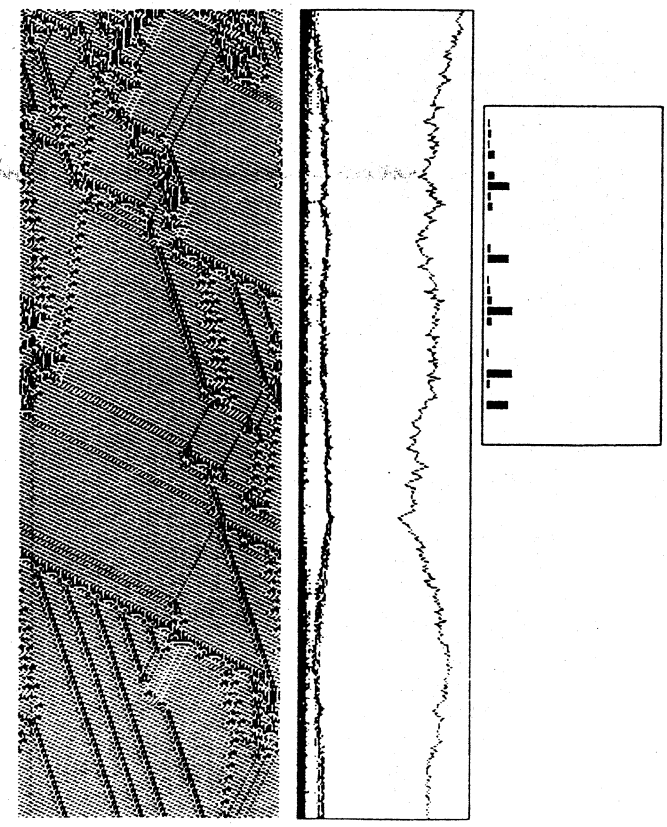

*K*5 rule = 63 be a5 83, λ ratio = 0.938, Z = 0.671875

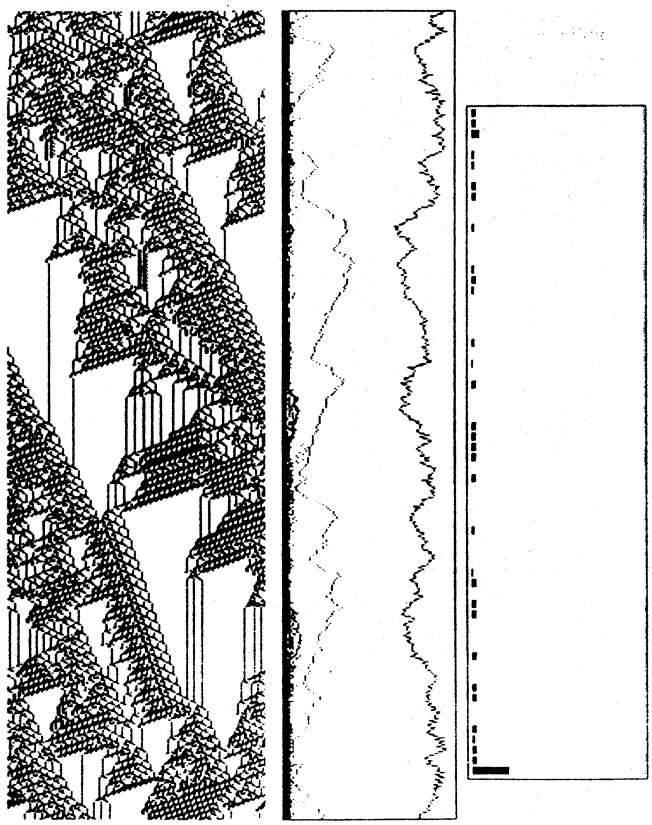

*K*6 rule = b3 87 b6 b8 8c d4 af a0
λ ratio = 0.938, Z = 0.726562

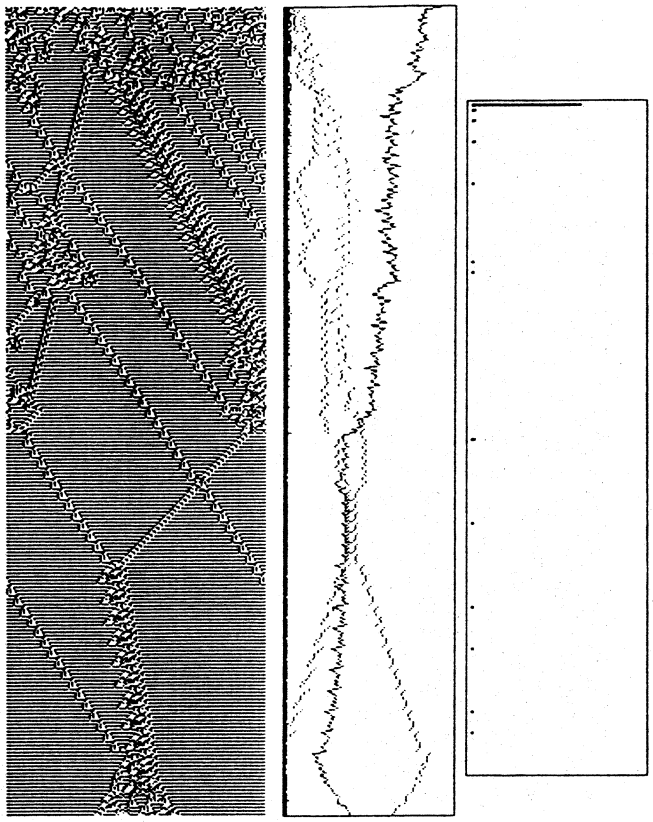

*K*7 rule = 16 42 44 f5 2d 01 de c7 0e de 02 4b 76 0b e4 ff
λ ratio = 0.984, Z = 0.521484

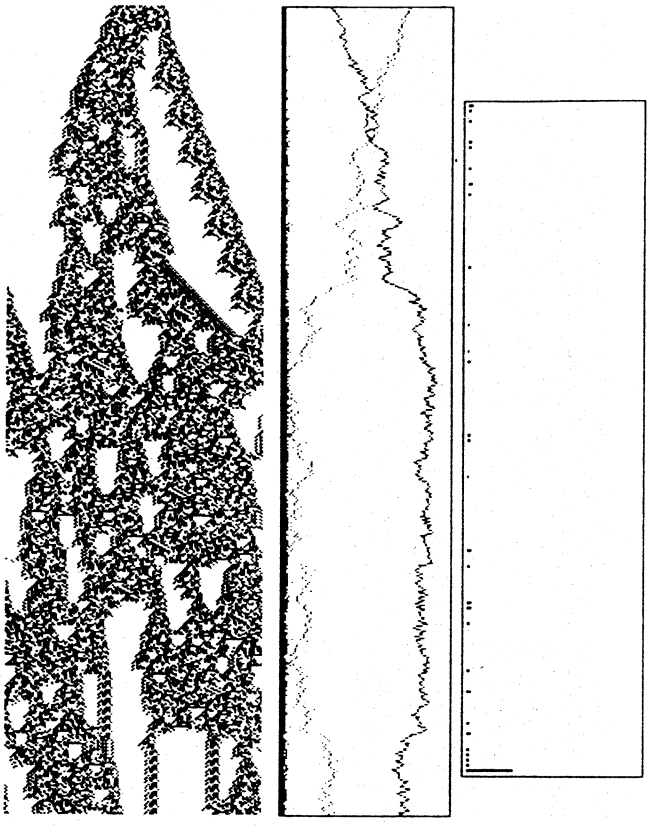

*K*7 rule = 3b 46 9c 0c e4 f7 fa 96 b9 3b 4d 3a b8 9e c0 e0
λ ratio = 0.958, Z = 0.591309

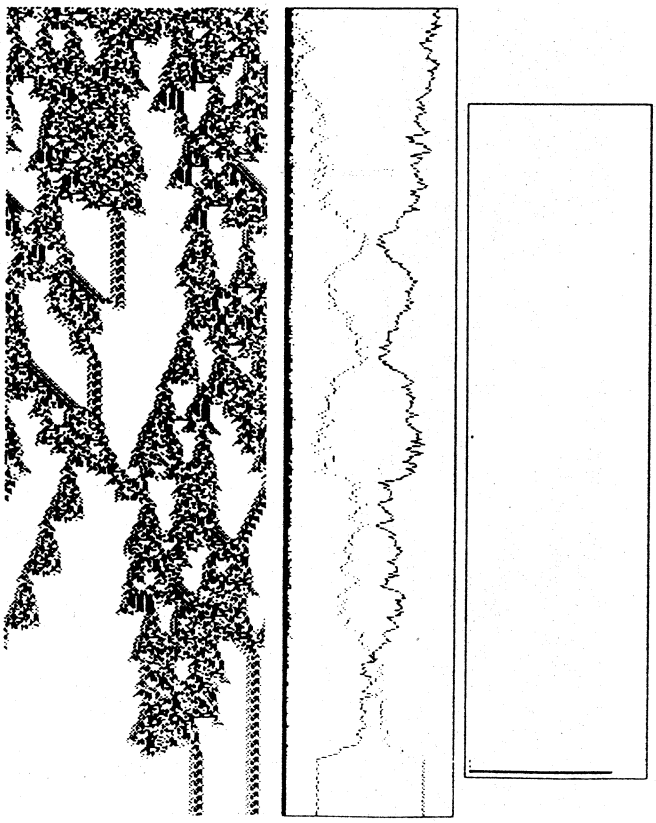

*K*7 rule = 3b 46 9c 0e e4 f7 fa 96 f9 3b 4d 32 b0 9e d0 e0
λ ratio = 0.938, Z = 0.578125

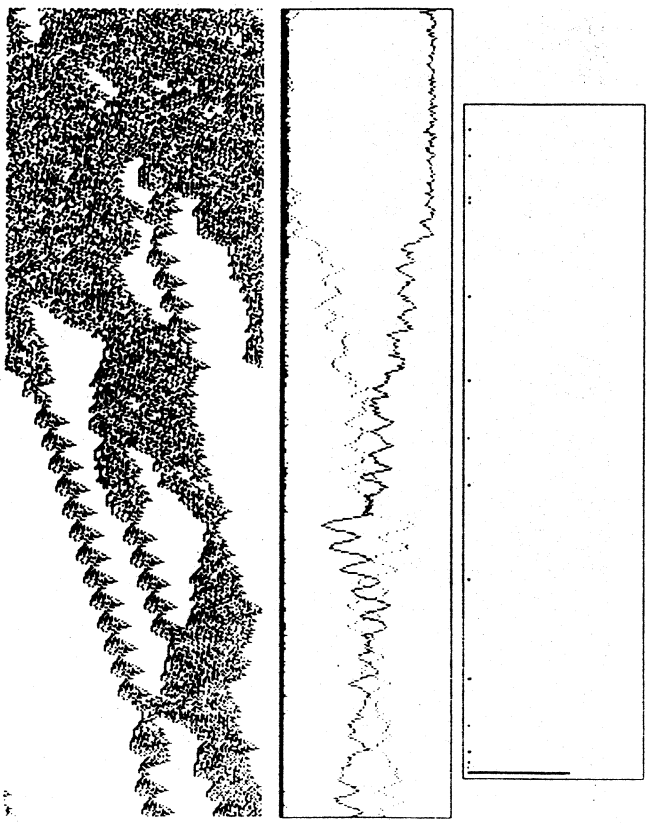

*K*7 rule = ef 80 af 6e 25 32 62 a6 2a 9f 98 b1 88 89 fb 40
λ ratio = 0.958, Z = 0.663086

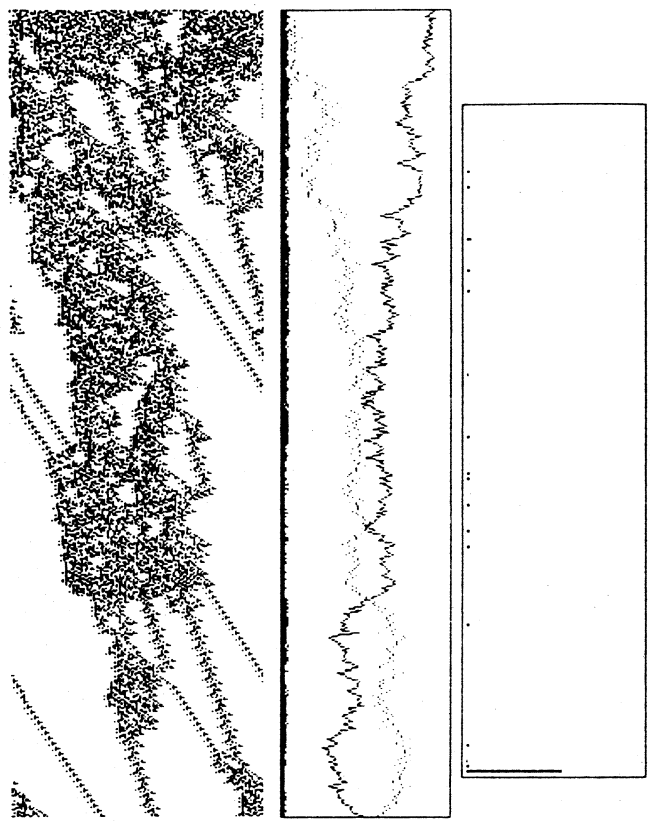

*K*7 rule = ed 88 27 ee 25 32 22 a6 2a 1f 9c 53 8c 89 fb 48
λ ratio = 0.953, Z = 0.682129

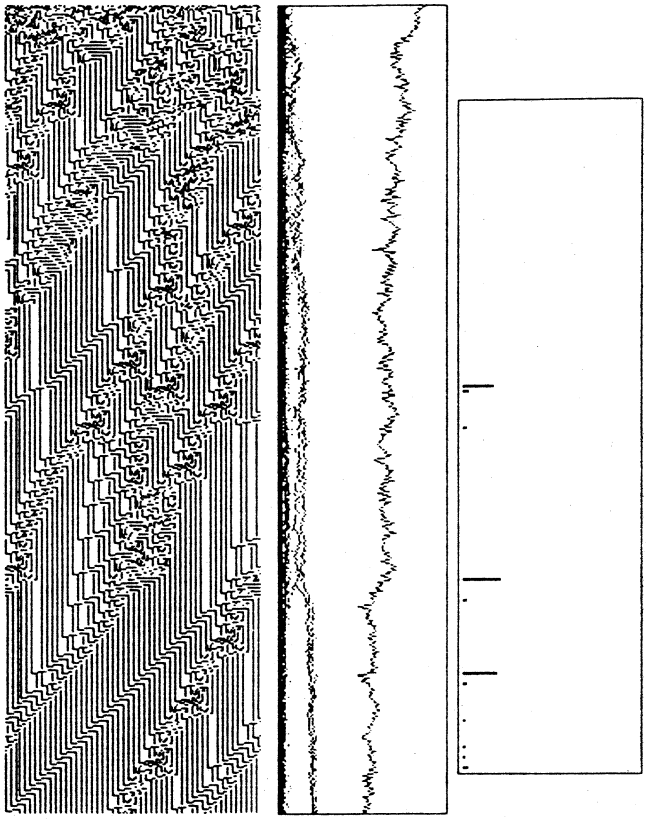

*K*7 rule = 2e fb df e2 2d aa 67 f0 45 c1 4b 08 24 a2 2e 2b
λ ratio = 0.906, Z = 0.517517

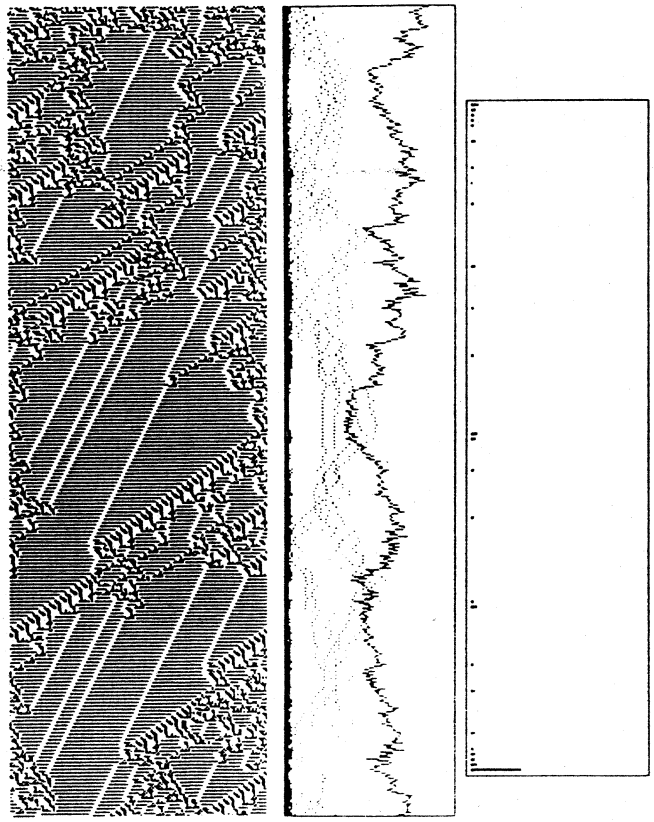

*K*7 rule = 00 1e 17 2d 67 1e 5f 21 3f 10 07 ff 37 be 07 21
λ ratio = 0.938, Z = 0.384766

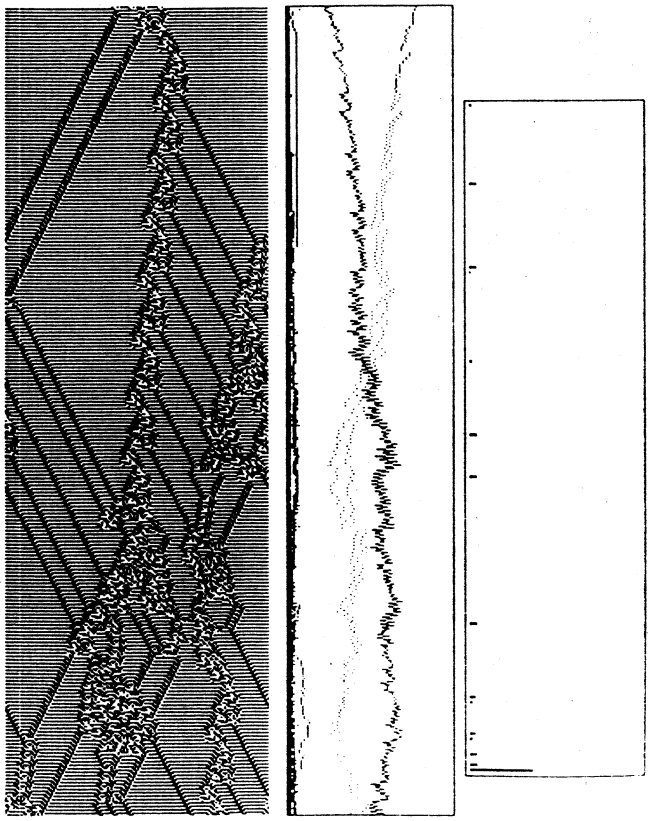

*K*7 rule = 0c f7 8a cf 30 4b 06 4f 24 fb 1e 8f bf 7d 4f df
λ ratio = 0.844, Z = 0.384766

Santa Fe Institute
1660 Old Pecos Trail, Suite A, Santa Fe, New Mexico 87501
505-984-8800; FAX 505-982-0565; email@santafe.edu